Resistance experiments on a systematic series of high speed displacement catamaran forms: Variation of length-displacement ratio and breadth-draught ratio

Article · January 1994

CITATIONS
77

READS
284

3 authors, including:

A.F. Molland
University of Southampton
131 PUBLICATIONS **2,074** CITATIONS
SEE PROFILE

Pat Couser
Bentley Systems
24 PUBLICATIONS **147** CITATIONS
SEE PROFILE

ISSN 0140-3818
SSSU 71

UNIVERSITY OF SOUTHAMPTON

DEPARTMENT OF SHIP SCIENCE

FACULTY OF ENGINEERING AND APPLIED SCIENCE

RESISTANCE EXPERIMENTS ON A SYSTEMATIC SERIES OF HIGH SPEED DISPLACEMENT CATAMARAN FORMS: VARIATION OF LENGTH-DISPLACEMENT RATIO AND BREADTH-DRAUGHT RATIO

A.F. Molland, J.F. Wellicome and P.R. Couser

Ship Science Report 71

March 1994

Resistance Experiments on a Systematic Series of High Speed Displacement Catamaran Forms: Variation of Length-Displacement Ratio and Breadth-Draught Ratio

A.F. Molland, J.F. Wellicome and P.R.Couser

Ship Science Report No. 71
University of Southampton

March 1994

Contents

Nomenclature

Symbols and some values used in the report:

Demihull	One of the hulls which make up the catamaran
Fn	Froude Number, $[v/\sqrt{gL}]$
Rn	Reynolds Number, $[vL/\nu]$
v, U_0	Velocity [ms^{-1}]
W_{tank}	Tank width
H_{tank}	Tank depth
L, L_{BP}	Demihull length between perpendiculars [m]
A	Static wetted surface area [m^2]
B	Demihull maximum beam [m]
T	Demihull draught [m]
T_{stem}	Draught at stem [m]
S	Separation between catamaran demihull centrelines [m]
∇	Volume of displacement [m^3]
Δ	Mass displacement in freshwater [kg]
C_B	Block coefficient
C_P	Prismatic coefficient
$L/\nabla^{\frac{1}{3}}$	Length : displacement ratio, $[L/\nabla^{\frac{1}{3}}]$
R_T	Total resistance
C_T	Coefficient of total resistance $[R_T/\ \frac{1}{2}\ \rho A v^2]$
R_W	Wave resistance
C_W	Coefficient of wave resistance $[R_W/\ \frac{1}{2}\ \rho A v^2]$
R_{WP}	Wave pattern resistance
C_{WP}	Coefficient of wave pattern resistance $[R_{WP}/\ \frac{1}{2}\ \rho A v^2]$
C_F	Coefficient of frictional resistance [ITTC-57 Correlation line]
R	A measurement of resistance
$1+k$	Form factor
β	Viscous resistance interference factor
τ	Wave resistance interference factor
g	Acceleration due to gravity [9.80665 ms^{-2}]
ρ	Density of freshwater [1000 kg/ m^3]
ν	Kinematic viscosity of freshwater [1.141×10^{-6} m^2s^{-1} at 15°C]
δ	Boundary layer thickness [m]
δ_2	Boundary layer momentum thickness [m]
h	Turbulence stud height [m]
w	Turbulence stud width [m]
n	Number of turbulence studs
C_D	Stud drag coefficient
$\overline{U}$	Average velocity over stud [ms^{-1}]
l	Length of model
l_{laminar}	Average distance of studs from leading edge; length of model with laminar boundary layer [m]
$l_{\text{effective}}$	Effective length of plate for unstimulated turbulent b.l.
l_e	Length required for unstimulated turbulent b.l. to produce required momentum thickness
A_{laminar}	Area of hull in front of studs
D_{stud}	Turbulence stud drag [N]
$D_{\text{turbulent}}$	Viscous drag on turbulent part of hull [N]
D_{laminar}	Viscous drag on laminar part of hull [N]
$D_{\text{unstim. turb.}}$	Unstimulated, turbulent viscous hull drag [N]
α	Ratio of running to static wetted surface area
γ	Ship : Model scale factor
λ	Wavelength [m]

1 Introduction

The commercial applications of high speed displacement catamarans has increased significantly over the past few years. Little information is, however, available for carrying out powering estimates for such vessels, particularly in the high speed range.

Work on the resistance of high speed displacement catamarans has been ongoing over a number of years at the University of Southampton[4, 5] in an effort to improve the understanding of their resistance components and to provide design data.

This report describes an extensive series of model tests on catamarans in calm water. The experimental programme is a development of the earlier work[4, 5] in which a small series of three catamaran models were tested. The current work has extended the parametric investigation to cover changes in Breadth:Draught ratio (B/T) and a wider range of Length:Displacement ratio ($L/\nabla^{\frac{1}{3}}$). As in the earlier work, an approach comprising total resistance measurements together with wave pattern analysis was utilised. A wide range of hull separations was tested and, overall, the experiments covered over 40 model configurations, each over a speed range up to a Froude Number of unity.

The information collected and presented in this report contributes to a further understanding of the resistance components of catamarans and provides resistance data for practical use at the preliminary design stage.

The work described formed part of a wider research programme, funded by SERC through MTD Ltd over a two year period, which included the development of theoretical methods for the prediction of the wave resistance of catamarans. The theoretical work is the subject of a separate report[11].

2 Description of Models

Details of the models used in the investigation are given in TABLES I and II. The models were built from high density polyurethane foam using the NC cutting machine described in[10]. This manufacturing technique was able to produce models to a good level of accuracy at relatively low cost.

It should be noted that Models 3b, 4b and 5b had already been tested some three years earlier and their results published in[5]. The results for these models are included in the present report for comparison and discussion since they form the basis from which the current wider series of models was developed. Some retests were in fact carried out on Model 4b to confirm and validate the current test procedure. Also, some element of doubt about the earlier results for Model 5b led to the retest of that model in monohull mode and confirmation of the results for the catamaran modes.

The models were of round bilge form with transom sterns, Fig 1, and were derived from the NPL round bilge series[8]. This hull broadly represents the underwater form of a number of catamarans in service or currently under construction. The models were firstly tested as monohuls and, in the catamaran configurations, Separation:Length ratios (S/L) of 0.2, 0.3, 0.4 and 0.5 were tested.

The model towing force was in the horizontal direction. The towing point in all cases was situated at the longitudinal centre of gravity and at an effective height one third of the draught above the keel. The models were fitted with turbulence stimulation comprising trip studs of 3.2mm diameter and 2.5mm height at a spacing of 25mm. The studs were situated 37.5mm aft of the stem. No underwater appendages were attached to the models. For some of the smaller displacement models it was necessary to apply a counter balance. Care was taken with its application whereby the effect on accuracy was negligible.

3 Facilities and Tests

3.1 General

All the model experiments were carried out in the Southampton Institute of Higher Education test tank which has the following principal particulars:

Length	:	60.0m
Breadth	:	3.7m
Water Depth	:	1.85m
Maximum Carriage Speed	:	4.6 ms^{-1}

The tank has a manned carriage which is equipped with a dynamometer for measuring model total resistance together with various computer and instrumentation facilities for automated data acquisition.

Calm water total resistance, running trim, sinkage and wave pattern analysis experiments were carried out for all the models. All tests were carried out where possible over a speed range up to a little over $Fn = 1.0$. Over the Froude Number range 0.1 to 1.0 the corresponding Reynolds Number (Rn) range for the models was 0.5×10^6 to 5.5×10^6.

3.2 Wave Pattern Resistance

A wave pattern analysis based on multiple longitudinal cuts was developed and applied to all the models. The analysis system was fully automated and consisted of four resistance wave probes, a microcomputer based data acquisition system and data analysis which enabled wave pattern analysis and resistance determination during standard resistance tests.

All wave probes were located at an optimum longitudinal position for longest possible wave traces, whilst transverse positions were chosen to obtain a suitable cosine term in the wave series for every harmonic. This had an important effect on the stability of the analysis which enabled the results to be effectively independent of the transverse positioning of the probes. The analysis method was based on a combined matrix solution of four longitudinal wave traces. The method accounted for short wave traces without truncation errors.

A full description of the apparatus and analysis method is given by Insel[4]

3.3 Trim and Sinkage Measurements

Trim and sinkage were monitored for all the tests. Trim (positive bow up) was measured by means of a potentiometer mounted on the tow fitting; accuracy of the measurement was within $\pm 0.05°$. Sinkage (positive downwards) was measured by means of a linear displacement potentiometer with a measurement accuracy within ± 0.1mm.

3.4 Bow Down / Transom Emerged Tests

A test case was carried out to derive the form factor for one of the models by running the model bow down with transom emerged. This technique was, for example, mentioned in the dicussion to Ref[5]. It has a number of limitations, but investigation into its potential uses was considered worthwhile.

3.5 Longitudinal Centre of Gravity

Before the start of the experimental investigation it was envisaged that the influence of variation of LCG on resistance would be investigated in a systematic way over a range of models.

Preliminary experimental studies were carried out which indicated that whilst some change in model running attitude occurred due to the change in LGC position, changes in resistance were negligible. This relative insensitivity of resistance to effective change in LCG was also noted by Marwood and Bailey[8]. The decision was therefore taken not to pursue the LCG investigation in a systematic manner. The decision was further influenced by the fact that the primary tasks of the overall experimental investigation were to investigate the effects on resistance of $L/\nabla^{\frac{1}{3}}$, B/T and S/L. This would entail an extensive

programme of tank tests covering over forty model configurations, each over a range of speeds. It was considered that the best use of available resources would be to concentrate effort on the above parameters and to investigate them properly.

4 Data Reduction and Corrections

All resistance data were reduced to coefficient form using fresh water density ($\rho = 1000$ kg/ m^3), static wetted surface area (A) and model speed (u):

$$\text{Resistance Coefficient} = \frac{\text{Resistance}}{\frac{1}{2}\rho A u^2}$$

Corrections were applied as necessary to the measured data and these, together with possible alternative approaches to data reduction are described in the following sections:

4.1 Temperature Correction

The model tests were carried out over a period of 18 months. During this time the water temperature varied from approximately 15°C to 18.5°C. The total resistance measurements were corrected to the standard temperature of 15°C by modifying the frictional resistance component. The correction which has been applied is as follows:

$$C_{T_{15}} = C_{T_{test}} - C_{F_{test}} + C_{F_{15}}$$

The correction should be slightly larger due to the form factor being greater than unity. However, the correction is in any case small and the above equation is considered to be sufficiently accurate.

4.2 Resistance due to Turbulence Studs

Turbulence studs were attached to all models as described in Section 2. A detailed investigation of their influence on model drag was carried out, and this is described in Appendix A. It was found that, whilst there was additional drag on the studs, this is to a certain extent negated by the laminar region upstream and the boundary layer momentum thickness increase down stream due to the studs. A stud drag correction was applied to all the measured resistance data along the lines described in Appendix A, although the investigation indicates that the net correction would be relatively small.

4.3 Wetted Surface Area

Static wetted surface area was used to nondimensionalise the resistance measurements. A detailed investigation into the use of running wetted surface area was carried out, and this is described in Appendix B. The conclusions in Appendix B indicate that whilst the use of running wetted surface might provide a better understanding of the physical components of resistance, it does not affect model to ship extrapolation providing both model and full scale coefficients are based on running wetted surface area. Running wetted surface area is difficult to measure experimentally in a routine manner, and will not be available for a new design. From a practical viewpoint it is necessary to use the static wetted surface area, and it has therefore been applied in the current work.

4.4 Tank Blockage and Shallow Water

As in the previous work viscous blockage effects on the models were neglected. The largest model cross-section was much less than 0.5% of the tank cross-section. The application of a tank wall correction was investigated by Insel[4], but theoretical calculations indicated that the maximum interference would be less than 1%. Hence correction for this effect was not applied.

Shallow water effects were also neglected. The tank critical Froude Number ($Fn_{H_{\text{tank}}} = 0.95$) corresponded to a model Froude Number of 1.02. Thus the models were being operated in the subcritical range, although the higher speed runs approached the critical Fn and this may have caused a slight increase in wave resistance.

4.5 Variation in Wetted Surface Area between Models of Same Displacement

It should be noted from TABLE II that for a given displacement there is a change in wetted surface area with change in B/T. The 'a' models ($B/T = 1.5$) in particular show an increase in wetted surface area compared with the 'b' models ($B/T = 2.0$)

As mentioned earlier the data have been nondimensionalised using wetted surface area. It should therefore be appreciated that resistance comparisons based on a fixed displacement or resistance per unit displacement, would be affected slightly by these changes in wetted surface area.

5 Presentation of Data

The basic presentation of the experimental data follows the same approach as that adopted in the earlier work[5] and is summarised as follows:

$$C_{T_{cat}} = (1 + \phi k)\sigma C_F + \tau C_W \tag{1}$$

where:
C_F is obtained from the ITTC-57 correlation line.
C_W is the wave resistance coefficient for the demihull in isolation.
$(1 + k)$ is the form factor for the demihull in isolation.
ϕ is introduced to take account of the pressure field change around the demihull.
σ takes account of the velocity augmentation between the two hulls and would be calculated from an integration of local frictional resistance over the wetted surface.
τ is the wave resistance interference factor.

It is difficult to separate the two factors ϕ and σ by experimental measurements. For practical purposes, therefore, ϕ and σ are combined into a viscous resistance interference factor β. Where:

$$(1 + \phi k)\sigma = (1 + \beta k)$$

whence:

$$C_{T_{cat}} = (1 + \beta k)C_F + \tau C_W \tag{2}$$

Noting that for the demihull in isolation, $\beta = 1$ and $\tau = 1$.

The measured experimental data are presented in Figs 2 to 31. Figures 2 to 12 give the total and wave pattern resistance data for the demihulls (or monohulls) in isolation whilst Figs 14 to 23 give the data for the catamaran configurations. In these diagrams the wave pattern resistance C_{WP} is plotted downward from the total resistance C_T, in the form $(C_T - C_{WP})$. The estimates of $(1+k)$ or $(1+\beta k)$ are also shown in the diagrams, these lines being set to the lower envelope of the $(C_T - C_{WP})$ curves when they settle at an approximately constant level above the ITTC friction line at higher Froude Numbers.

Results of the trim and sinkage measurements are presented in Figs 24 to 31.

From a practical viewpoint it is not necessary to confine the user to the particular values of $(1+k)$ or $(1+\beta k)$ derived in this work. Following the earlier work, for example, some concern was expressed over their magnitudes and application (see discussion to[5]), and this subject is discussed later (Section 6.5). For these reasons, residuary resistance coefficients C_R (derived from $C_T - C_{F_{ITTC}}$) have been calculated from the experimental data and are presented in Figs 32a, 32b, 32c and 32d for the monohulls and Figs 33 to 46 for the catamarans. These curves provide the data in a form suitable for practical powering applications and an overall comparison of the residuary components for the various hull configurations. The user is able to choose a suitable $(1+k)$ or $(1+\beta k)$ from this work or other sources. For an estimate of the ship total resistance coefficient it can be shown that, for the monohulls:

$$C_{T_{ship}} = C_{F_{ship}} + C_{R_{model}} - k(C_{F_{model}} - C_{F_{ship}}) \tag{3}$$

and for catamarans:

$$C_{T_{ship}} = C_{F_{ship}} + C_{R_{model}} - \beta k(C_{F_{model}} - C_{F_{ship}}) \tag{4}$$

Use of these equations requires a knowledge of model C_F. Based on the model length of 1.6m and a kinematic viscosity for fresh water of 1.14×10^{-6} it can be shown that:

$$C_{F_{model}} = \frac{0.075}{[\log_{10}(Fn \times 5.56 \times 10^6) - 2]^2} \tag{5}$$

Residuary resistance interference factors, used later in comparing the performance of the various hull configurations, are presented in Figs 47 to 60. Form and viscous interference factors are presented in Figs 61 to 71 and are summarised in TABLE III.

The experimental data for C_T, C_{WP}, trim and sinkage for all model configurations over a range of speeds, together with residuary resistance coefficients C_R derived from these data, are tabulated at the back of the report.

6 Discussion of Results

6.1 Correlation with Earlier Tests

As mentioned in Section 2, representative models from the earlier experimental programme were retested in order to confirm and validate the current test procedure.

Figures 2a and 2b show the results of the retests of the monohull Model 4b and catamaran Models 4b with S/L=0.3. In both cases the total resistance values show good agreement with the earlier results. The wave pattern resistance values are in acceptable agreement, showing levels of scatter expected for this component. It should be noted that the error margins for the monohull (Fig 2a) are greater than for the catamaran (Fig 2b) because of the smaller forces being measured on the dynamometer and the smaller amplitude of the waves in the wave resistance analysis. Also, results for Fn less than about 0.2 cannot always be relied upon since the measured forces were very small and subject to poor repeatability due to flow fluctuations and vortex shedding. Thus results at these very low Fn can be subject to quite large experimental errors.

These tests on the same models were carried out more than three years apart and satisfactorily demonstrate the repeatability of the results and the experimental procedure.

6.2 Total Resistance and Wave Pattern Resistance

6.2.1 Results for Monohulls

Figures 3 to 12 show the experimental results for the monohull tests. It is to be noted that the results from the earlier tests of monohull Model 5b showed some inconsistencies when compared with the current tests. This model was therefore retested. The results for C_T were about 5% higher than the original results, and the updated data are used in this report.

The total resistance curves are of similar shape with the main resistance hump reducing as the models become finer.

The results of the wave pattern measurements are included in Figs 3 to 12 and are plotted downwards from the total resistance values. The results display a hump (or decrease in measured wave pattern resistance) at a Froude Number of about 0.4 before settling down at an approximately constant level above the ITTC correlation line at higher Froude Numbers. Observations during the tests indicate that the large hump is due primarily to transom stern and wave breaking effects in this speed range when the transom is just about to run clear.

Figures 13a, 13b and 13c show comparisons between the total resistance measurements and those for models from Series 64[13] which had reasonably similar hull characteristics. It can be seen that although the absolute magnitudes are different the general shape of the curves is very similar. The unfamiliar resistance curves for Models 6a, 6b and 6c are duplicated in the Series 64 results; some of these results are even more extreme for the most slender models. This is due to the very small component of wave resistance for these slender hulls. The main hump normally associated with the resistance curve is due to the wave resistance of the model. As the models become more slender they have less wave resistance and hence their resistance curve tends to a shape similar to that of the flat plate friction line. This is even more apparent in the resistance curves of the most slender Series 64 forms.

6.2.2 Results for Catamarans

Figures 14 to 23 show the experimental results for the catamaran tests. These are a broadly consistent set of results and provide the total and wave pattern resistance over the ranges of hull parameters and hull separations tested.

It is noted that for some of the fuller models there was some difficulty in obtaining satisfactory data at the lowest S/L, ($S/L = 0.2$) due to substantial wave breaking between the hulls. This curtailed testing at higher speeds (Figs 14a and 16a).

The comparison between the results for the different hull parameters and hull separations is discussed later in Sections 6.4 and 6.5.

6.3 Running Trim and Sinkage

The interference effects on the running trim and sinkage can be seen in Figs 24 to 31. The overall results and trends are in broad agreement with published monohull data such as Lahtiharju[7] and Tanaka et al[12].

In all cases, trim angle interference is important between $Fn = 0.3$ and $Fn = 0.7$ where the catamaran displays significantly higher trim angles than the monohull, but generally approaches the monohull trim angle as the S/L is increased. It is seen that as Length:Displacement ratio is increased (when going from Models 3 to 6) there is a decrease in running trim. As B/T is increased for a given Length:Displacement ratio (when going from Models 'a' to 'c') the changes in running trim are relatively small.

In general, as Length:Displacement ratio is increased (when going from Models 3 to 6) there is a decrease in running sinkage. As B/T is increased for a given Length:Displacement ratio (when going from Models 'a' to 'c') there tends to be an increase in sinkage or lift effects for the fuller models, particularly at higher speeds (e.g. Figs 29a, 30a, 31a).

6.4 Residuary Resistance; Effect of Hull Parameters

The experimental results are presented in term of residuary resistance coefficient C_R in Figs 32 to 46, where the residuary coefficient has been derived from $C_T - C_{F_{ITTC}}$. As discussed in Section 5, this presentation is used in order to provide a readily available tool for powering purposes and a means of comparing the relative merits of changes in the hull form parameters.

6.4.1 Monohulls

The residuary resistance coefficients for the monohulls are shown in Figs 32a, 32b, 32c and 32d.

The results in Fig 32a, for fixed $B/T = 2.0$, clearly show the influence of Length:Displacement ratio as it is increased from Model 3b to 6b. With increase in Length:Displacement ratio the main resistance hump becomes less pronounced and the Froude Number at which it occurs decreases slightly.

Figures 32b, 32c and 32d show the influence of B/T (1.5, 2.0, 2.5) at each Length:Displacement ratio. The influence of B/T is seen mainly in the lower Froude Number range up to about 0.6, and differences between the results of up to 10% due to changes in B/T can occur in this region. In the highest Froude Number range, at speeds often representing service speeds for this type of hull form, Models 'c' with the highest $B/T = 2.5$ tend to have the highest resistance coefficient; the differences between it and the lower B/T ratios tends to be of the order of 3% to 4%. In general the curves tend to cross and recross and no consistent trends are apparent. A similar lack of trend is also seen in the Series 64 data[13] (Fig 13).

6.4.2 Catamarans

Figures 33 to 42 give the results for each of the catamaran models for changes in S/L. The monohull is also shown on each Figure. The general trend in all cases is that as the hull separation is increased, the resistance decreases and the main resistance hump occurs at decreasing Froude Numbers. It is noted that, in the higher speed range, changes in hull separation tend to have a relatively small effect. There is however an increase in residuary resistance for the catamaran compared with the monohull, and this increase becomes a larger proportion of the monohull residuary resistance as Length:Displacement ratio increases from Model 3 to Model 6.

Figures 43 to 46 show comparisons for changes in Length:Displacement and B/T ratios for given S/L values. The results for a fixed $B/T = 2.0$ (Figs 43a, 44a, 45a and 46a) show, for each S/L, the same general trend as those displayed by the monohulls, with resistance decreasing as Length:Displacement ratio is increased. The results for fixed Length:Displacement ratio and changes in B/T show various trends. For the highest Length:Displacement ratio (Models 6a – 6c), Model 6a with the smallest B/T tends to have the largest resistance coefficient. For the low Length:Displacement ratio (Models 4a – 4c) the trend has been reversed and Model 4a (with the smallest B/T) tends to have the lower resistance coefficient over much of the Froude Number range beyond the resistance hump speed.

6.4.3 Residuary Resistance Interference Factors

The results for the ratio of catamaran residuary resistance coefficient to monohull residuary resistance coefficient for the various catamaran configurations are shown in Figs 47 to 60. As has been found earlier[5] there are significant oscillations in the interference factor in the lower Froude Number range, with a slight shift in the phasing with change in S/L and a general decrease in amplitude of interference factor as S/L is increased. In the higher Froude Number range S/L has a much smaller effect on the interference; also, the amplification between the monohull and catamaran gets larger with increasing Length:Displacement ratio, as was noted in Section 6.4.2, ranging from a value of about 1:10 for the lowest Length:Displacement ratio (Model 3) up to a mean of about 1.35 for the largest Length:Displacement ratio (Model 6).

6.5 Viscous Resistance and Form Factors

6.5.1 General

Form factors $(1+k)$ for the monohulls and form factors for the catamarans including viscous interference $(1+\beta k)$ were obtained by deducting the wave pattern resistance from the total resistance as described in Section 5.

The basic experimental results, Figs 3 to 23 include the $C_T - C_{WP}$ curves and an estimated position of the $(1+k)C_F$ line in the case of monohulls and $(1+\beta k)C_F$ in the case of the catamarans. The resulting values of $(1+k)$ and $(1+\beta k)$ for the various configurations are shown in Figs 61 to 71 and are summarised in TABLE III. As discussed in Section 5, these factors may not necessarily be used directly for design or resistance scaling purposes, but they do provide a broad indication of changes in viscous resistance and viscous interference due to changes in Length:Displacement, B/T and S/L ratios.

6.5.2 Monohulls

For the monohulls, inspection of Figs 61 to 63 and TABLE III indicates a decrease in $(1+k)$ with increasing Length:Displacement ratio and a corresponding trend with Length:Breadth ratio (Models 3 to 6). This was also determined by Insel[5], and might be expected physically. For each Length:Displacement ratio there is however an insignificant change in $(1+k)$ with change in B/T ratio.

6.5.3 Catamarans

For the catamarans, inspection of Figs 61 to 71 and TABLE III indicates $(1+\beta k)$ values to be higher than the corresponding monohull $(1+k)$ values, indicating $\beta > 1$ and suggesting some viscous interference between the hulls as well as the form effect of the demihulls. Part of this increase could be negated by the increase in wave breaking between the hulls at some speeds in the case of the catamarans leading to decreased values of C_{WP} and subsequent overestimates of $(1+\beta k)$. Observations at the time of the tests suggest that, in most cases, this effect should not be significant.

As was seen in the earlier tests[5], changes in $(1+\beta k)$ due to S/L are small and do not show a regular trend. There is seen to be a general trend for a slight decrease in $(1+\beta k)$ between models 'a' to 'c' (as B/T increases from 1.5 to 2.5); this effect is more pronounced at the lower S/L ratios. These trends are not fully what, intuitively, would be expected physically. Whilst the decrease in $(1+\beta k)$ with increasing B/T might follow from an increasing wave pattern resistance with increasing B/T, some increase in viscous resistance might have been expected, due to the greater acceleration of the flow through the tunnel. However there is a corresponding decrease in draught with increasing beam. These results do, however, have implications for the choice of basic hull parameters since they indicate, for a given S/L, some reduction in wave interference and wave resistance with decrease in B/T, particularly with lower Length:Displacement ratios. It should be noted however that there is an increase in wetted area for the lowest B/T form which could reduce some of this gain, and that at higher speeds the wave pattern resistance is the smaller portion of the total resistance.

6.5.4 Bow Down / Transom Emerged Tests

The results of the bow down / transom emerged tests for catamaran Model 4a at $S/L = 0.5$ are shown in Fig 72a, 72b, and 72c.

In the slow speed test, Fig 72a, the results with the transom immersed (normal trim condition) are much more erratic than with the transom emerged. This is likely to be due to the highly turbulent, chaotic wake and vortex / eddy shedding caused by the deeply immersed transom.

The slow speed tests, Fig 72a, indicate a $(1 + \beta k)$ value of 1.55 for the normal trimmed condition and 1.37 for the transom emerged case. Using Prohaska's method; Figs 72b and 72c, similar values for $(1 + \beta k)$ are found. TABLE III indicates a value of 1.44 for this model.

These results tend to confirm earlier deductions that viscous form and interaction effects are present, although they may be smaller than the values suggested by the $(C_T - C_{WP})$ method.

Taken overall, and compared with the normal trim condition, the $(1+\beta k)$ derived from the bow down / transom emerged tests is in broad agreement with the value obtained from the wave pattern analysis. In both cases the transom was running clear, indicating that when the transom is immersed and not releasing it has a substantial effect on the flow resulting in an increase in resistance.

It is finally noted that the slow speed bow down / transom emerged tests should be treated with caution due partly to the low resistance forces measured at low speed and the fact that the forward trimmed hull form will be different (although not necessarily significantly) from the actual normal trimmed condition.

7 Conclusions and Recommendations

7.1 The results of the investigation provide further insight into the influence of hull parameters on the resistance components of high speed displacement catamarans, and offer a very useful extension to the available resistance data for this vessel type.

7.2 Length:Displacement ratio was found to be the predominant hull parameter, resistance decreasing with increasing Length:Displacement ratio as might be expected for higher speed displacement vessels.

7.3 The effect of B/T on resistance was not large. Changes in resistance due to changes in B/T were however identified in particular ranges of speed and Length:Displacement ratio which could warrant attention at the hull design stage. In the main, increase in B/T ratio led to an increase in resistance in the lower Length:Displacement ratio range and a decrease in resistance at the highest Length:Displacement ratio.

7.4 The catamaran displays significantly higher running trim angles than the monohull, but generally approaches the monohull angle as S/L is increased. Changes in running trim due to changes in B/T are relatively small.

As B/T is increased there is an increase in running sinkage / lift effects for the fuller models, particularly at higher speeds.

7.5 Form factors for the catamarans were consistently higher than the corresponding monohulls, suggesting some viscous interference between the hulls as well as the form effect of the demihulls.

7.6 Bow down / transom emerged tests indicated that the viscous form and interference factors may be lower than those derived directly from the total minus wave pattern resistance results. Whilst the total minus wave pattern resistance method provides very useful information on the general changes in wave pattern and viscous resistance, further work is required to justify and confirm the magnitude of the total viscous term.

Based on observations during the tests a significant presence of spray and wave breaking was not apparent. Any presence of either or both of these components would however lead to a reduction in the derived viscous form factors.

Work pertaining specifically to the quantification of the spray and wave breaking components, where present, would form a useful contribution to the full understanding of the resistance breakdown for this vessel type and improve the resistance scaling procedure.

Acknowledgements

The work described in this report covers part of a research project funded by SERC through MTD Ltd. under research grant Ref. Nos. GR/H17992, SHP107/MHV 2.

References

[1] D. Bailey. The NPL high speed round bilge displacement hull series. Maritime Technology Monograph No. 4, Royal Institution of Naval Architects, 1976.

[2] S.F. Hoerner. *Fluid Dynamic Drag.* S.F. Hoerner, 1965.

[3] G. Hughes and J.F. Allan. Turbulence stimulation on ship models. *SNAME*, 59, 1951.

[4] M. Insel. *An Investigation into the Resistance Components of High Speed Displacement Catamarans.* PhD thesis, University of Southampton, 1990.

[5] M. Insel and A.F. Molland. An investigation into the resistance components of high speed displacement catamarans. *Transactions of the Royal Institution of Naval Architects*, 1992.

[6] D.P. Jones. Turbulence stud effect on model resistance. BEng Report No. 39, Department of Ship Science, University of Southampton, 1976.

[7] E. Lahtiharju, T. Karppinen, M. Hellevaara, and T. Aitta. Resistance and seakeeping of fast transom stern hulls with systematically varied form. *SNAME Transactions*, 99:85–118, 1991.

[8] W.J. Marwood and D. Bailey. Design data for high-speed displacement hulls of round-bilge form. Ship Report No. 99, National Physical Laboratory, 1969.

[9] J.H. McCarthy. Collected experimental resistance component and flow data for three surface ship model hulls. DTNSRDC Report 85/011, 1985.

[10] A.F. Molland. A new NC-Controlled three axis model cutting machine. *The Naval Architect*, October 1989.

[11] A.F. Molland, J.F. Wellicome, and P.R. Couser. Theoretical prediction of the wave resistance of slender hull forms in catamaran configurations. Ship Science Report No. 72, Department of Ship Science, University of Southampton, March 1994.

[12] H. Tanaka, K. Nakatake, S. Araki, M. Nakato, and T. Ueda. Cooperative resistance tests with geosim models of a high-speed semi-displacement craft. *Journal of The Society of Naval Architects of Japan*, 169, 1990/91.

[13] H.Y.H Yeh. Series 64 resistance experiments on high-speed displacement forms. *Marine Technology*, July 1965.

Appendix A

A The effect of turbulence studs on model resistance

A.1 Introduction

Trip studs are put near the leading edge of the model to induce a turbulent boundary layer. When analysing the model data account should be taken of the effect of these studs on the model resistance. The approach that follows is based on the work done by Hughes and Allan[3], Jones[6] and Hoerner[2]. There are three main points that must be taken into consideration when calculating the effect of the turbulence studs on model resistance.

- The additional drag on the model due to the studs.
- The increase in momentum thickness of the boundary layer caused by the studs.
- The laminar region in front of the studs.

The following sections deal with the above aspects.

A.2 Boundary Layer Fundamentals

There are basically two boundary layer regimes which are of interest for these calculations:

Laminar Flow The steady part of the boundary layer that follows the contours of the body smoothly. The stream tubes are essentially parallel and do not mix.

Turbulent Flow When the boundary layer becomes irregular and disordered. Random velocity vectors are added to the flow to produce an eddying flow with substantial mixing. Turbulence components are typically 20% of the mean flow velocity.

Equations used to describe the boundary layer in these two regimes are given below; however, several equations apply to both.

The Reynolds number R_{n_x} at a point x from the leading edge is given by:

$$R_{n_x} = \frac{xU_0}{\nu} \tag{6}$$

The average skin friction coefficient over part of the model can be calculated from the momentum thicknesses of the boundary layer at these points:

$$C_{F_{AB}} = \frac{2(\delta_{2_B} - \delta_{2_A})}{\overline{AB}} \tag{7}$$

Thus if A is at the leading edge then the skin friction coefficient is described by the momentum thickness at the point of interest, x:

$$C_{F_x} = \frac{2(\delta_{2_x})}{x} \tag{8}$$

A.3 Laminar Flow

The boundary layer thickness δ at a point x from the leading edge is given by:

$$\delta = \frac{5.5x}{\sqrt{R_{n_x}}} \tag{9}$$

The momentum thickness δ_2 of the boundary layer at a point x from the leading edge is given by:

$$\delta_2 = \frac{0.66x}{\sqrt{R_{n_x}}} \tag{10}$$

The mean friction coefficient C_F, at a point x from the leading edge, is calculated from the momentum thickness:

$$C_F = \frac{2\delta_2}{x} = \frac{1.328}{\sqrt{R_{n_x}}} \tag{11}$$

The velocity profile $u(y)$ within the boundary layer can then be modeled as:

$$u(y) = U_0 \sin\left(\frac{\pi y}{2\delta}\right) \tag{12}$$

A.4 Turbulent Flow

Similar equations can be found for the turbulent region. The boundary layer thickness δ at a point x from the leading edge is given by:

$$\delta = \frac{0.154x}{\sqrt[7]{R_{n_x}}} \tag{13}$$

The momentum thickness δ_2 of the boundary layer at a point x from the leading edge is given by:

$$\delta_2 = \frac{n\delta}{(n+1)(n+2)} \tag{14}$$

where $n \approx 7$

The mean friction coefficient C_F, at a point x from the leading edge, is calculated from the momentum thickness, or the ITTC C_F formula:

$$C_F = \frac{2\delta_2}{x} = \frac{0.075}{(\log R_{n_x} - 2)^2} \tag{15}$$

A.5 Calculation of Stud Drag

The drag on the studs can be calculated as follows:

$$D_{\text{stud}} = \tfrac{1}{2}\,\rho h w n \overline{U}^2 C_D \tag{16}$$

Where h, w, n are the stud height, width and number respectively; C_D is the drag coefficient, typically 0.95 – 1.0 and $\overline{U}$ is the mean velocity over the stud.

The mean velocity over the stud must be calculated since part of the stud will be in the boundary layer and part in the free stream. The mean velocity is calculated by integrating the volume flow past the stud and dividing by the height of the stud:

$$\overline{U} = \frac{\int_0^h u(y)dy}{h} = \frac{1}{h}\int_0^\delta u(y)dy + \frac{U_0}{h}(h-\delta) \tag{17}$$

The velocity profile is substituted from equation 12 and integrated thus:

$$\overline{U} = \frac{U_0}{h}\left[\delta\left(\frac{2}{\pi} - 1\right) + h\right] \tag{18}$$

or substituting for the boundary layer thickness from equation 9 we get:

$$\overline{U} = U_0\left[1 - \frac{1.997}{h}\sqrt{\frac{x\nu}{U_0}}\right] \tag{19}$$

It should be noted that, due to hull shape, the local 'free stream' velocity, in way of the studs will be slightly less than the actual free stream velocity, but this effect has been neglected in the current analysis.

A.6 Effect of Stud on Boundary layer

Figure 1 shows how the model and full scale boundary layers differ. The model boundary layer starts as a laminar boundary layer which is then tripped by the studs. The drag on the studs increases the momentum thickness of the boundary layer at this point. This effectively reduces the C_F value over the turbulent part of the model.

The increase in momentum thickness caused by n studs (total for both sides) of height h, width w and drag coefficient C_D, can be calculated as follows:

$$\text{Average force per unit area on studs} = \tfrac{1}{2}\,\rho\frac{hwn}{2T_{\text{stem}}}C_D\overline{U}^2 = \rho U_0^2 \delta_{2_{\text{stud}}}$$

Where T_{stem} is the draught at the studs. Re-arranging, this becomes:

$$\delta_{2_{\text{stud}}} = \frac{hwnC_D}{4T_{\text{stem}}}\left(\frac{\overline{U}}{U_0}\right)^2 \tag{20}$$

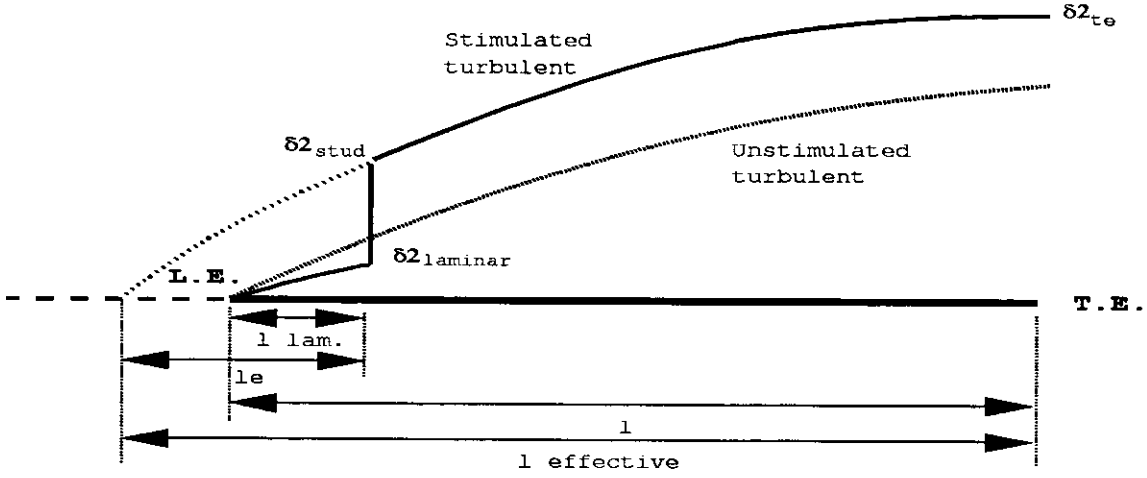

Figure 1: Development of Boundarylayer Momentum Thickness δ_2

This additional momentum thickness should be added to the laminar momentum thickness just before the studs to give the total momentum thickness:

$$\delta_{2_{\text{total at stud}}} = \delta_{2_{\text{stud}}} + \delta_{2_{\text{laminar}}} \tag{21}$$

Where $\delta_{2_{\text{laminar}}}$ is obtained from equation 10 calculated with Reynolds number corresponding to the average distance of the studs from the leading edge, l_{laminar}.

An equivalent model length for the turbulent flow can be calculated; this is the model length that would be required to produce a purely turbulent boundary layer, without stimulation, with this momentum thickness at this point. There are two ways of doing this.

Firstly calculate the turbulent boundary layer thickness corresponding to this momentum thickness from equation 14. This thickness can then be substituted into a re-arranged version of equation 13 to obtain the length from the studs to a fictitious leading edge, l_e, corresponding to an unstimulated fully turbulent boundary layer, as shown below:

$$\delta = \frac{(n+1)(n+2)}{n}\delta_2 \tag{22}$$

(from equation 14)

$$l_{\text{e}} = \sqrt[6]{\frac{\delta^7 U_0}{2.054 \times 10^{-6}\nu}} \tag{23}$$

(from equation 13)

Secondly by assuming a value for x, calculating R_{n_x} and hence ITTC C_F. The corresponding momentum thickness can then be calculated from equation 8 and this procedure iterated until suitable convergence.

Both methods should yield similar results, though the second method has been used for these calculations.

The friction drag on the part of the hull behind the studs (turbulent region) can be calculated by considering the difference in momentum thicknesses at the trailing edge and just behind the studs and substituting in equation 7

The momentum thickness at the trailing edge is calculated from the appropriate ITTC C_F value corresponding to the Reynolds number based on the effective model length $l_{\text{effective}}$ which is given by:

$$l_{\text{effective}} = l - l_{\text{laminar}} + l_{\text{e}} \tag{24}$$

where l is the overall model length and the momentum thickness is given by:

$$\delta_{2_{\text{te}}} = \frac{l_{\text{effective}} C_{F_{\text{effective}}}}{2} \tag{25}$$

The overall skin friction coefficient for the turbulent region, $C_{F_{\text{turbulent}}}$, is then given by:

$$C_{F_{\text{turbulent}}} = \frac{2\left(\delta_{2_{\text{te}}} - \delta_{2_{\text{total at stud}}}\right)}{(l - l_{\text{laminar}})} \tag{26}$$

The drag on this part of the hull, $D_{\text{turbulent}}$, can then be calculated:

$$D_{\text{turbulent}} = \tfrac{1}{2}\,\rho(A - A_{\text{laminar}})\,U_0^2 C_{F_{\text{turbulent}}} \tag{27}$$

In a similar way, the skin friction coefficient, $C_{F_{\text{laminar}}}$, for the laminar region can be calculated:

$$C_{F_{\text{laminar}}} = \frac{2\delta_{2_{\text{laminar}}}}{l_{\text{laminar}}} \tag{28}$$

and hence the drag on this part of the model, D_{laminar} calculated:

$$D_{\text{laminar}} = \tfrac{1}{2}\,\rho(A_{\text{laminar}})\,U_0^2 C_{F_{\text{laminar}}} \tag{29}$$

The skin friction coefficient, $C_{F_{\text{unstimulated turbulent}}}$, for the laminar region can easily be calculated from the ITTC C_F value using a Reynolds number based on the model length; and the skin friction drag, $D_{\text{unstimulated turbulent}}$, calculated for the model.

Hence the correction that must be obtained to the model resistance is:

$$\text{drag correction} = D_{\text{unstimulated turbulent}} - D_{\text{turbulent}} - D_{\text{laminar}} - D_{\text{stud}} \tag{30}$$

Results of these calculations are given in table 1

Table 1: Stud correction for model 6b at two speeds

U_0 [m/s]	R_{measured} [N]	D_{stud} [N]	$D_{\text{turbulent}}$ [N]	D_{laminar} [N]	$D_{\text{unstimulated turb.}}$ [N]	Correction [N]	Correction [%]
2.0	3.5	0.140	1.642	0.047	1.767	-0.062	1.8
4.0	8.9	0.610	5.713	0.134	6.199	-0.260	2.9

A.7 Summary

The investigation has indicated the various effects on drag due to the turbulence studs.

The correction for model 6b was seen to amount to about 2% to 3% of the measured resistance. This model is one of the most affected by the stud correction and the effect on the other models was less.

A stud drag correction was applied to all the measured resistance data along the lines of the method described above.

Appendix B

B The use of static or running wetted surface area

B.1 Introduction

Since this project is built on previous work carried out at the University of Southampton a similar analysis and presentation was used for the work. However in response to queries raised by the original work[5] it was decided to investigate the running wetted surface areas of these models.

B.2 Photographic estimate

An estimate of the running wetted surface area was made from photographs of the wave profile along the outside of the hull. Due to the lack of a suitable camera mount the wave profile along the inside of the tunnel could not be recorded photographically but a visual estimate was made and at larger hull spacings the two wave profiles were similar. Estimates of running wetted surface areas were made from the photographs and were found to follow published data[8].

Some regression analysis was performed on the data and it was found that the data could be accurately modeled by:

$$\left[\frac{WSA_{\text{Run}}}{WSA_{\text{Stat}}}\right]\% = A.Fn^2 + 100 \tag{31}$$

where the constant A is determined from the L/B ratio of the model.

B.3 Analysis using running wetted surface area

The effect of re-analysing the resistance data with the running wetted surface area was to reduce the $C_T - C_W$ by the same proportion. This reduced the form factor.

Note:

$$C_T = \frac{R_T}{C}; C_W = \frac{R_W}{C}; \Rightarrow C_T - C_W = \frac{R_T - R_W}{C} \tag{32}$$

where:

$$C = \tfrac{1}{2}\,\rho A v^2 \tag{33}$$

if the new wetted surface area is increased by a factor α then:

$$C_{T_\alpha} = \frac{R_T}{\alpha C}; C_{W_\alpha} = \frac{R_W}{\alpha C} \tag{34}$$

therefore:

$$C_{T_\alpha} - C_{W_\alpha} = \frac{R_T - R_W}{\alpha C} \tag{35}$$

$$C_{T_\alpha} - C_{W_\alpha} = \frac{1}{\alpha}(C_T - C_W) \tag{36}$$

$$(1+k) = \frac{C_T - C_W}{C_F} \tag{37}$$

$$(1+k)_\alpha = \frac{C_{T_\alpha} - C_{W_\alpha}}{C_F} \tag{38}$$

$$(1+k)_\alpha = \frac{1}{\alpha}(1+k) \tag{39}$$

This re-analysis reduced the form factors by around 5%

B.4 Effect of re-analysis on full scale extrapolation

An analysis of the effect of using the running wetted surface area as compared with the static wetted surface area for the calculation of full scale resistance estimates was made.

It can be shown that, in general, using consistently either static or running wetted surface area, makes very little difference to the full scale resistance estimates. The small changes arise from the fact that the form factor is 'averaged' over the speed range.

Effect of wetted surface area on full scale resistance estimates:

$$R_{T_{\text{Ship}}} = \tfrac{1}{2}\,\rho A_{\text{Ship}} v^2_{\text{Ship}} C_{T_{\text{Ship}}} \tag{40}$$

where:

$$C_{T_{\text{Ship}}} = (1+k)C_{F_{\text{Ship}}} + C_W \tag{41}$$

thus:

$$R_{T_{\text{Ship}}} = \tfrac{1}{2}\,\rho A_{\text{Ship}} v^2_{\text{Ship}} \left[(1+k)C_{F_{\text{Ship}}} + C_W\right] \tag{42}$$

now

$$(1+k) \approx \frac{C_{T_{\text{Model}}} - C_W}{C_{F_{\text{Model}}}} \tag{43}$$

approximately because it is the result of a fitted line which approximates the above expression over the speed range. or:

$$(1+k) \approx \frac{R_{T_{\text{Model}}} - R_{W_{\text{Model}}}}{\frac{1}{2}\,\rho A_{\text{Model}} v^2_{\text{Model}}} \cdot \frac{1}{C_{F_{\text{Model}}}} \tag{44}$$

Thus if the actual wetted surface area is greater than the static wetted surface area by a factor α then this will lead to a reduction of form factor by the same amount. substituting gives:

$$R_{T_{\text{Ship}}} = \frac{\frac{1}{2}\,\rho A_{\text{Ship}} v^2_{\text{Ship}}}{\frac{1}{2}\,\rho A_{\text{Model}} v^2_{\text{Model}}} \left[\left(R_{T_{\text{Model}}} - R_{W_{\text{Model}}}\right)\frac{C_{F_{\text{Ship}}}}{C_{F_{\text{Model}}}} + R_{W_{\text{Model}}}\right] \tag{45}$$

now γ = scale factor $= \dfrac{L_{\text{Ship}}}{L_{\text{Model}}} = \sqrt{\dfrac{A_{\text{Ship}}}{A_{\text{Model}}}} = \left(\dfrac{v_{\text{Ship}}}{v_{\text{Model}}}\right)^2$ thus:

$$R_{T_{\text{Ship}}} = \gamma^3 \left[\left(R_{T_{\text{Model}}} - R_{W_{\text{Model}}}\right)\frac{C_{F_{\text{Ship}}}}{C_{F_{\text{Model}}}} + R_{W_{\text{Model}}}\right] \tag{46}$$

Thus it can be seen that so long as consistent areas, related by the scale factor γ^2, are used, then scaled resistance is independent of the wetted surface area used.

Note from equation 42, and substituting for C_W from equation 43:

$$R_{T_{\text{Ship}}} = \tfrac{1}{2}\,\rho A_{\text{Ship}} v^2_{\text{Ship}} \left[C_{T_{\text{Model}}} - \underbrace{(1+k)\left(C_{F_{\text{Model}}} - C_{F_{\text{Ship}}}\right)}_{\text{+ve since } C_{F_{\text{Model}}} > C_{F_{\text{Ship}}}}\right] \tag{47}$$

Thus as (1+k) decreases, as for the case where it has been calculated from running wetted surface areas, so the full scale resistance estimate will increase

$$(1+k) \rightarrow \frac{1+k}{\alpha} \text{ if } WSA \rightarrow \alpha \cdot WSA \tag{48}$$

B.5 Calculation of Running Wetted Surface Area for Catamarans

There are several difficulties associated with calculating the running wetted surface area of the catamarans:

- Difficulty in photographing the wave profile along the inside of the hull
- Obstruction of view from cross-members etc.
- The camera cannot be mounted perpendicular to the hull.
- The constructive interference of the two bow wave systems causes a large amplitude wave along the centre line of the model. This obscures the view of the wave profile along the hull.
- and most importantly, readings of wave height from the photos cannot be more accurate than plus or minus 2–5 mm.

Table 2: Running wetted surface areas for catamarans, Model 5b, Fn≈1.0

S/L	% of Monohull RWSA	% of Static WSA
0.2	100.9	120.3
0.3	not available	not available
0.4	100.3	119.6
0.5	100.0	119.2

Table 3: Length of hull (from aft end) affected by bow-wave from other demi-hull

S/L	Length [%]	
	Model 4c	Model 6a
0.2	62	54
0.3	35	27
0.4	7	0
0.5	0	0

Taking these factors into consideration, it is estimated that the running wetted surface areas cannot be calculated to an accuracy of greater than 5% by this method. However it is possible to use the photographic evidence to give some idea of the trends that occur. As has been previously mentioned the percentage increase of running over static wetted surface area can be modeled by a parabola. An investigation of the increase in wetted surface area for the catamaran case as compared with the monohull has been made. An analysis of wetted surface areas measured for model 5b, at a Froude number of approximately 1.0, showed that at an S/L ratio of 0.2 the catamaran running wetted surface area was approximately 1% greater than the monohull and at S/L = 0.4 the increase was down to less than 0.5% (see Table 2). These are very much less than the order of accuracy for this method. It is suggested that if running wetted surface areas are to be used then the catamaran wetted surface area can, for simplicity, be taken as twice the monohull running wetted surface area.

It can be seen (Table 3) that for S/L greater than 0.3, the wetted length of a demihull that is affected by the bow-waves produced by the other demihull is relatively small and this effect is only *one* side of the hull. The Kelvin wave pattern produces a wave envelope approximately 20° to the direction of travel. In the case of 4c, S/L=0.2; approximately the aft 1m of the hull will be impinged upon by this wave. However, in most cases far less of the hull will be affected. If this interaction causes an average increase in draught of 5mm over this 1m length of hull this will lead to approximately 5% increase in running wetted surface area over the monohull case (see Table 4). However this is compensated by the increase in dynamic lift (4mm for model 5b S/L=0.2 compared with monohull) for the catamaran, reducing the wetted surface area. It seems that both effects tend to cancel each other and with the data available it is very difficult to say which effect would dominate.

Table 4: Wavelength of waves traveling at various Froude numbers

Fn	λ [m]	$\frac{\lambda}{4}$ [m]
0.50	2.5	0.6
0.75	5.7	1.4
1.00	10.1	2.5

The wavelength and speed of a deep-water gravity wave are connected by the expression:

$$\lambda = 2\pi Fn^2 l \tag{49}$$

Note: $\frac{\lambda}{4}$ gives the length over which the free-surface is raised by the wave.

B.5.1 Implications of Catamaran Running Wetted Surface Area Changes

It has been shown that an increase in the wetted surface area used to non-dimensionalise the resistance data leads to a decrease in the form factors calculated. Also it has been noted that the running wetted surface areas for the catamarans tends (if at all) to increase as the models are brought together. Using these running wetted surface areas tend to reverse the expected trend of the viscous interference factors β. It is expected that β will be greatest for the closer spacings, and tend to unity as the separation approaches infinity. However, using form factors which have been reduced by approximately the same amounts to calculate β will increase the value of β obtained. Thus the re-analysis with running wetted surface areas will increase the values for viscous interference factors.

B.6 Summary

There are two main points of view from which this work can be regarded:

1. to provide a greater understanding of the physics of the problem and to develop a model which will simulate the physical properties of the flow.

2. to provide an easy to use design tool

The priority must be to understand, as much as possible, the physical nature of the problem. Once this has been achieved it will then be possible to develop a reliable, user-friendly design tool. In this work it is probably more correct to use the running wetted surface areas in calculating the resistance coefficients, form factors, and interference factors. It has however been shown that, if the wave drag is known, then the scaling to full scale resistance estimates is independent of the wetted surface area used (providing it is used consistently).

A thorough investigation into the implications of using running as opposed to static wetted surface areas has been made and the overall effects are relatively small:

- 'form factors' ($(1+k)$ or $(1+\beta k)$) can be reduced by around 3%–5%
- Overall, the viscous interference factors β would increase compared with the static wetted surface area analysis.
- There is possibly a slight increase in the running wetted surface area for catamarans as compared with monohulls. However this is limited to the closest spaced hulls, and is in any case very small.
- The above effect would tend to reduce the viscous interference factor β for the closer spacings, as compared with the other spacings. This is perhaps not as expected.
- The 'form factors', themselves, are not greatly affected; however it is known from experience that these small changes (especially in the monohull form factor) can have quite a large influence on the viscous interference factors β.

On the whole, it appears that the effects of using running compared with static wetted surface areas are small. Due to the problems associated with obtaining accurate estimates of wetted surface area and the lack of this information at the preliminary design stage it is suggested that the analysis be carried out using static wetted surface areas.

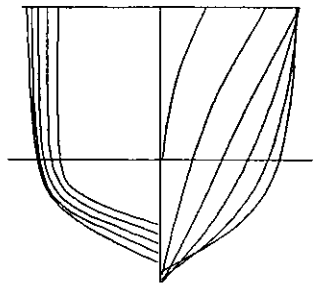

Model: 3b

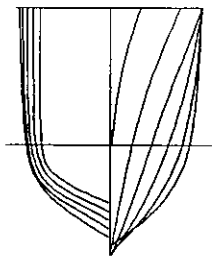

Model: 4a

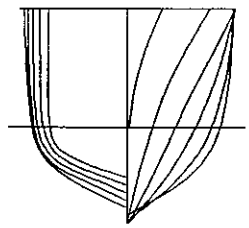

Model: 4b

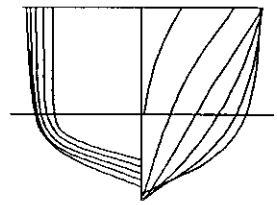

Model: 4c

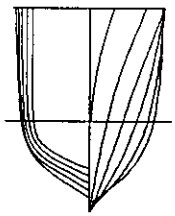

Model: 5a

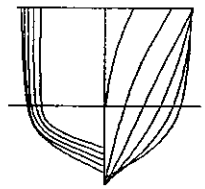

Model: 5b

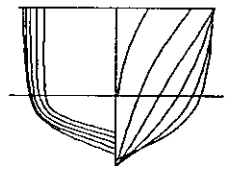

Model: 5c

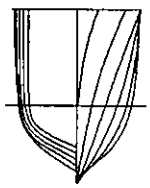

Model: 6a

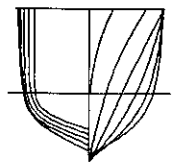

Model: 6b

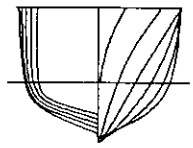

Model: 6c

Figure 1: Model Body Plans and Notation

TABLE I: Notation and Main Parameters of Models

$L/\nabla^{\frac{1}{3}}$	B/T			C_P
	1.5	2.0	2.5	
6.3	—	3b*	—	0.693
7.4	4a	4b*	4c	0.693
8.5	5a	5b*	5c	0.693
9.5	6a	6b	6c	0.693

* Tested by Insel[4, 5]

TABLE II: Details of the Models

Model	L[m]	L/B	B/T	$L/\nabla^{\frac{1}{3}}$	C_B	C_P	C_M	A[m^2]	LCB [% ⊠]
3b	1.6	7.0	2.0	6.27	0.397	0.693	0.565	0.434	-6.4
4a	1.6	10.4	1.5	7.40	0.397	0.693	0.565	0.348	-6.4
4b	1.6	9.0	2.0	7.41	0.397	0.693	0.565	0.338	-6.4
4c	1.6	8.0	2.5	7.39	0.397	0.693	0.565	0.340	-6.4
5a	1.6	12.8	1.5	8.51	0.397	0.693	0.565	0.282	-6.4
5b	1.6	11.0	2.0	8.50	0.397	0.693	0.565	0.276	-6.4
5c	1.6	9.9	2.5	8.49	0.397	0.693	0.565	0.277	-6.4
6a	1.6	15.1	1.5	9.50	0.397	0.693	0.565	0.240	-6.4
6b	1.6	13.1	2.0	9.50	0.397	0.693	0.565	0.233	-6.4
6c	1.6	11.7	2.5	9.50	0.397	0.693	0.565	0.234	-6.4

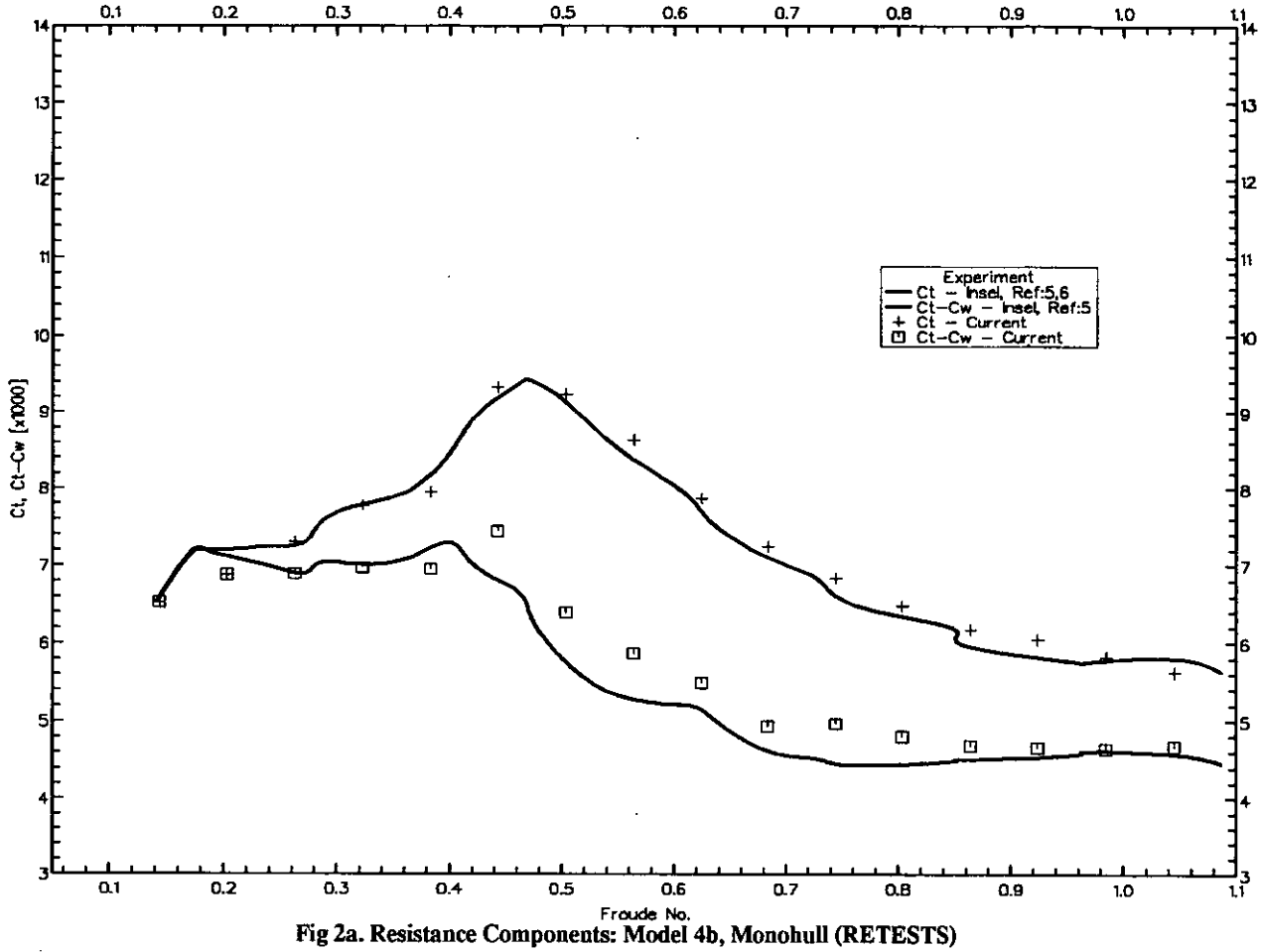

Fig 2a. Resistance Components: Model 4b, Monohull (RETESTS)

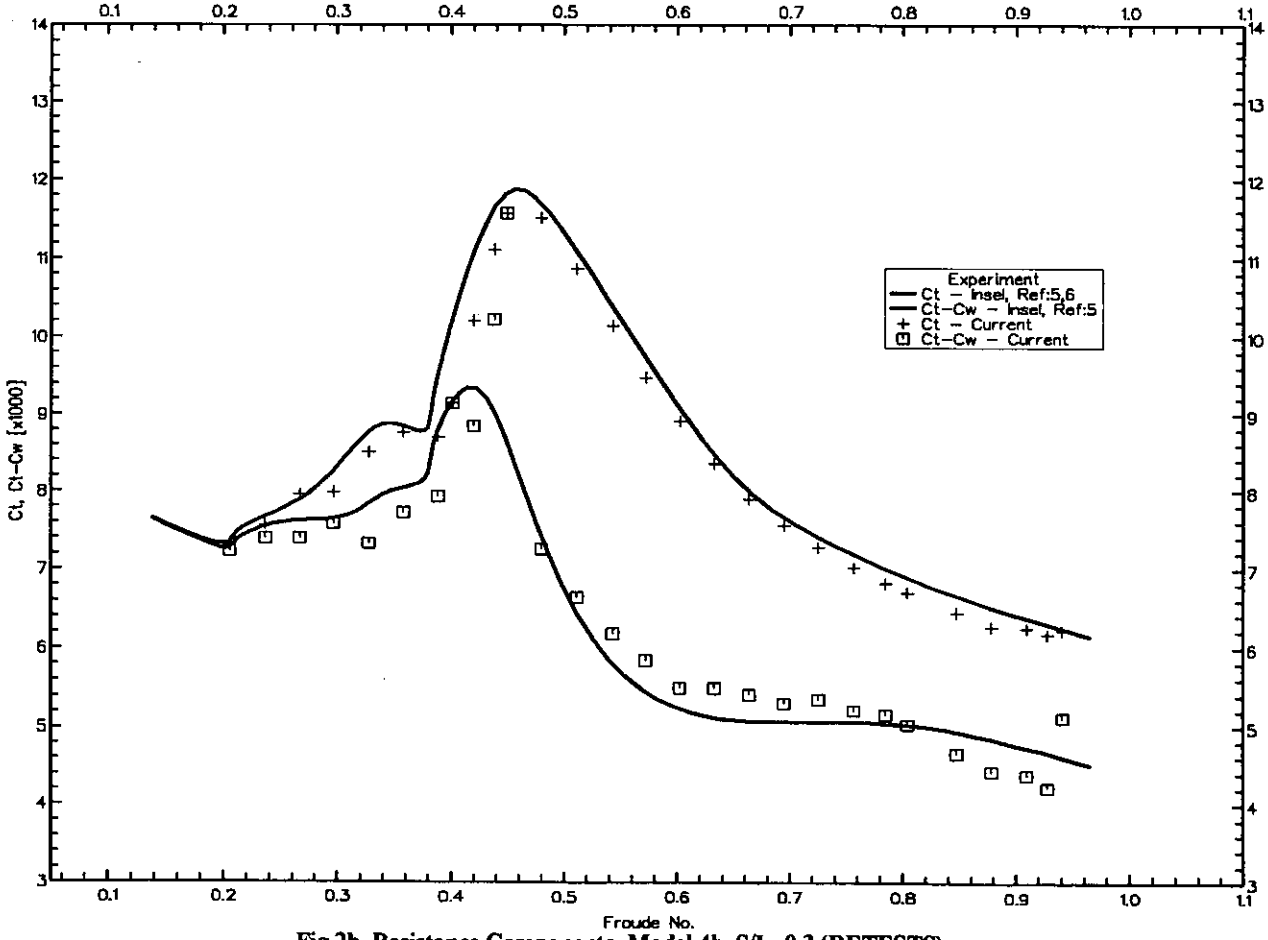

Fig 2b. Resistance Components: Model 4b, S/L=0.3 (RETESTS)

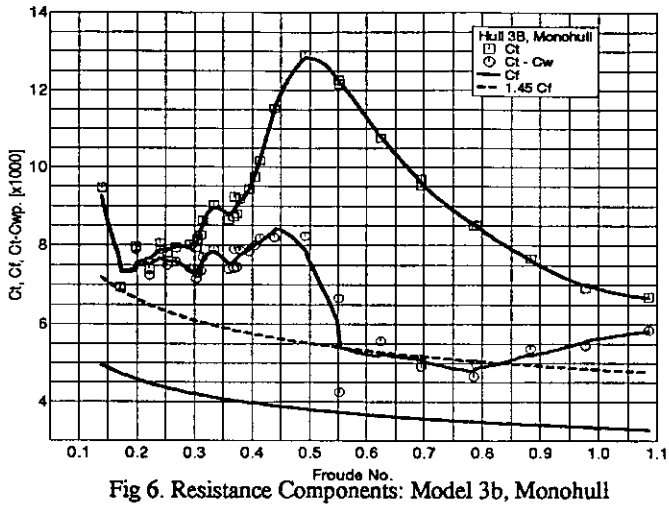

Fig 6. Resistance Components: Model 3b, Monohull

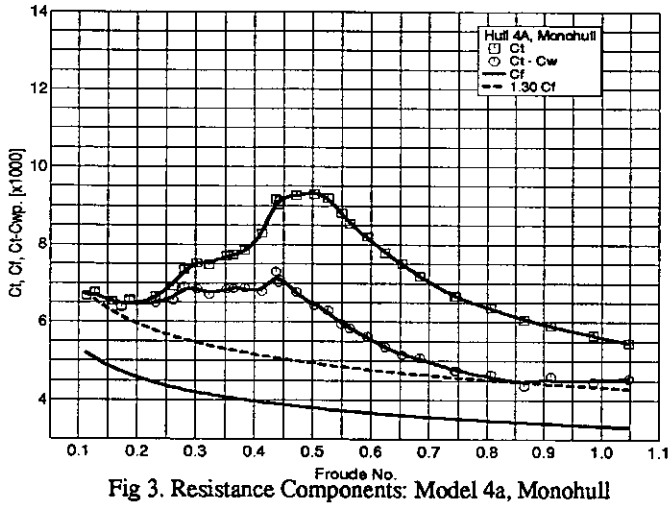

Fig 3. Resistance Components: Model 4a, Monohull

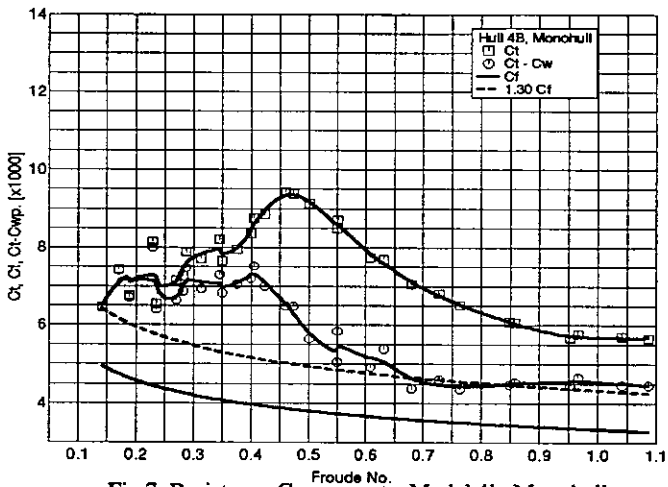

Fig 7. Resistance Components: Model 4b, Monohull

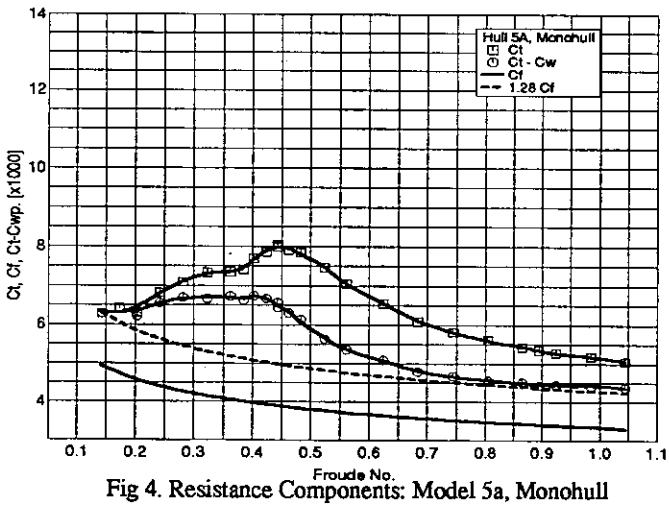

Fig 4. Resistance Components: Model 5a, Monohull

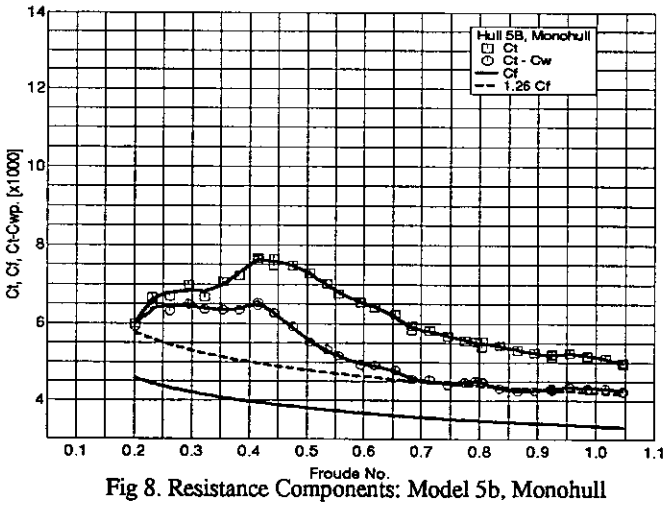

Fig 8. Resistance Components: Model 5b, Monohull

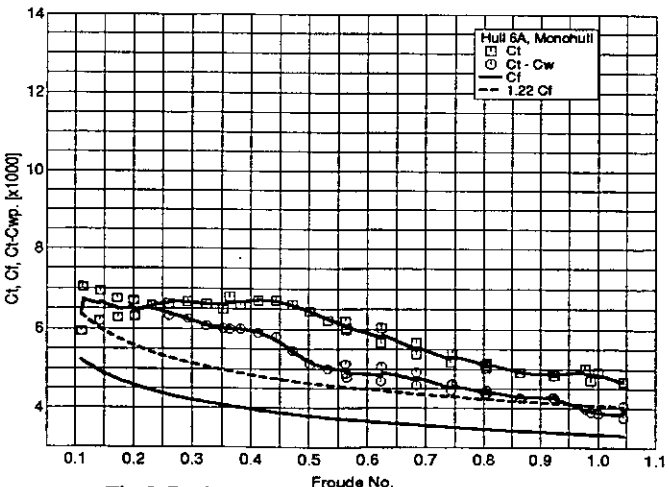

Fig 5. Resistance Components: Model 6a, Monohull

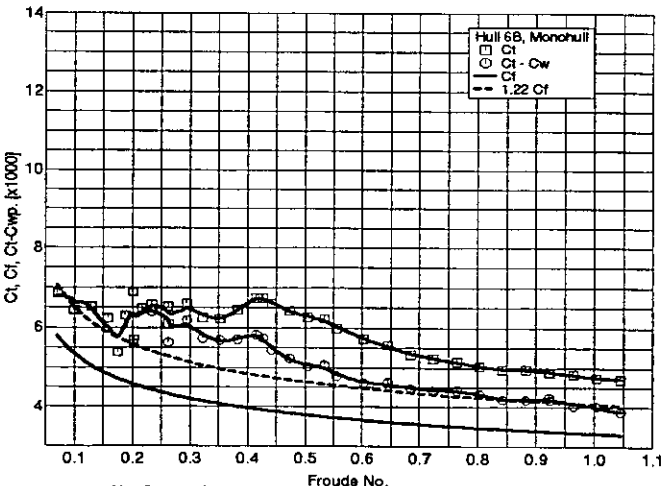

Fig 9. Resistance Components: Model 6b, Monohull

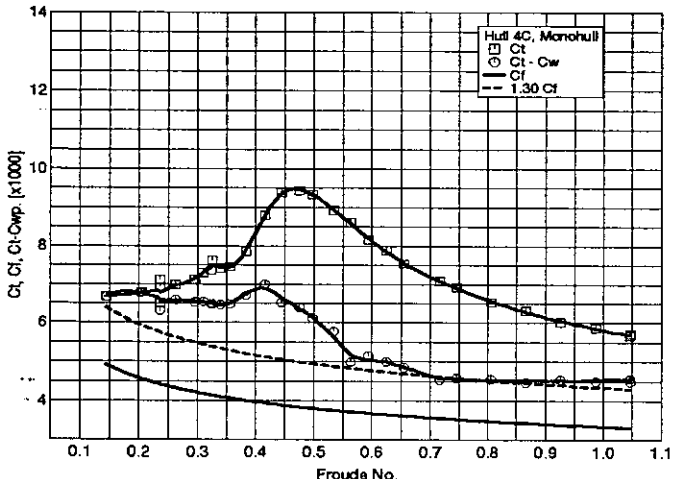

Fig 10. Resistance Components: Model 4c, Monohull

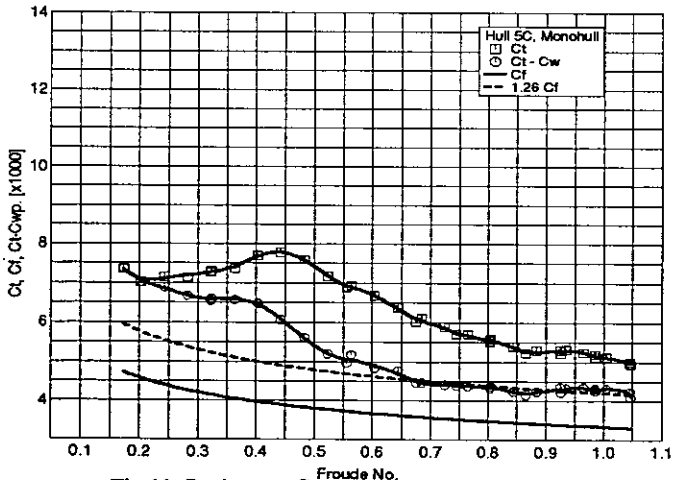

Fig 11. Resistance Components: Model 5c, Monohull

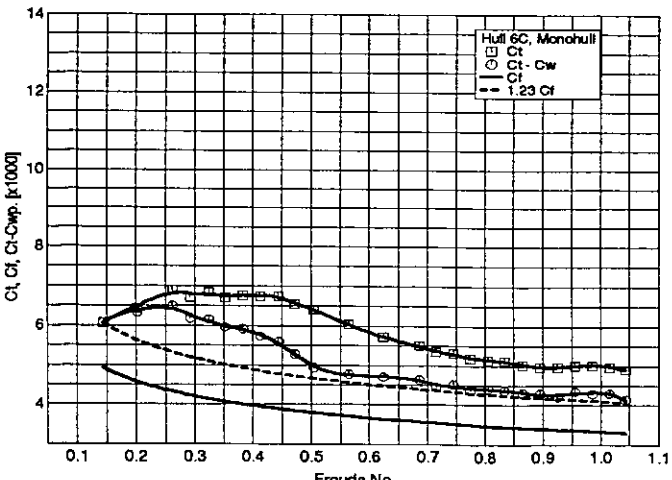

Fig 12. Resistance Components: Model 6c, Monohull

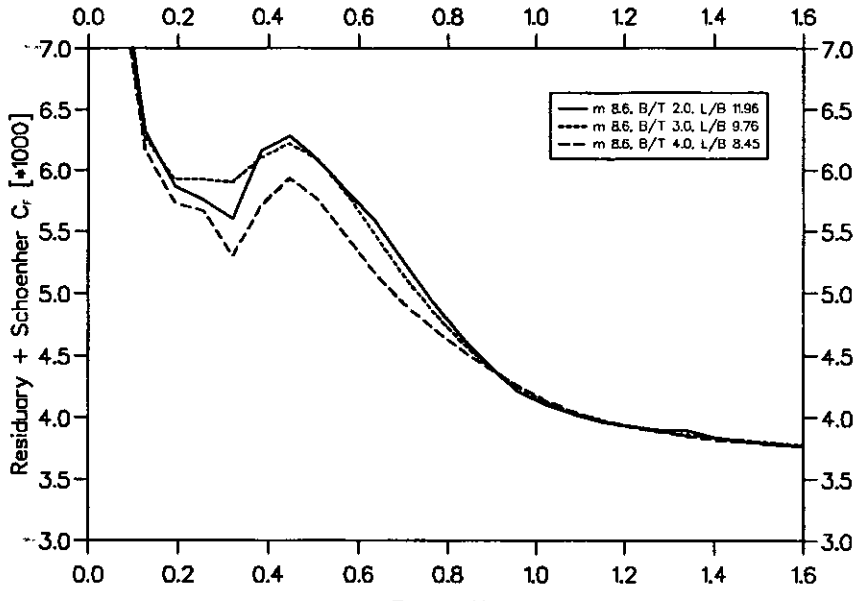

Fig 13a. Series 64: Models 862, 863 and 864

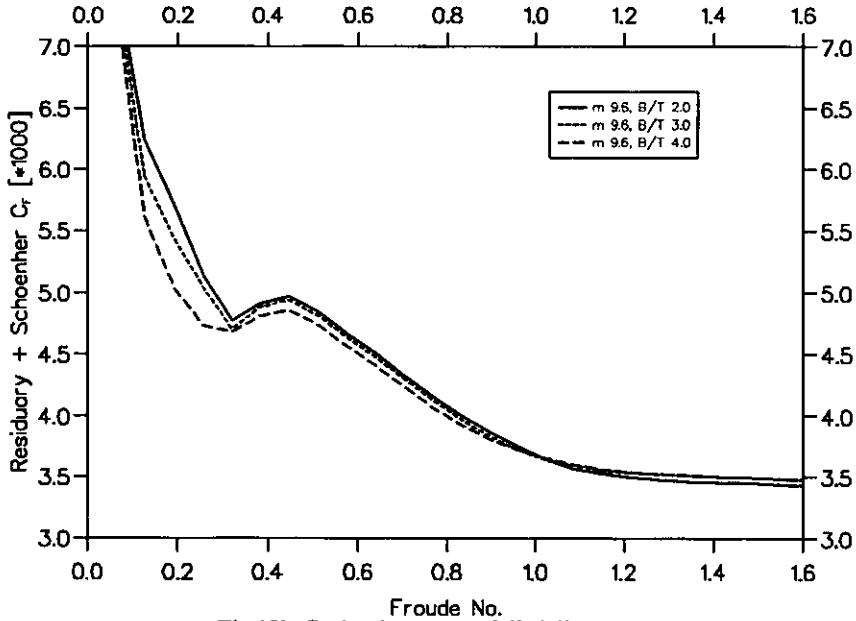

Fig 13b. Series 64: Models 962, 963 and 964

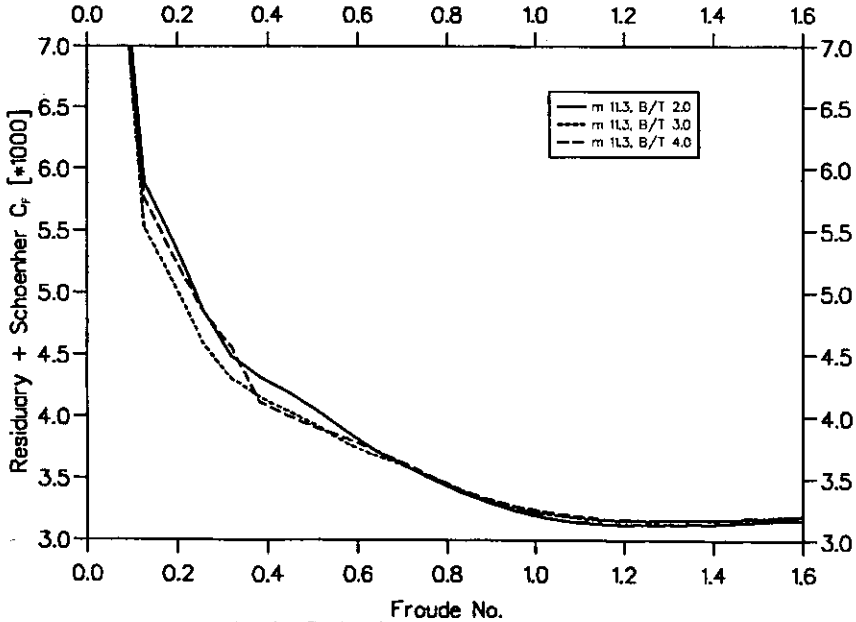

Fig 13c. Series 64: Models 112, 113 and 114

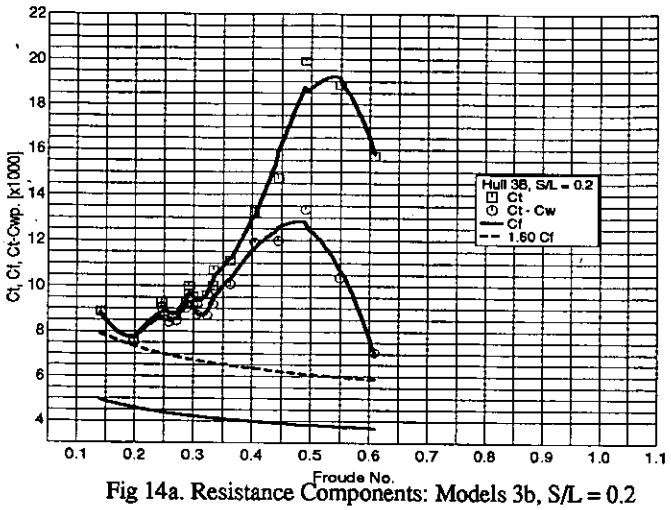

Fig 14a. Resistance Components: Models 3b, S/L = 0.2

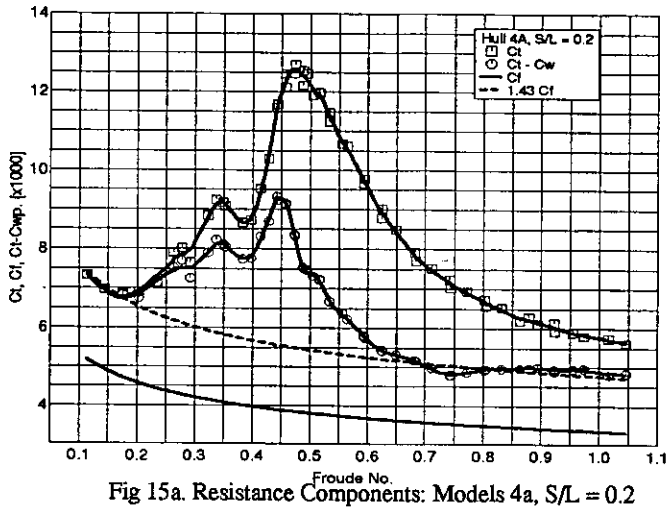

Fig 15a. Resistance Components: Models 4a, S/L = 0.2

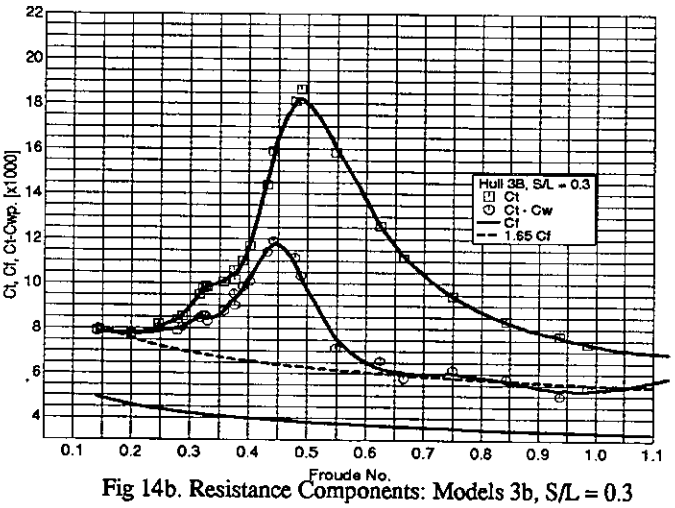

Fig 14b. Resistance Components: Models 3b, S/L = 0.3

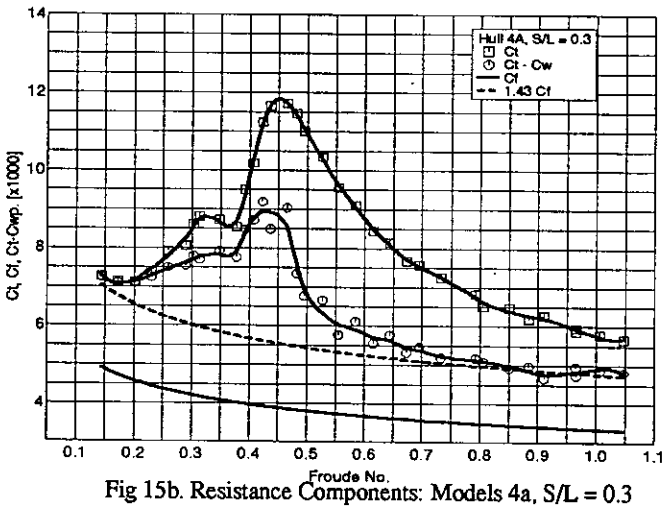

Fig 15b. Resistance Components: Models 4a, S/L = 0.3

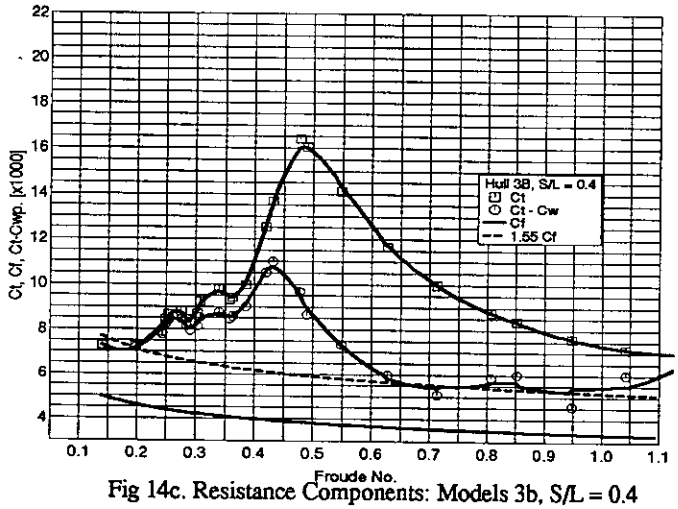

Fig 14c. Resistance Components: Models 3b, S/L = 0.4

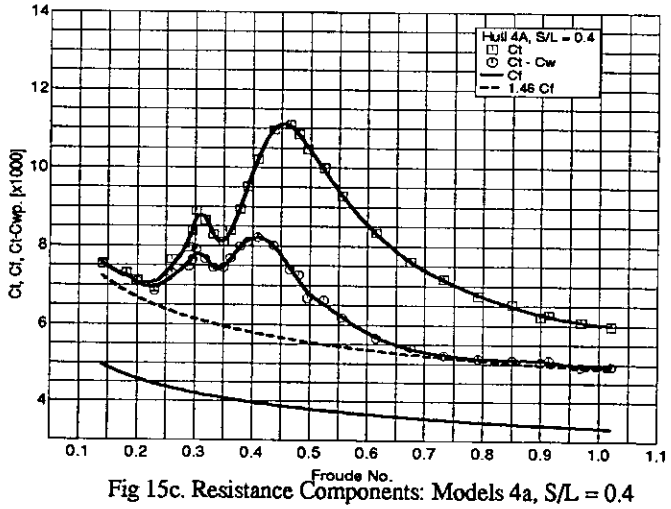

Fig 15c. Resistance Components: Models 4a, S/L = 0.4

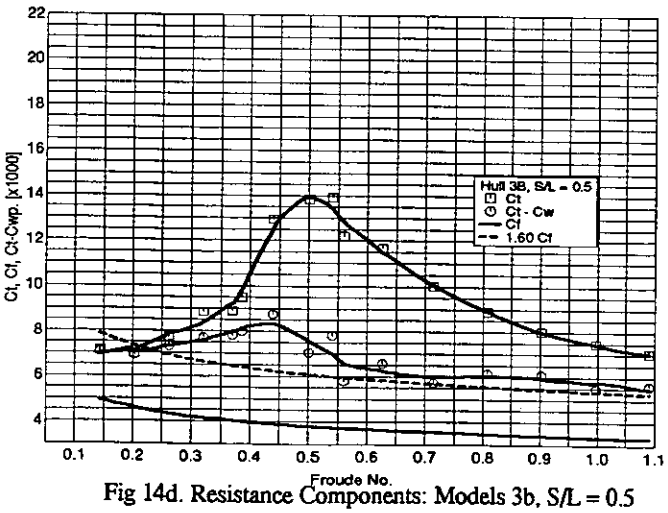

Fig 14d. Resistance Components: Models 3b, S/L = 0.5

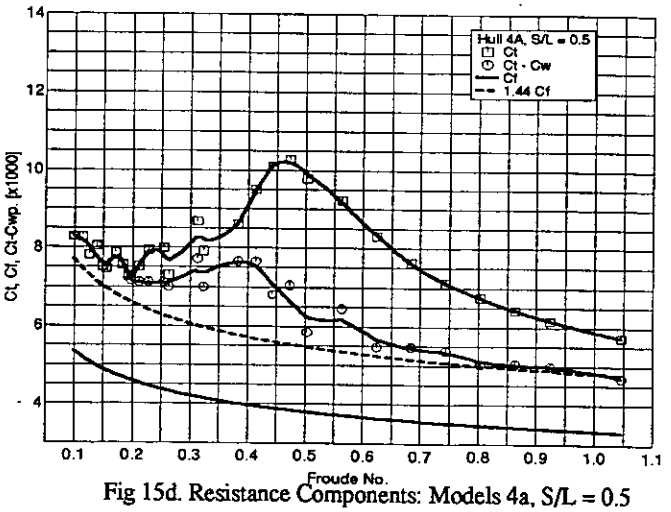

Fig 15d. Resistance Components: Models 4a, S/L = 0.5

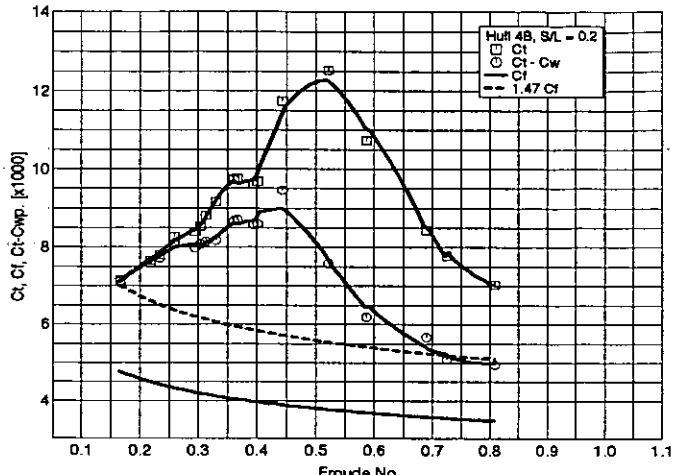

Fig 16a. Resistance Components: Models 4b, S/L = 0.2

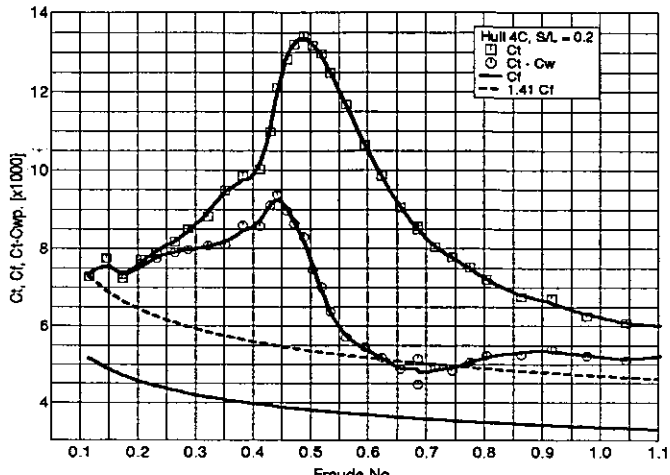

Fig 17a. Resistance Components: Models 4c, S/L = 0.2

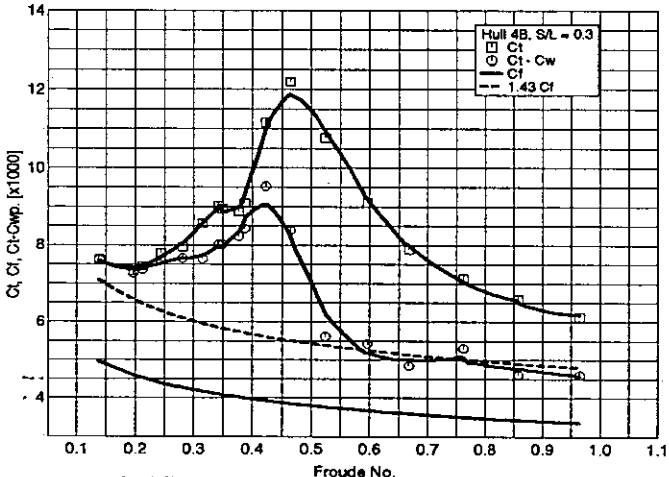

Fig 16b. Resistance Components: Models 4b, S/L = 0.3

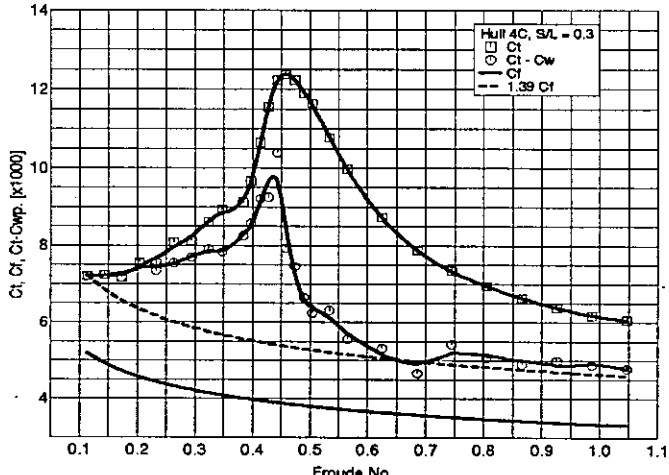

Fig 17b. Resistance Components: Models 4c, S/L = 0.3

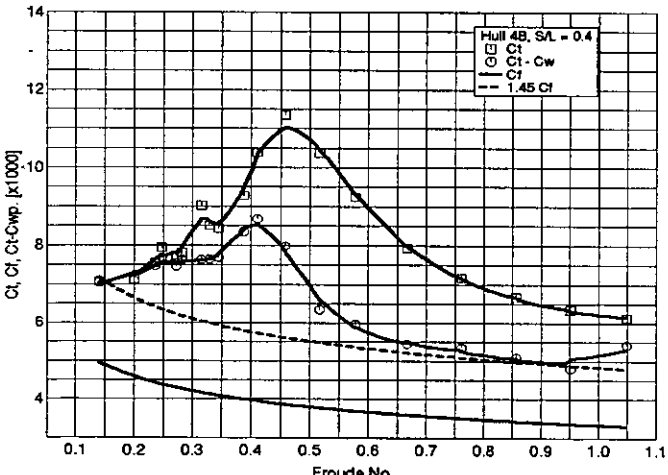

Fig 16c. Resistance Components: Models 4b, S/L = 0.4

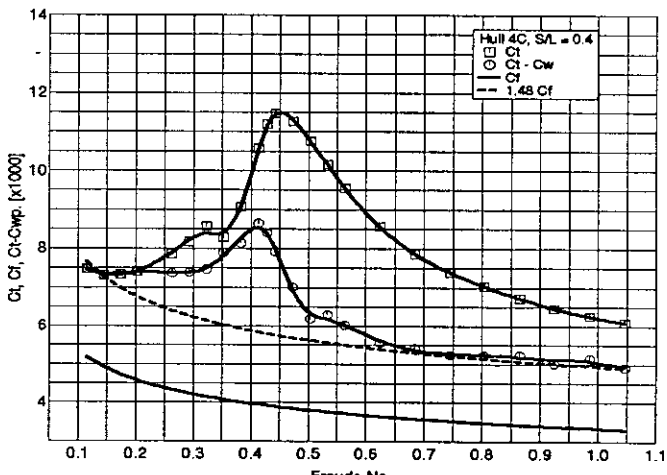

Fig 17c. Resistance Components: Models 4c, S/L = 0.4

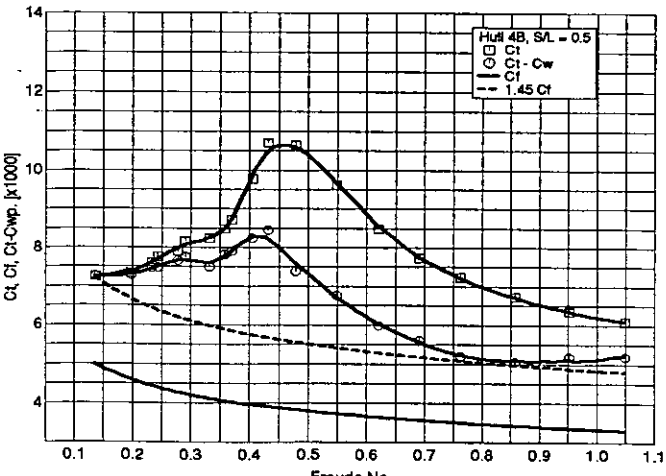

Fig 16d. Resistance Components: Models 4b, S/L = 0.5

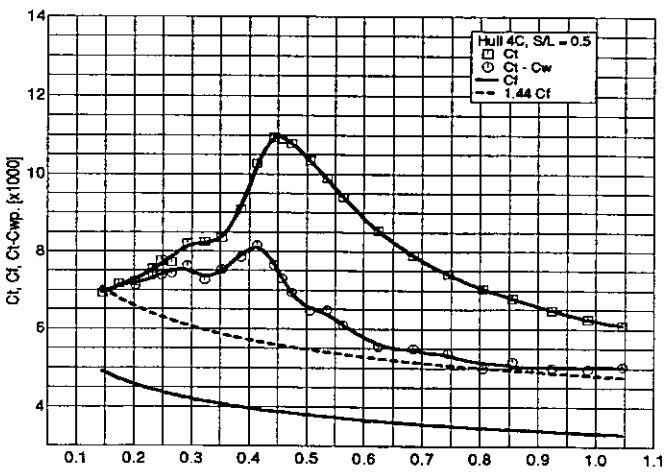

Fig 17d. Resistance Components: Models 4c, S/L = 0.5

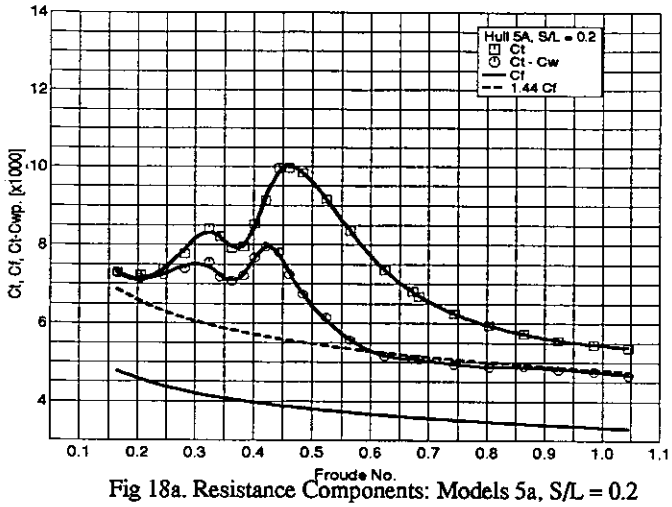

Fig 18a. Resistance Components: Models 5a, S/L = 0.2

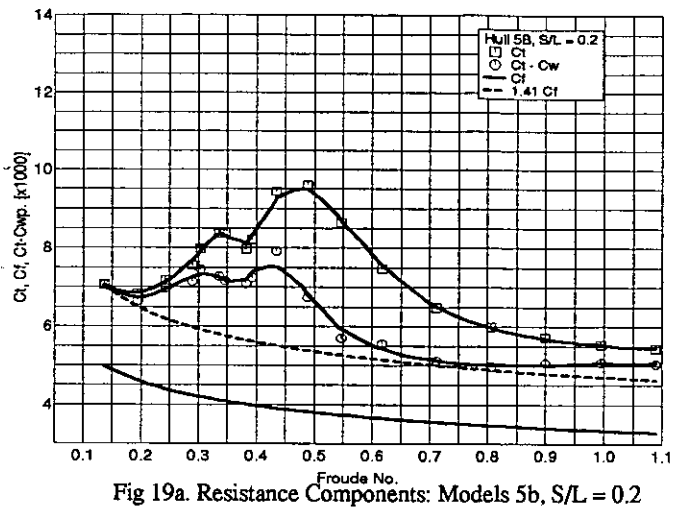

Fig 19a. Resistance Components: Models 5b, S/L = 0.2

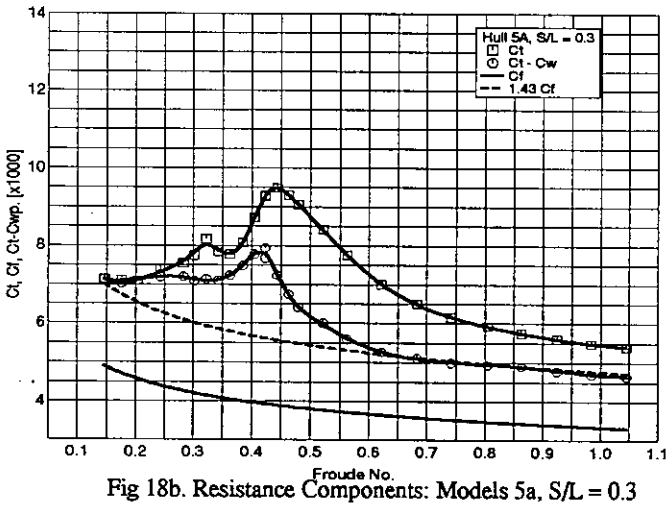

Fig 18b. Resistance Components: Models 5a, S/L = 0.3

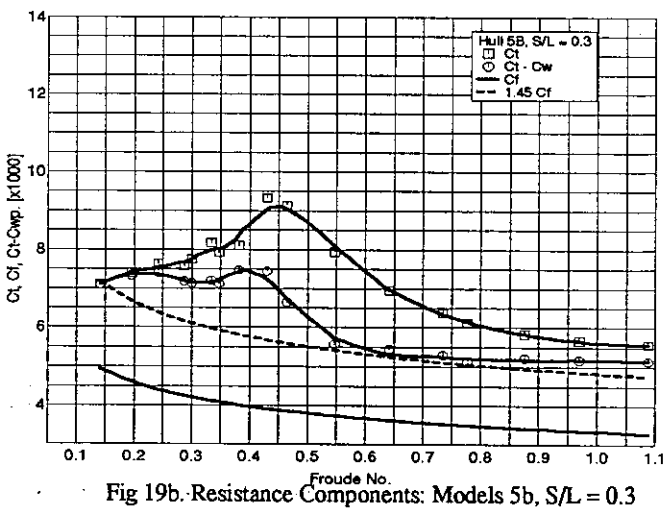

Fig 19b. Resistance Components: Models 5b, S/L = 0.3

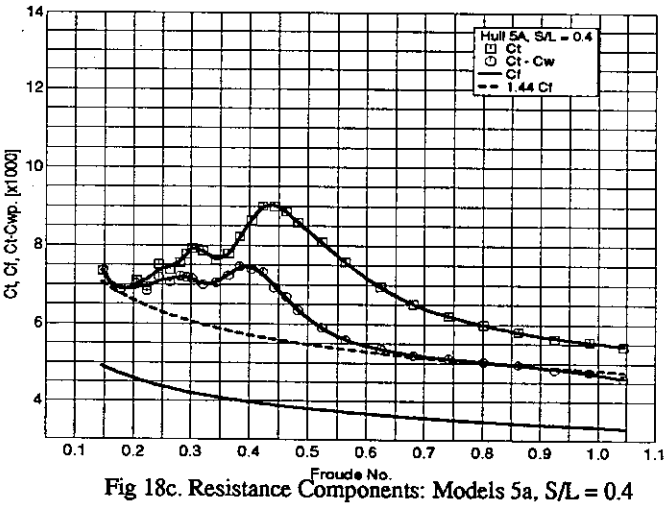

Fig 18c. Resistance Components: Models 5a, S/L = 0.4

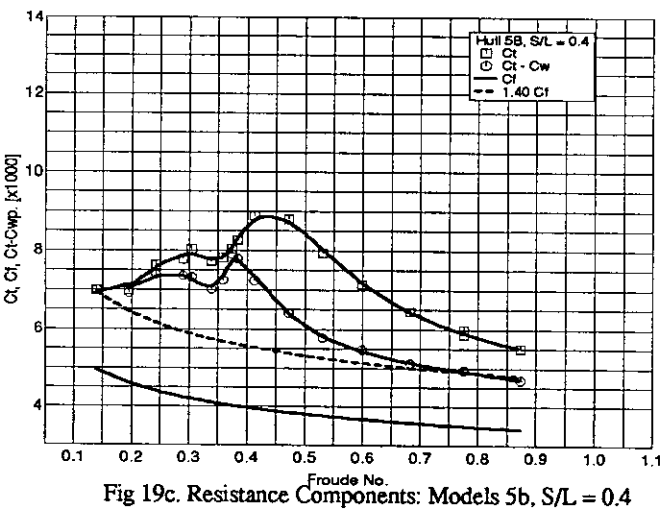

Fig 19c. Resistance Components: Models 5b, S/L = 0.4

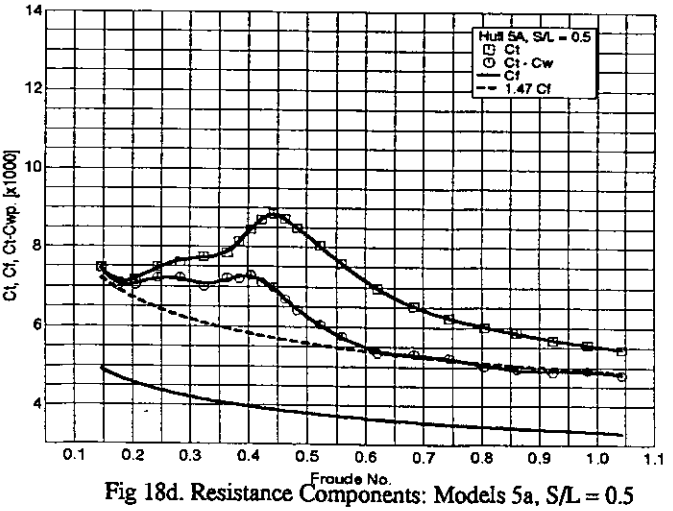

Fig 18d. Resistance Components: Models 5a, S/L = 0.5

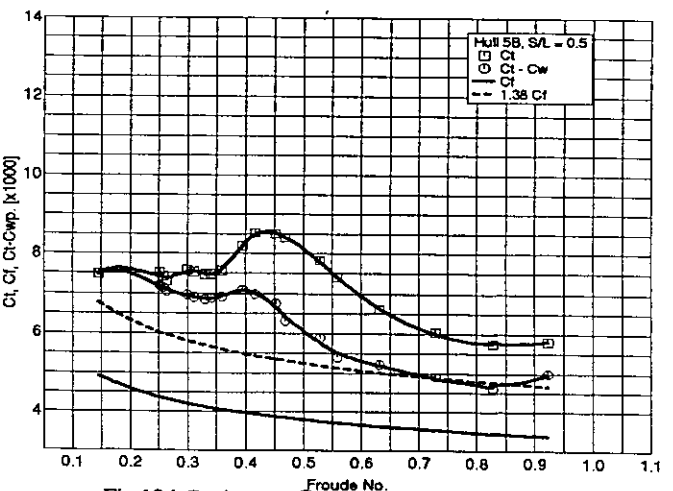

Fig 19d. Resistance Components: Models 5b, S/L = 0.5

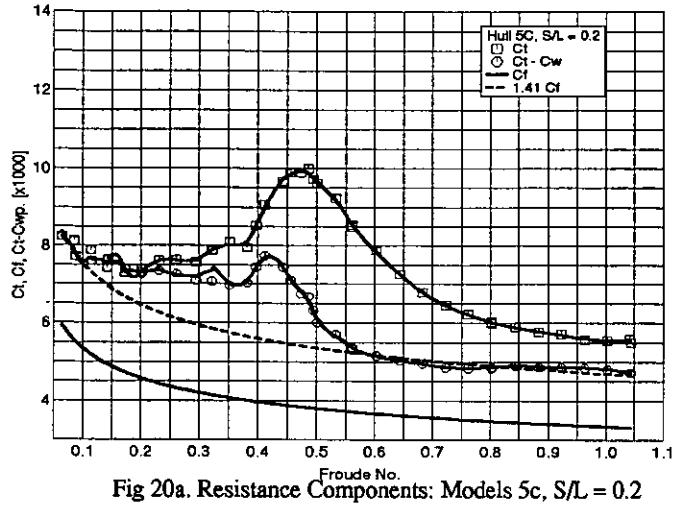

Fig 20a. Resistance Components: Models 5c, S/L = 0.2

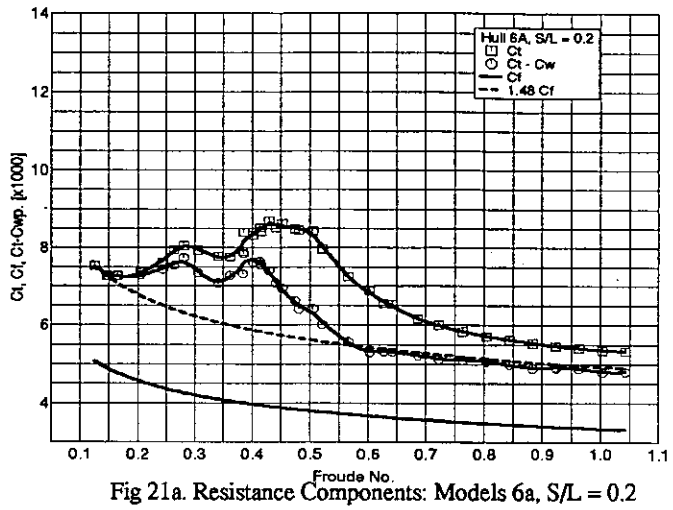

Fig 21a. Resistance Components: Models 6a, S/L = 0.2

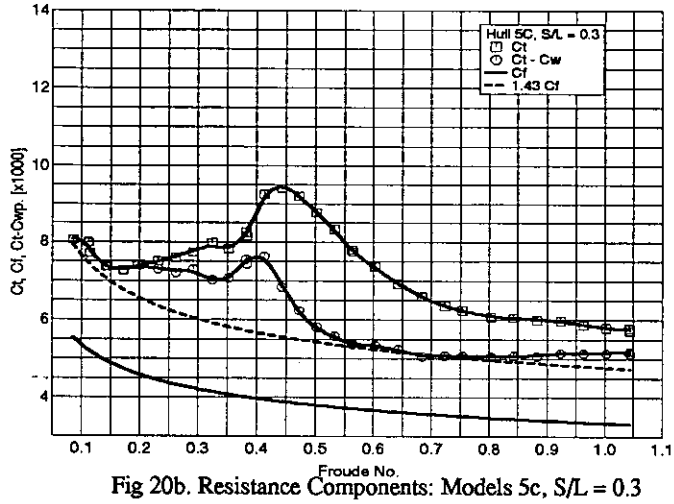

Fig 20b. Resistance Components: Models 5c, S/L = 0.3

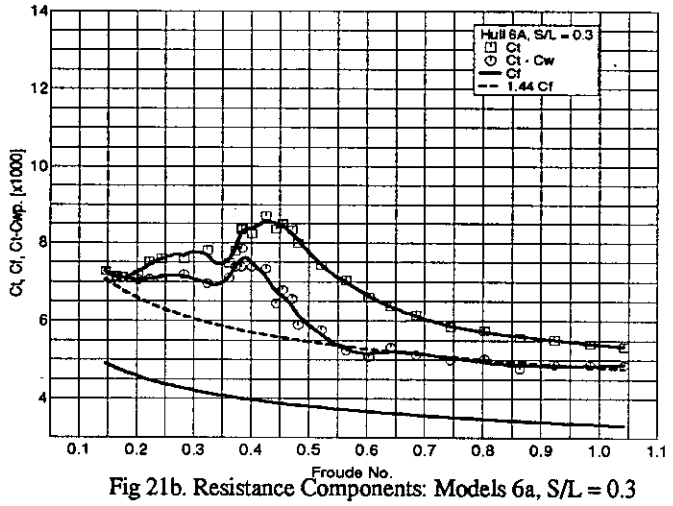

Fig 21b. Resistance Components: Models 6a, S/L = 0.3

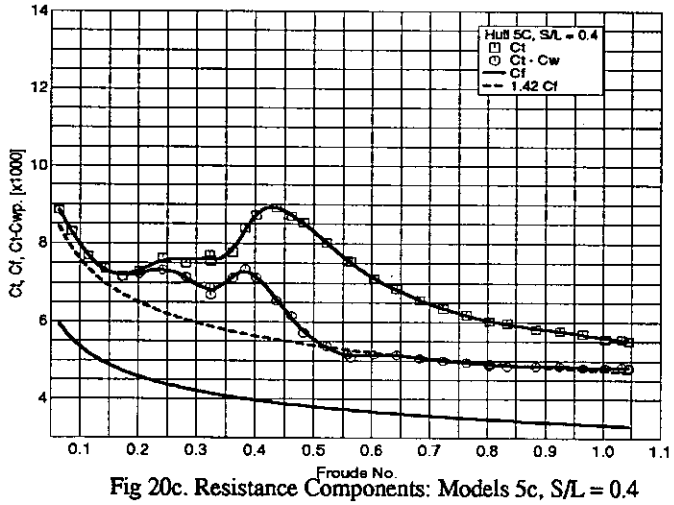

Fig 20c. Resistance Components: Models 5c, S/L = 0.4

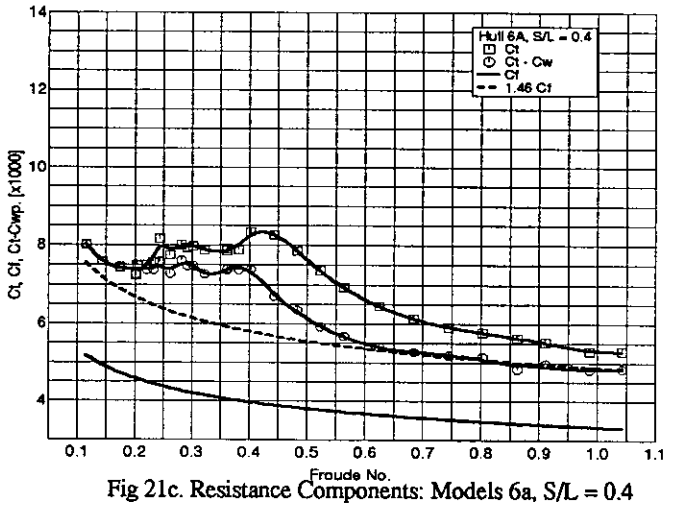

Fig 21c. Resistance Components: Models 6a, S/L = 0.4

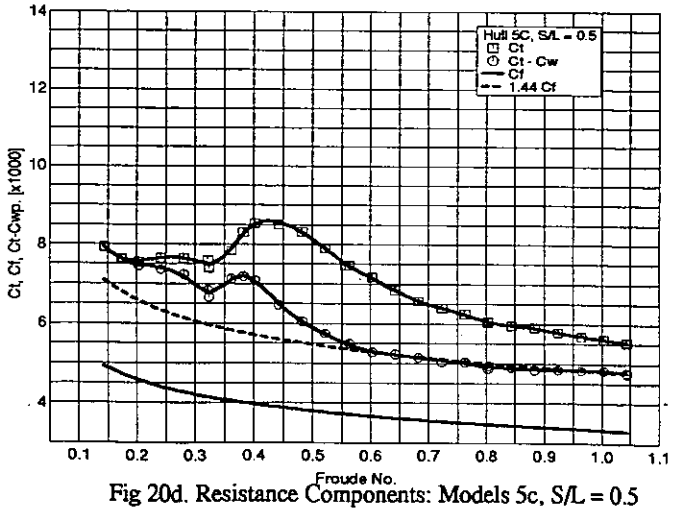

Fig 20d. Resistance Components: Models 5c, S/L = 0.5

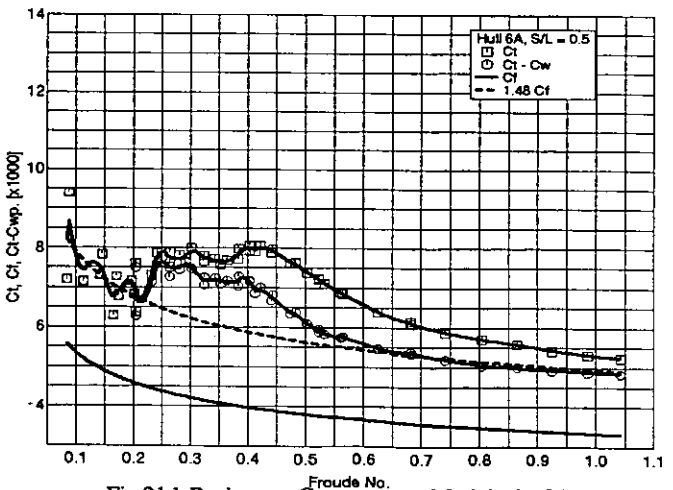

Fig 21d. Resistance Components: Models 6a, S/L = 0.5

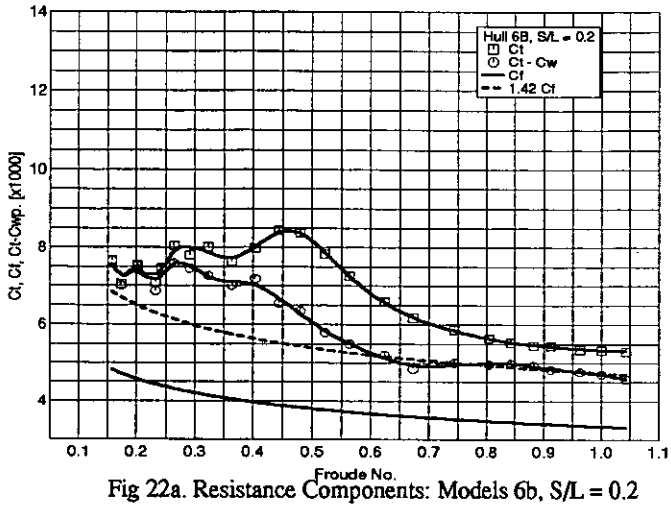

Fig 22a. Resistance Components: Models 6b, S/L = 0.2

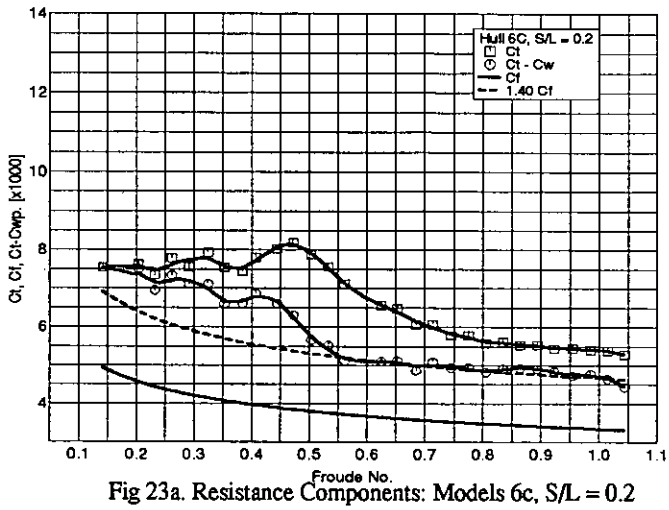

Fig 23a. Resistance Components: Models 6c, S/L = 0.2

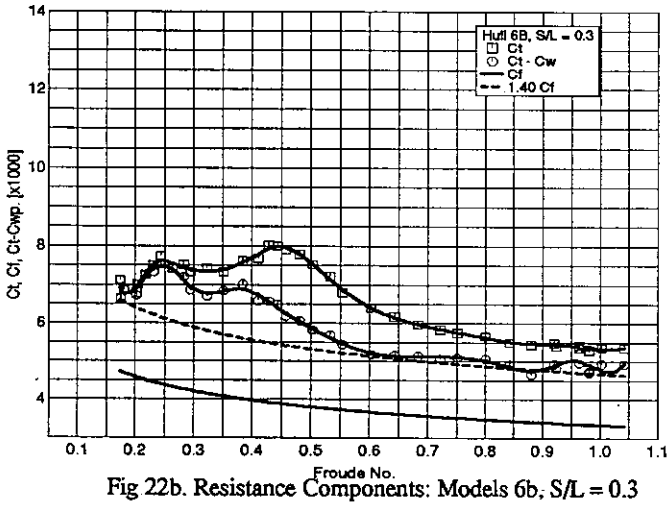

Fig 22b. Resistance Components: Models 6b, S/L = 0.3

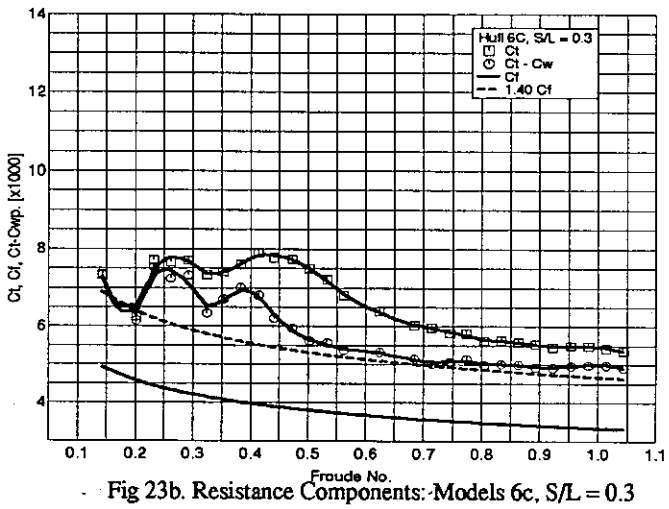

Fig 23b. Resistance Components: Models 6c, S/L = 0.3

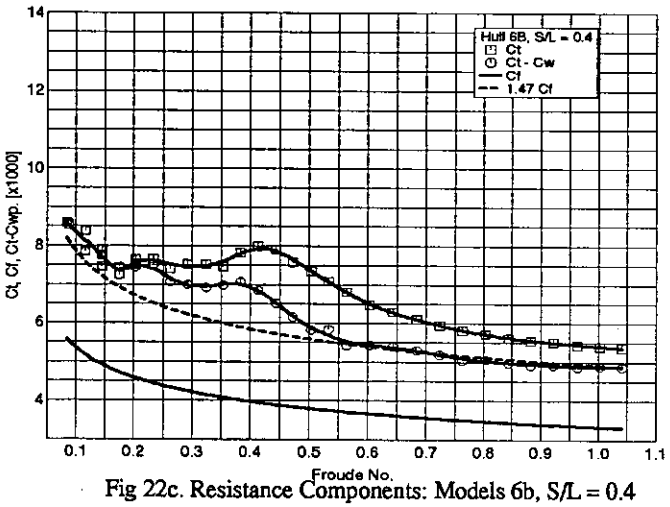

Fig 22c. Resistance Components: Models 6b, S/L = 0.4

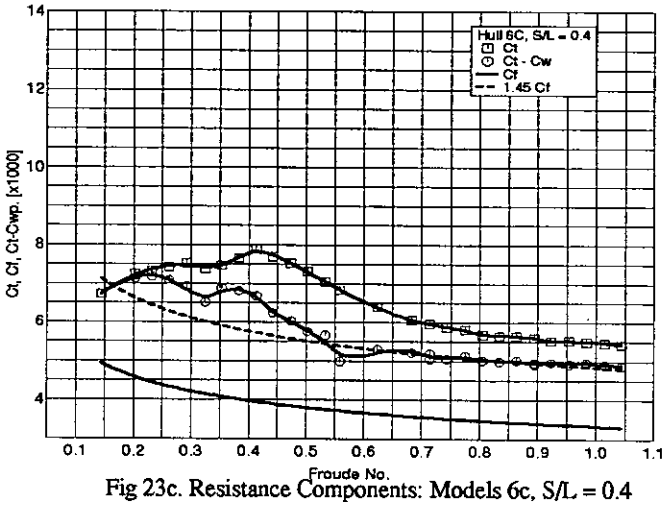

Fig 23c. Resistance Components: Models 6c, S/L = 0.4

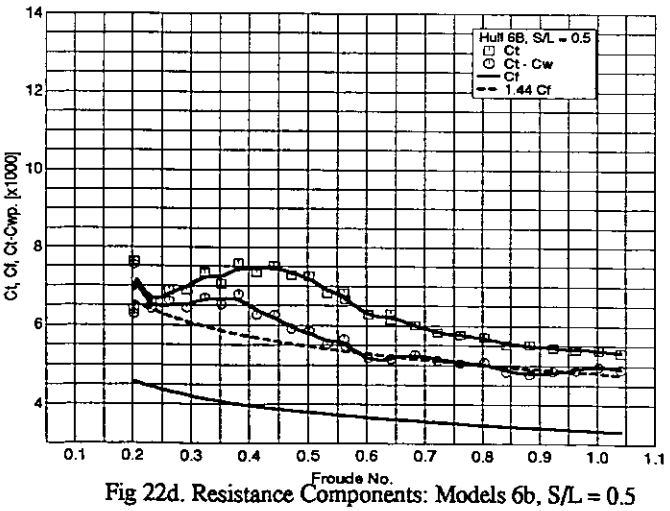

Fig 22d. Resistance Components: Models 6b, S/L = 0.5

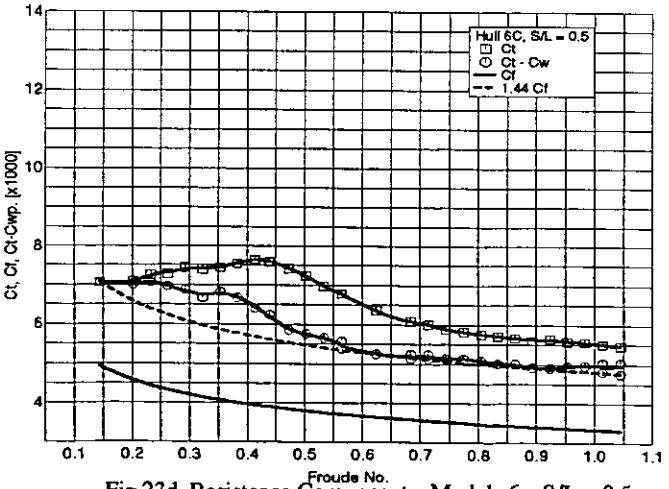

Fig 23d. Resistance Components: Models 6c, S/L = 0.5

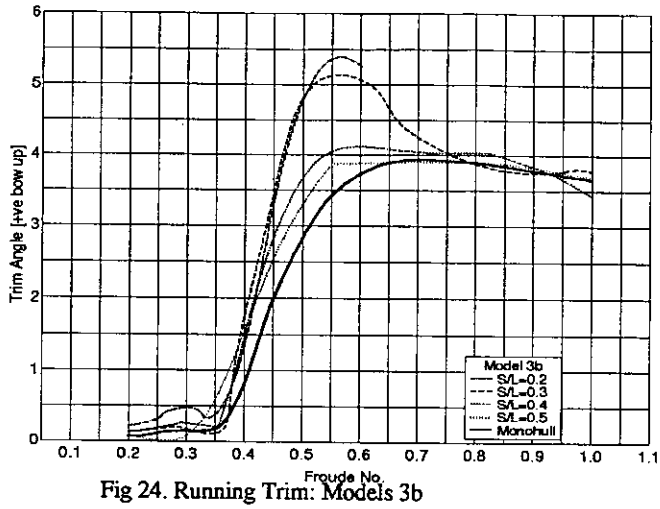

Fig 24. Running Trim: Models 3b

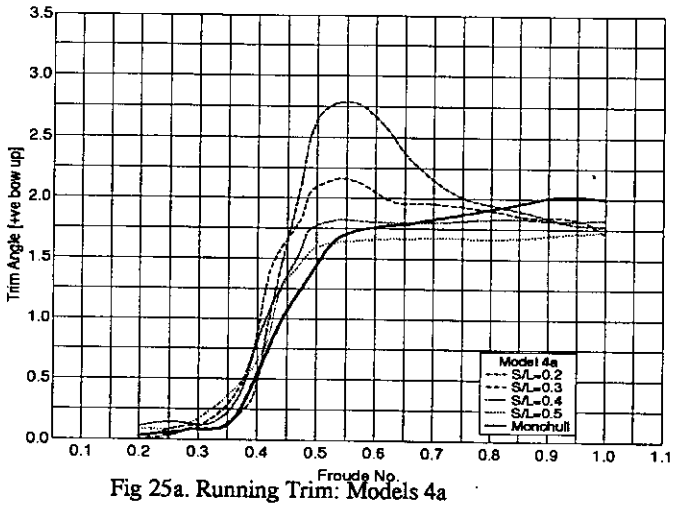

Fig 25a. Running Trim: Models 4a

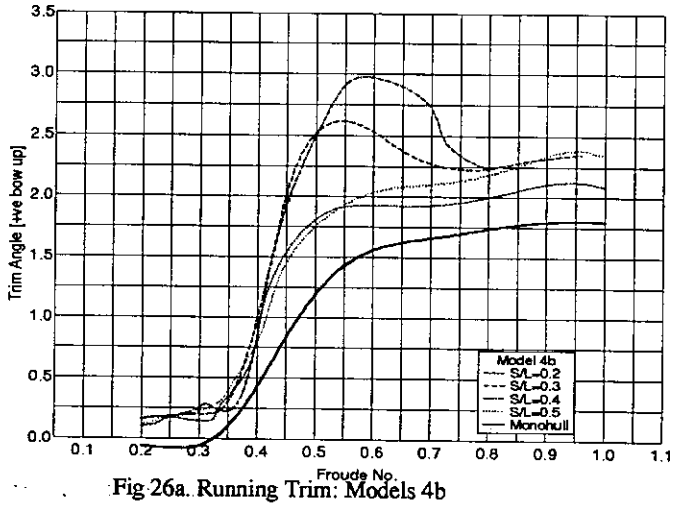

Fig 26a. Running Trim: Models 4b

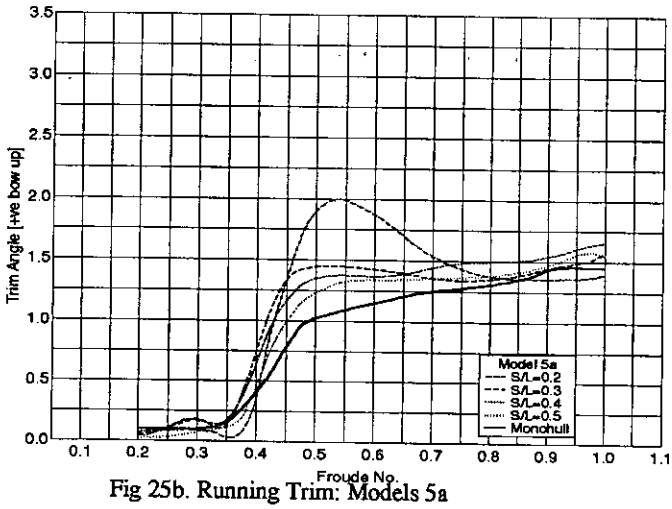

Fig 25b. Running Trim: Models 5a

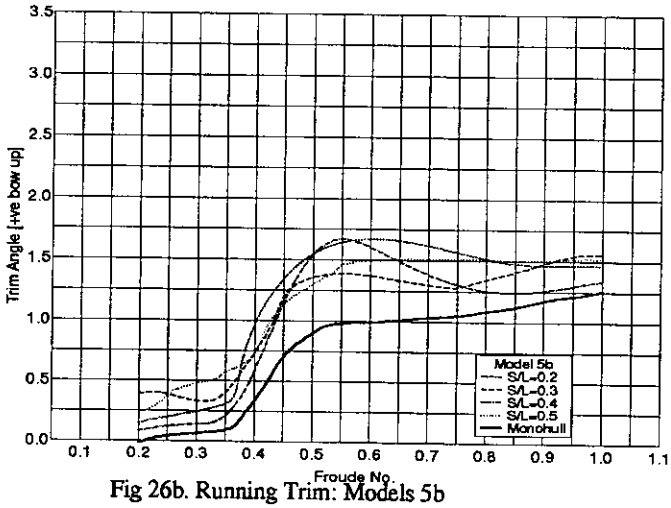

Fig 26b. Running Trim: Models 5b

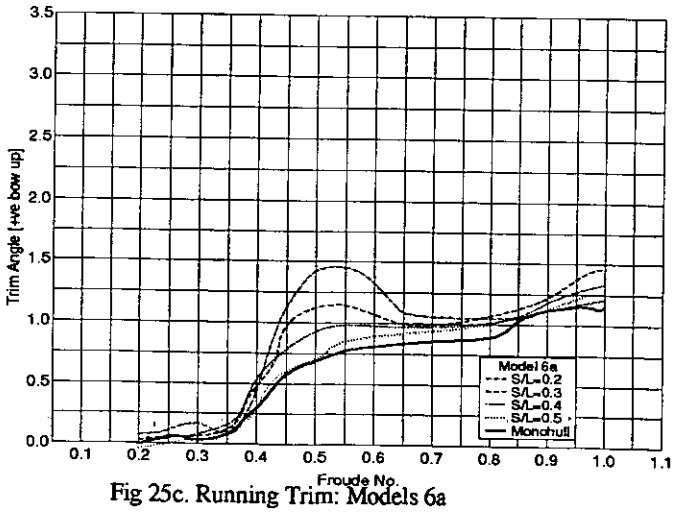

Fig 25c. Running Trim: Models 6a

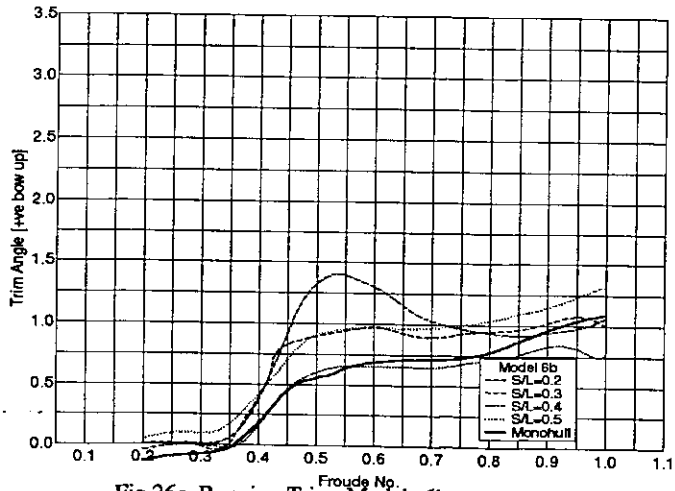

Fig 26c. Running Trim: Models 6b

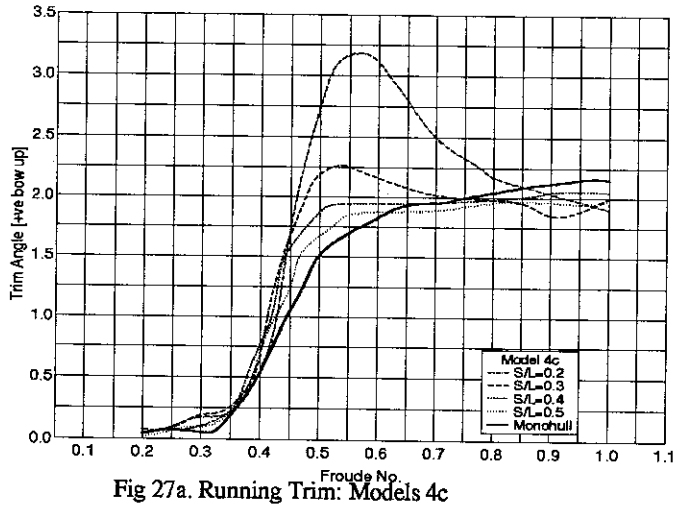

Fig 27a. Running Trim: Models 4c

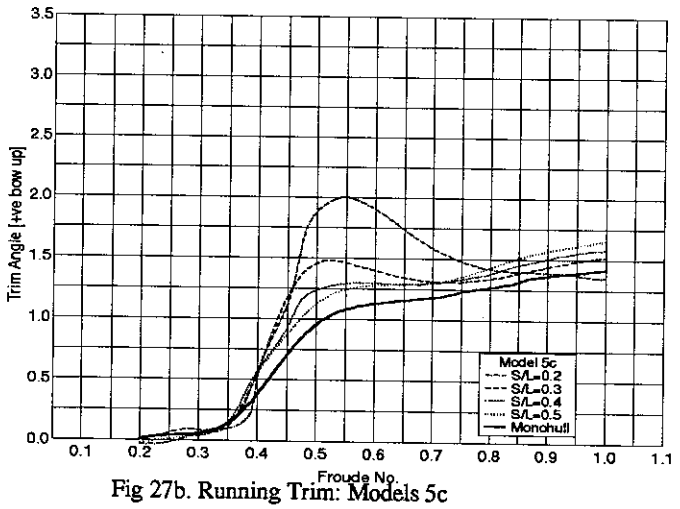

Fig 27b. Running Trim: Models 5c

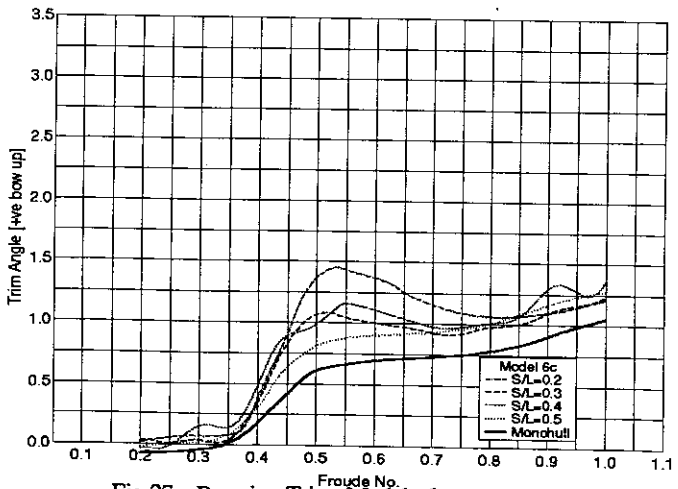

Fig 27c. Running Trim: Models 6c

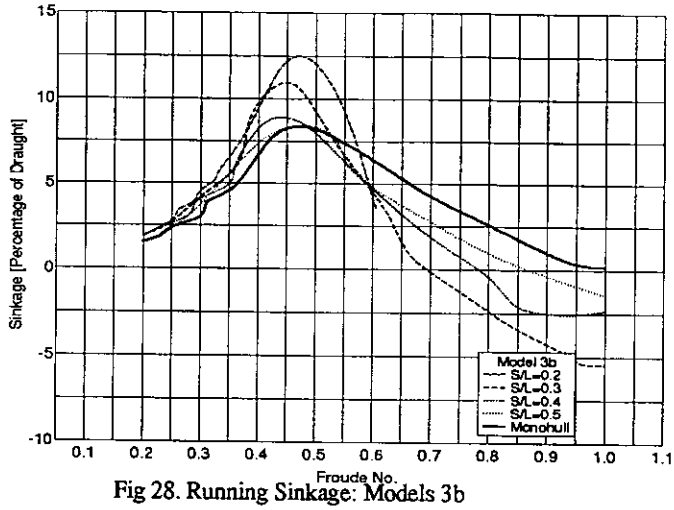

Fig 28. Running Sinkage: Models 3b

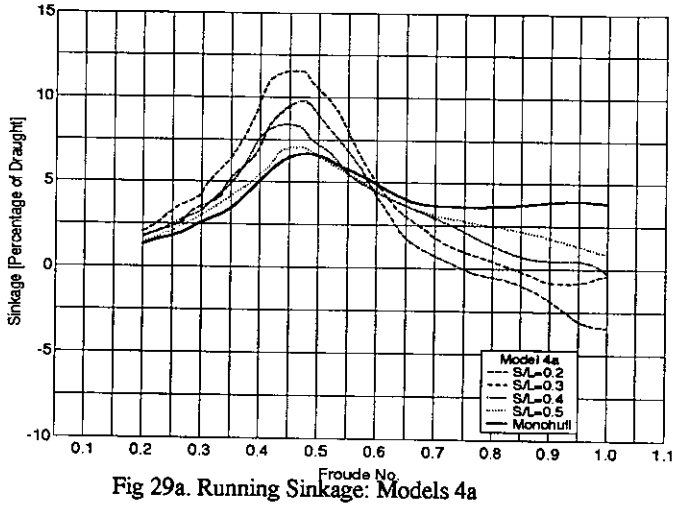

Fig 29a. Running Sinkage: Models 4a

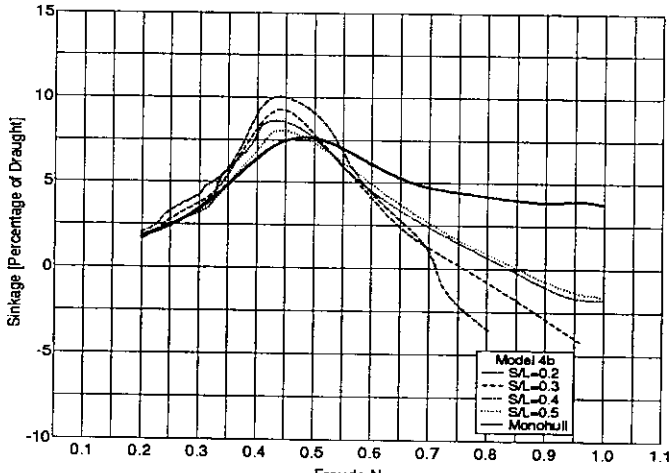

Fig 30a. Running Sinkage: Models 4b

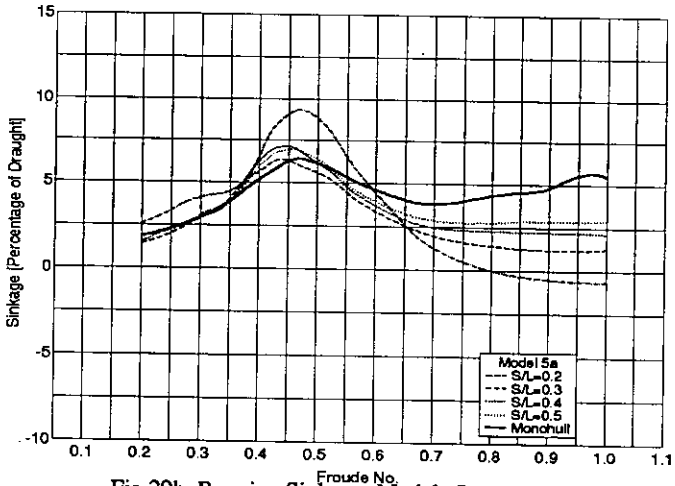

Fig 29b. Running Sinkage: Models 5a

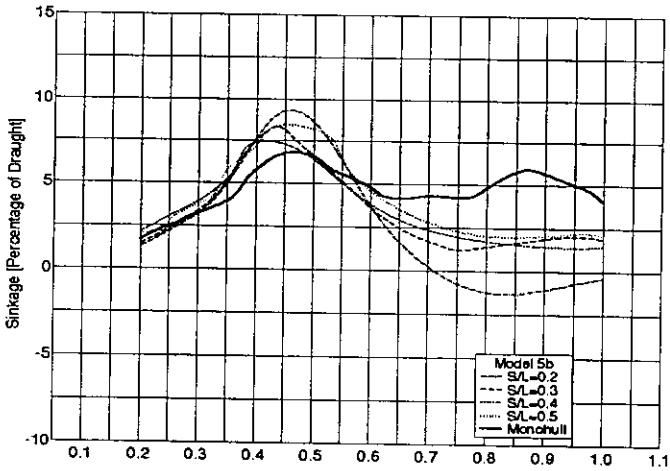

Fig 30b. Running Sinkage: Models 5b

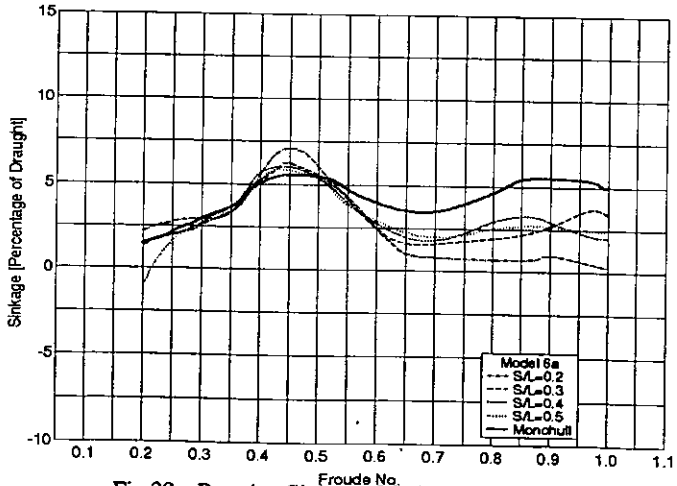

Fig 29c. Running Sinkage: Models 6a

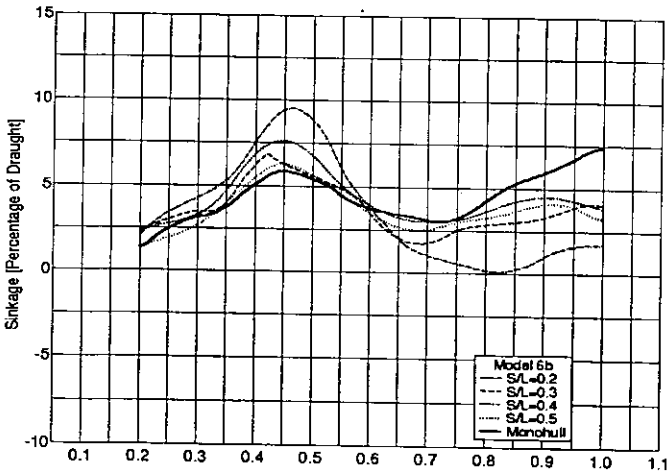

Fig 30c. Running Sinkage: Models 6b

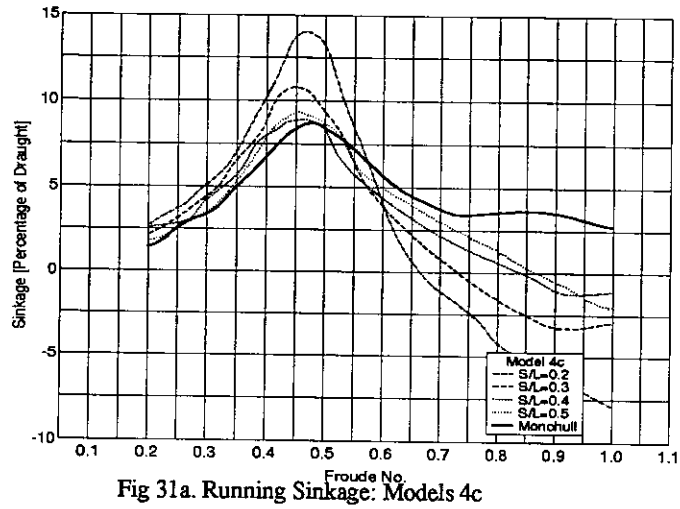

Fig 31a. Running Sinkage: Models 4c

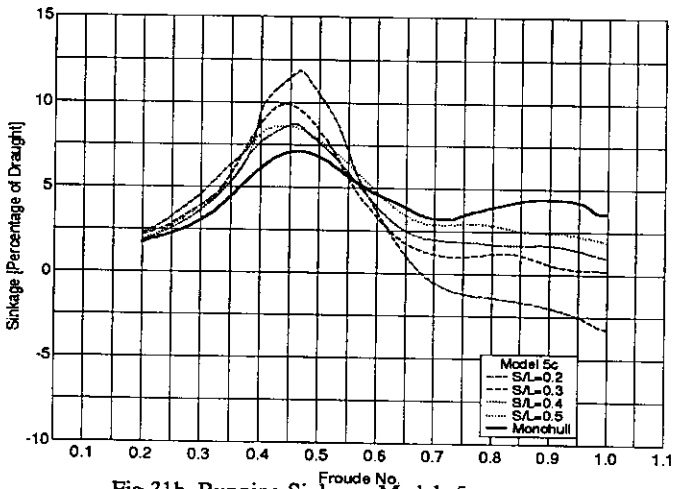

Fig 31b. Running Sinkage: Models 5c

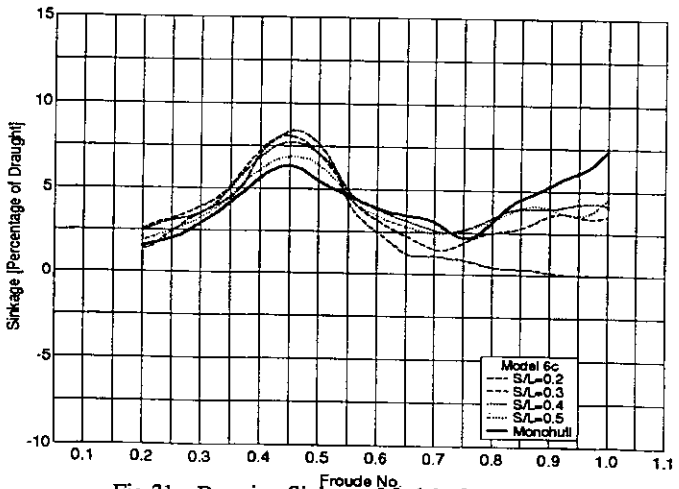

Fig 31c. Running Sinkage: Models 6c

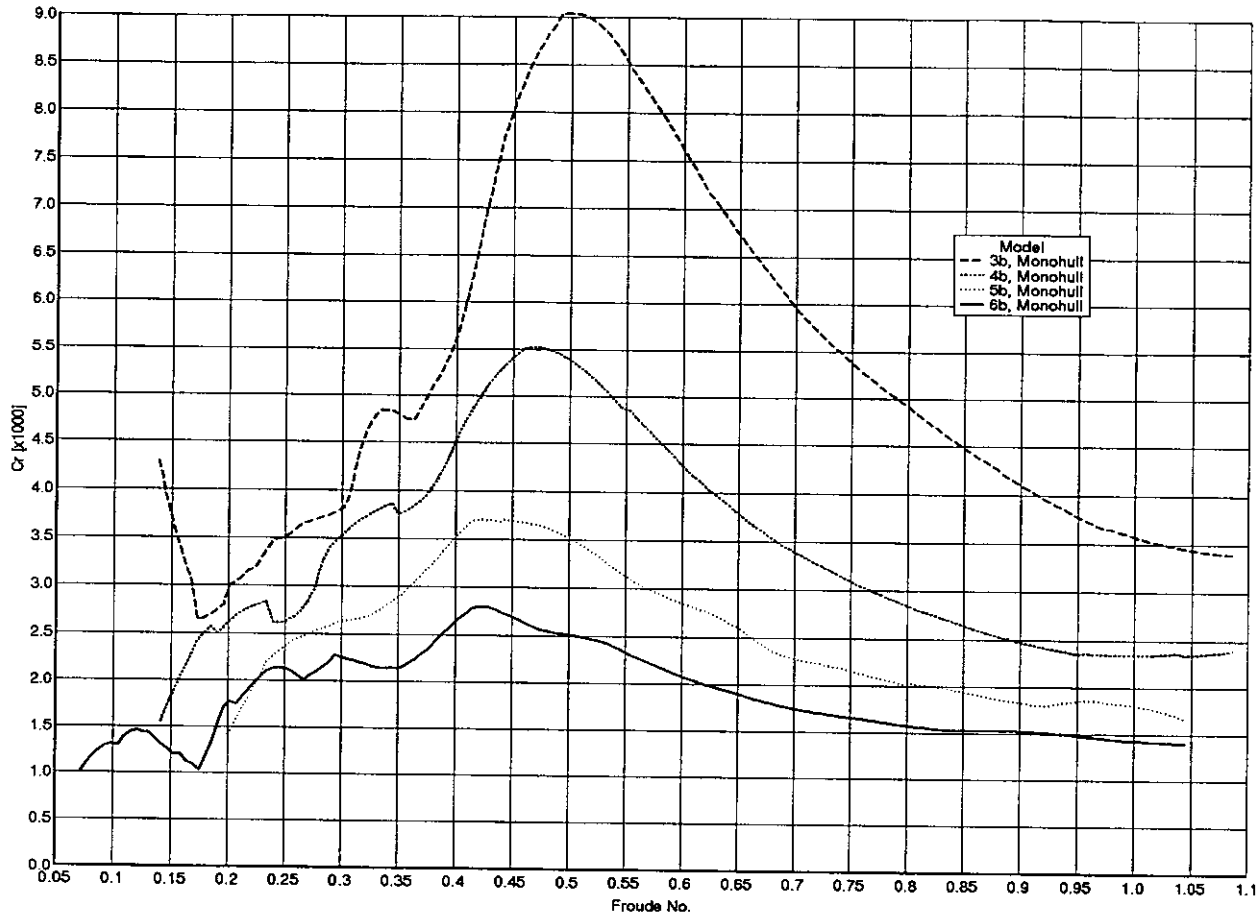

Fig 32a. Residuary Resistance: Models: 3b,4b,5b,6b (Monohull)

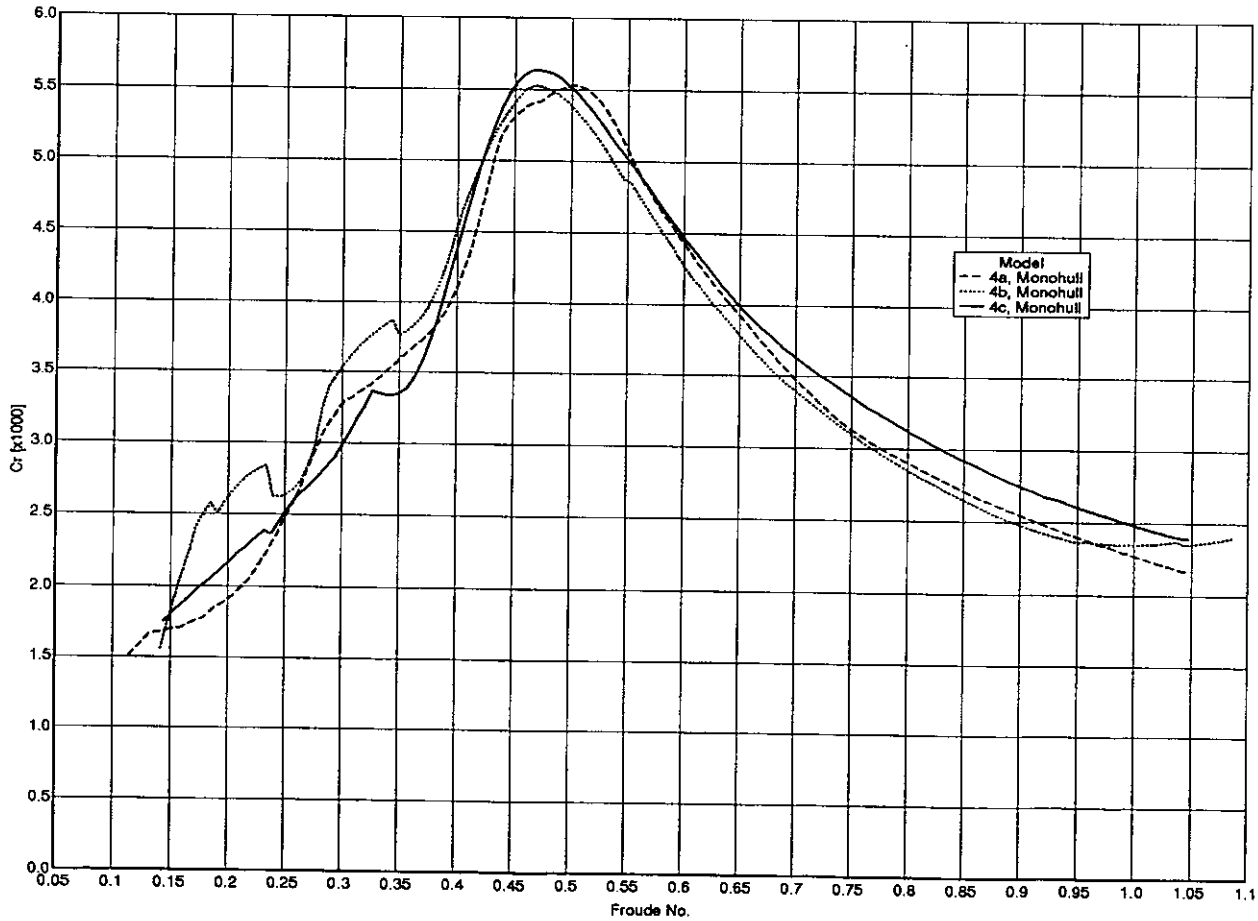

Fig 32b. Residuary Resistance: Models: 4a,4b,4c (Monohull)

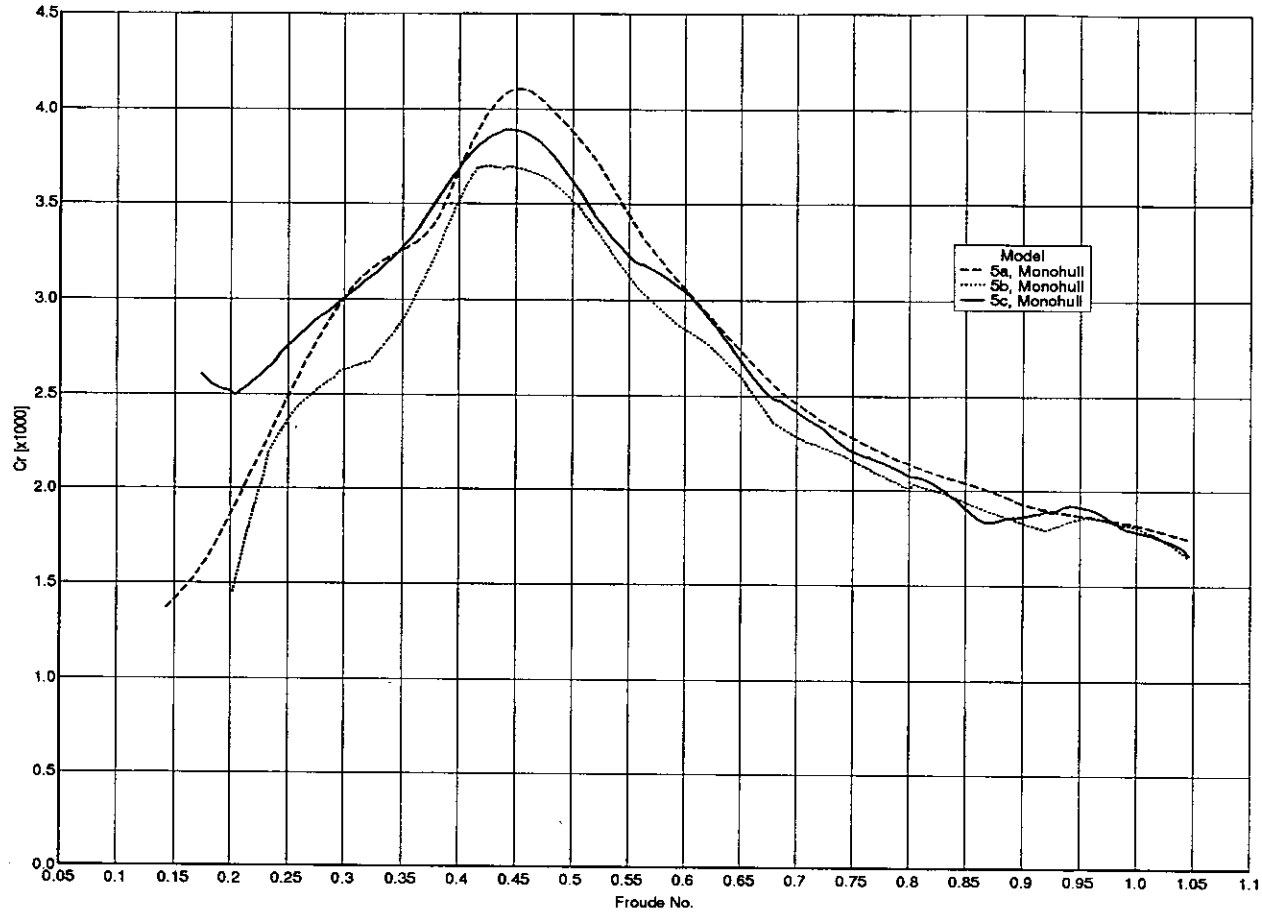

Fig 32c. Residuary Resistance: Models: 5a,5b,5c (Monohull)

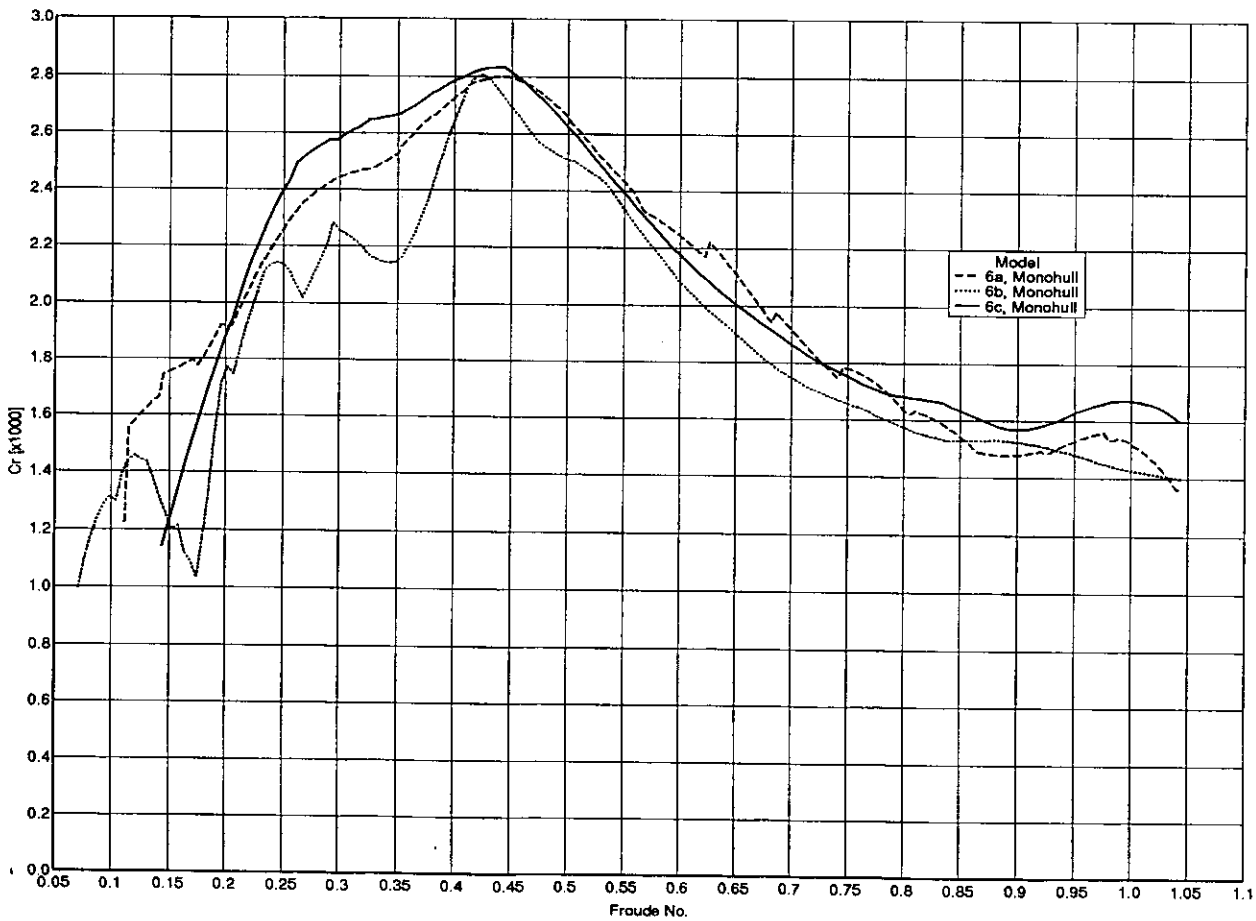

Fig 32d. Residuary Resistance: Models: 6a,6b,6c (Monohull)

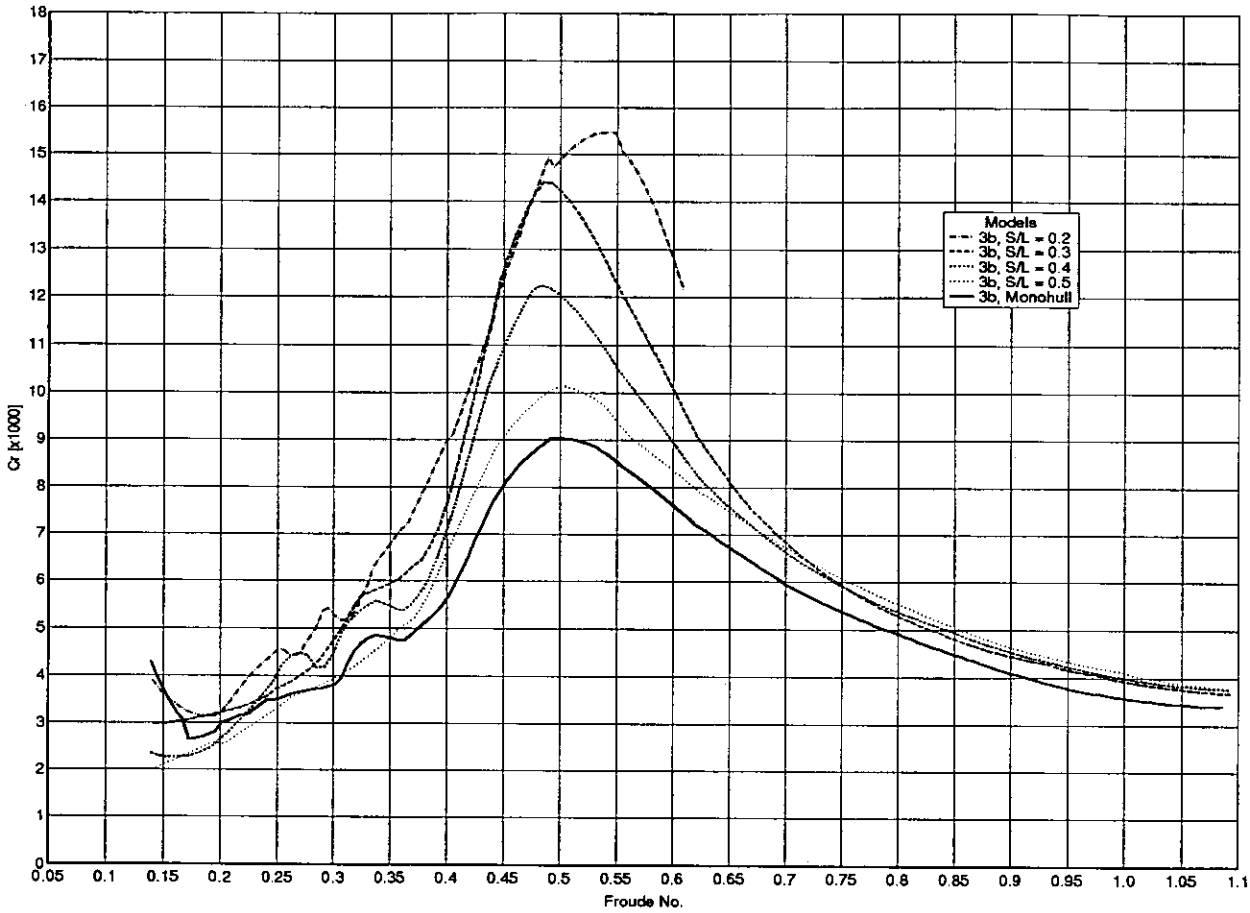

Fig 33. Residuary Resistance: Models: 3b

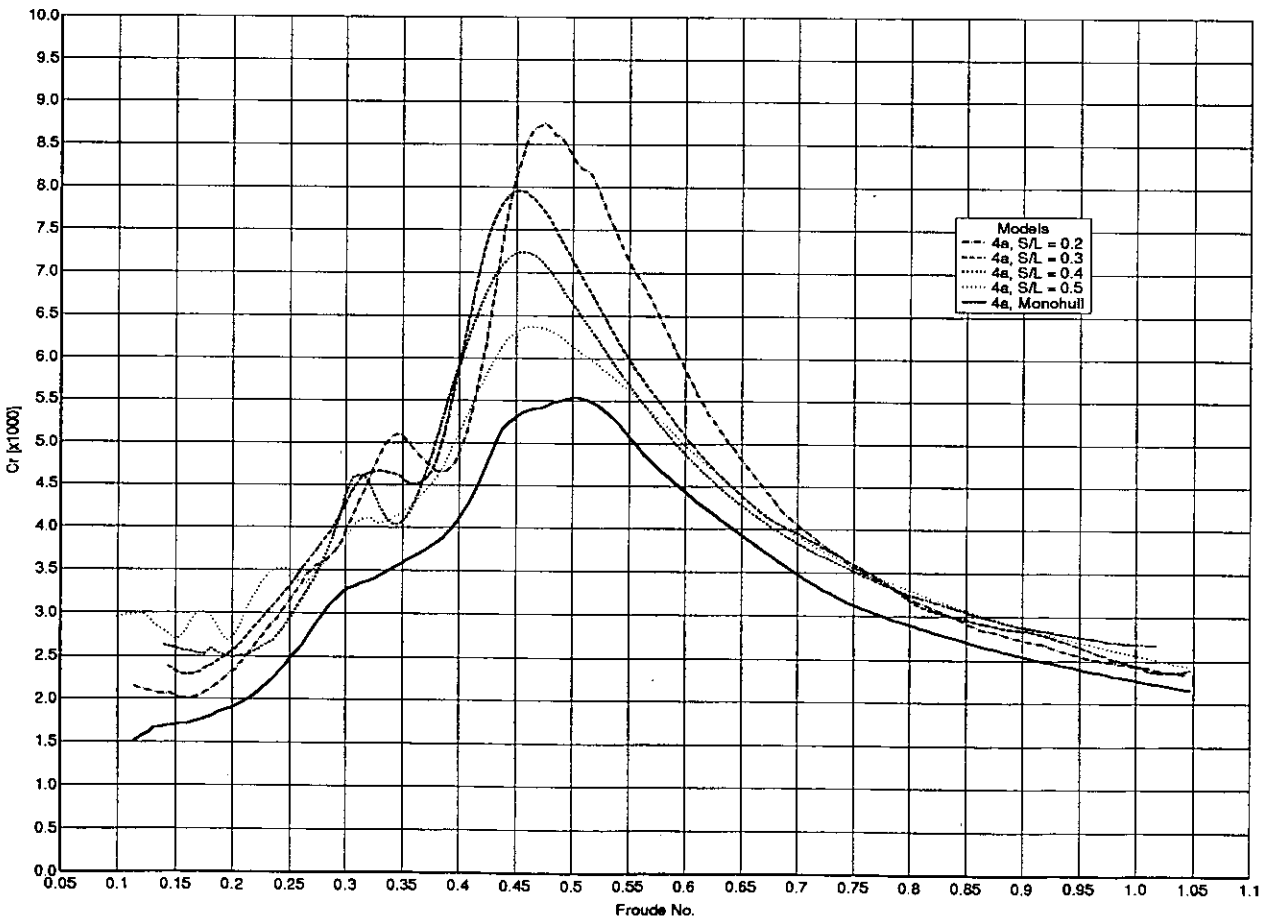

Fig 34. Residuary Resistance: Models: 4a

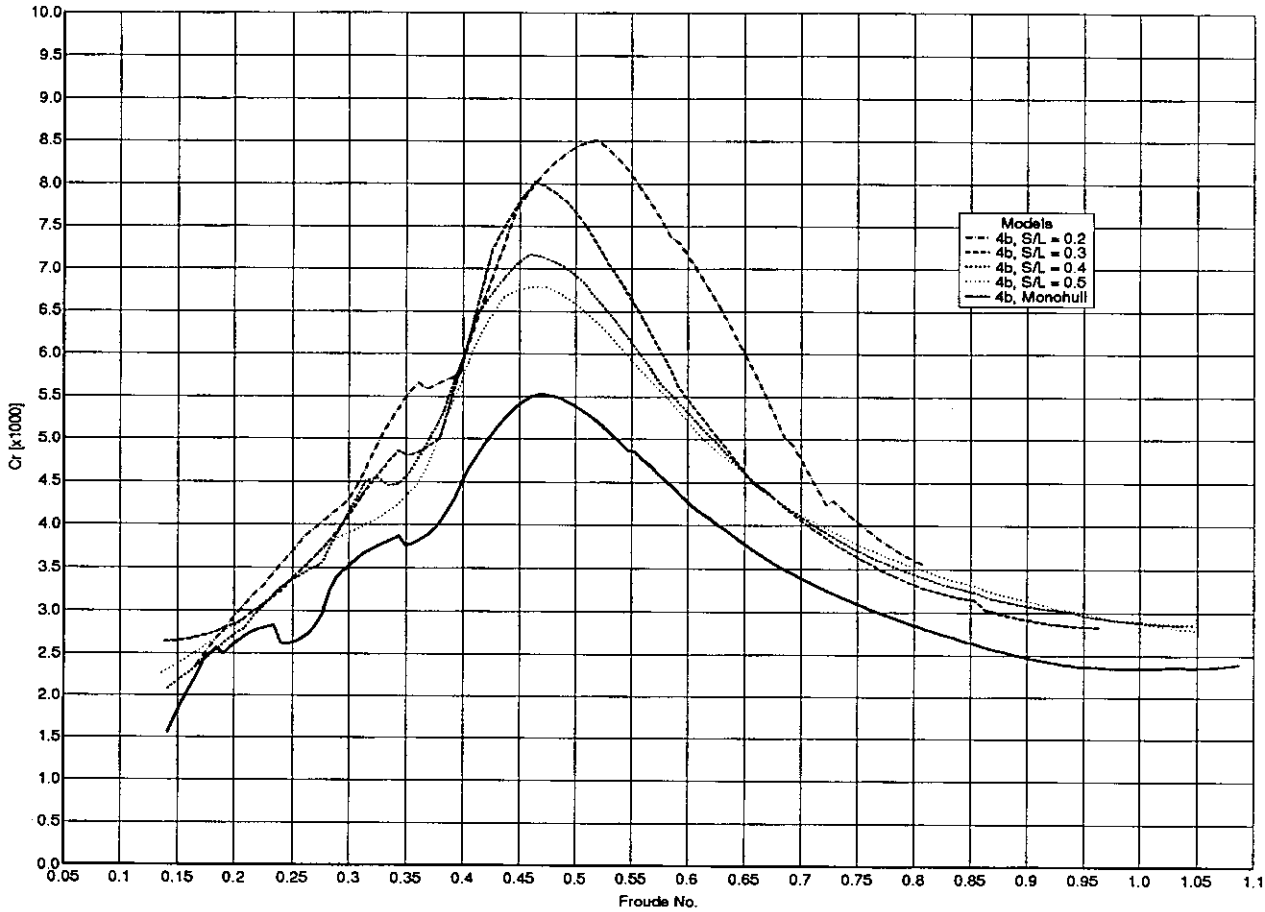

Fig 35. Residuary Resistance: Models: 4b

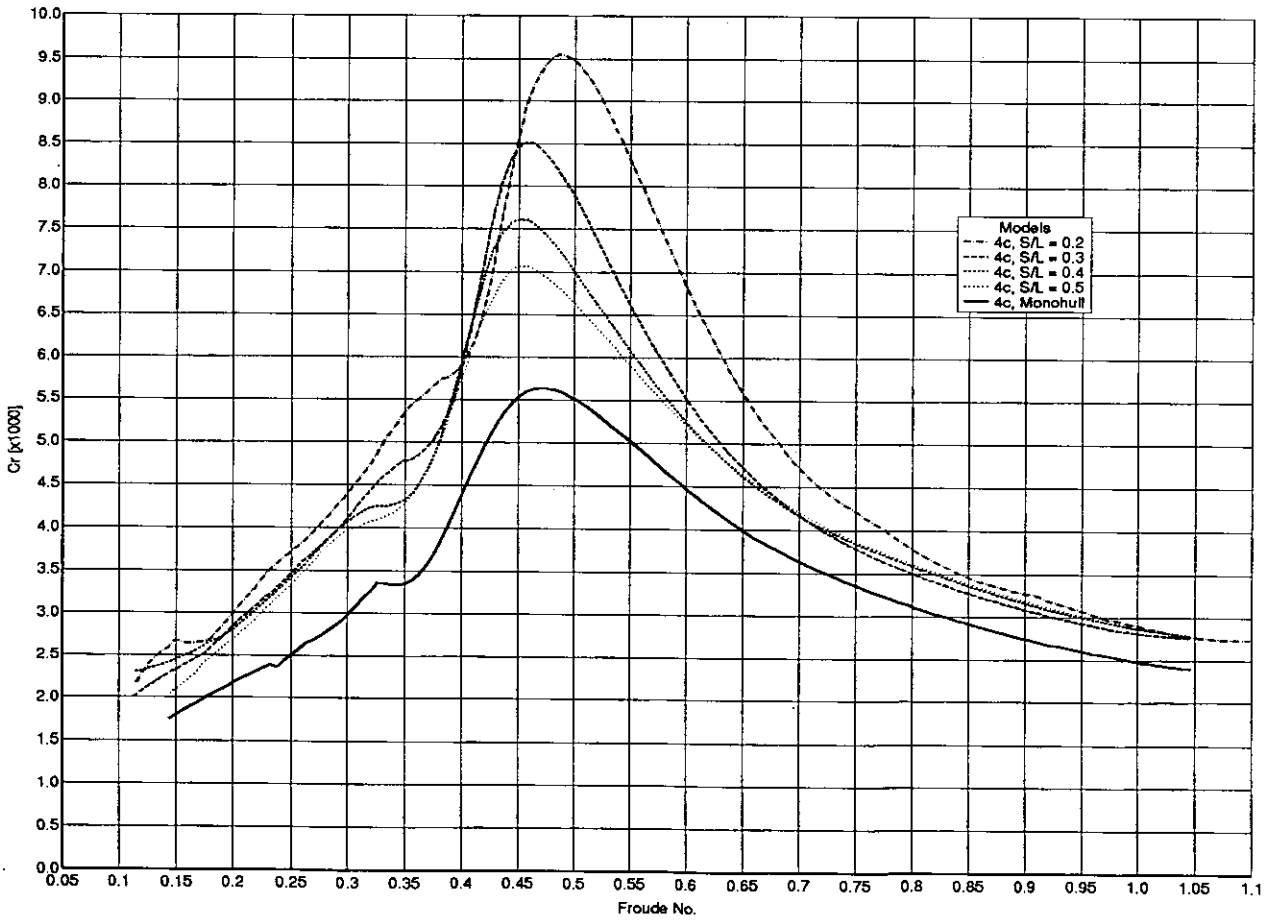

Fig 36. Residuary Resistance: Models: 4c

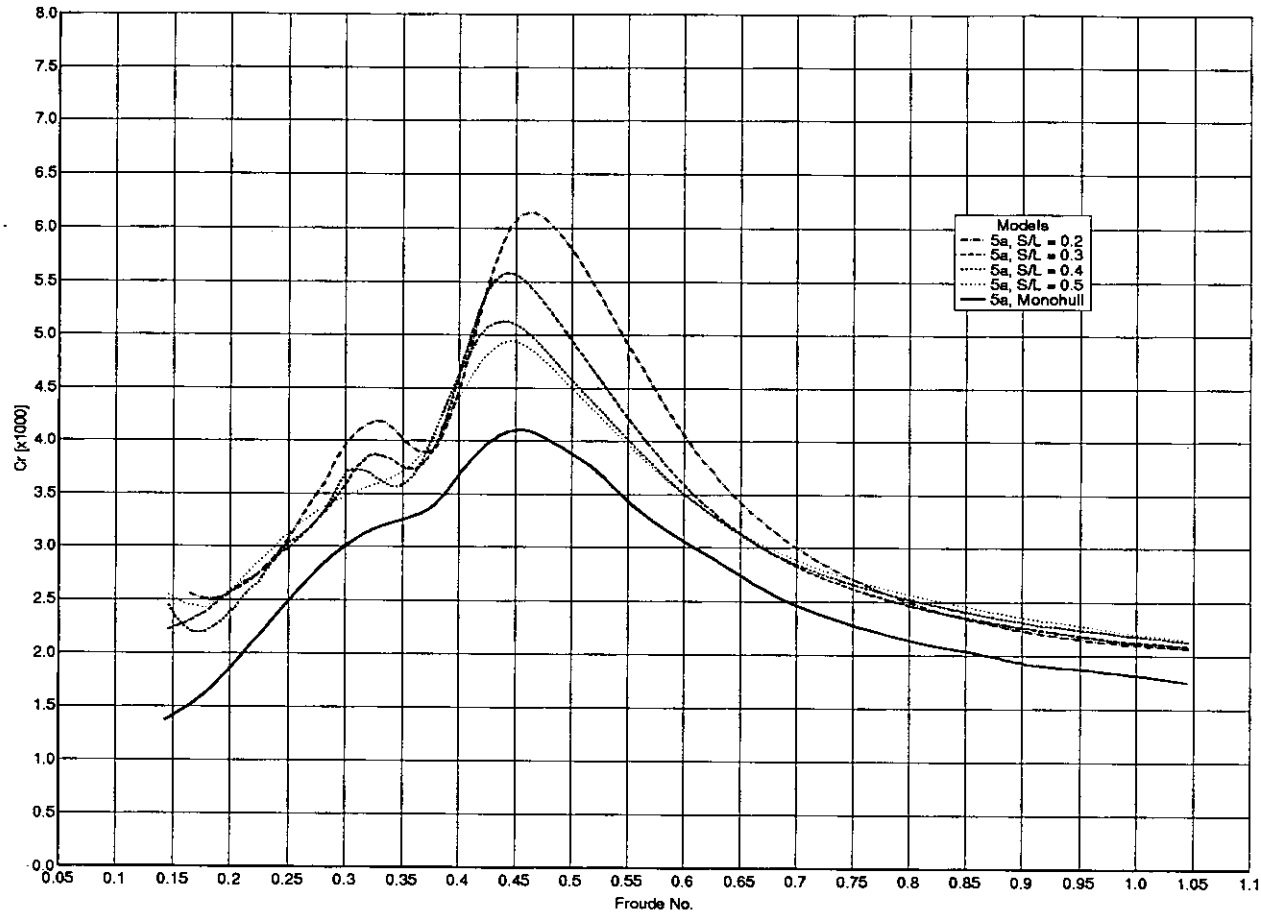

Fig 37. Residuary Resistance: Models: 5a

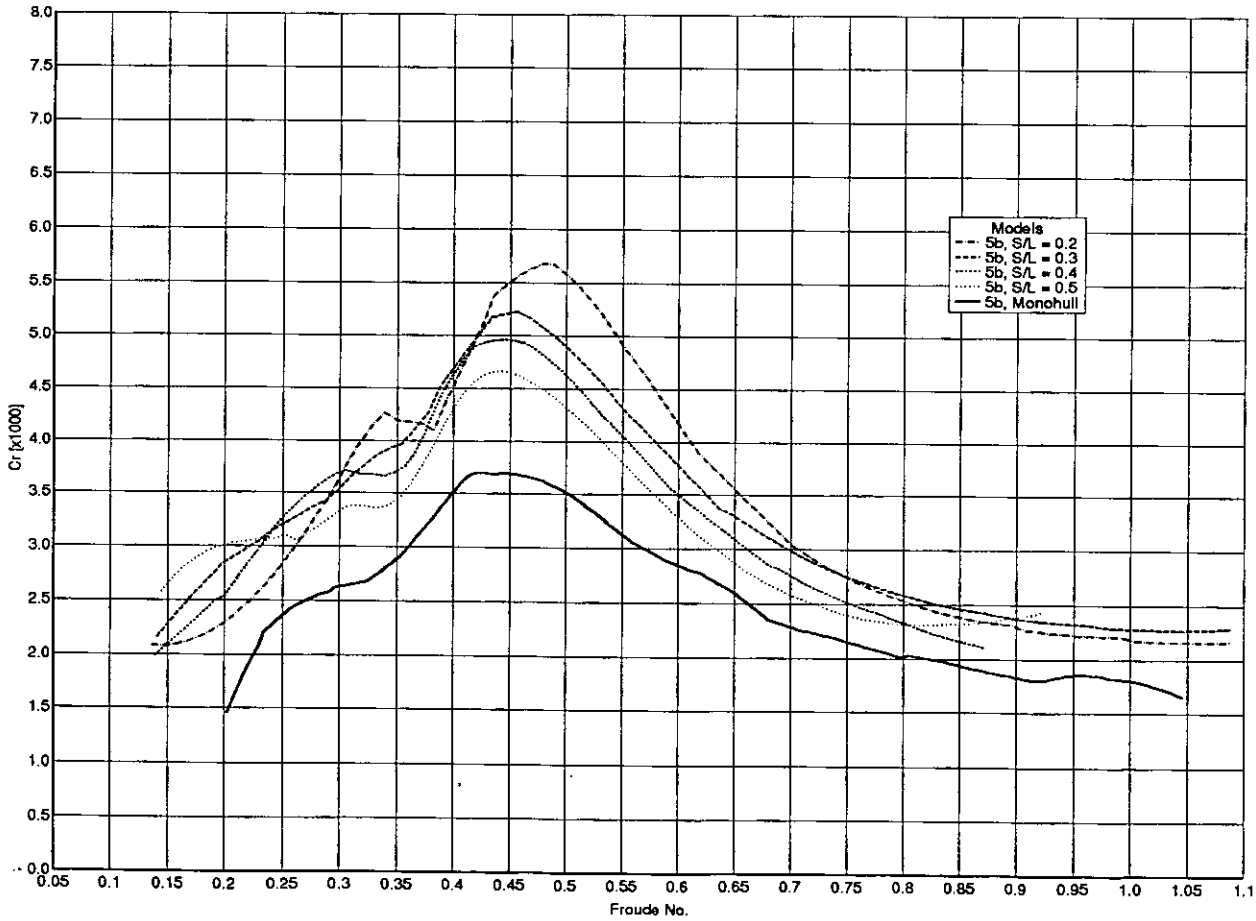

Fig 38. Residuary Resistance: Models: 5b

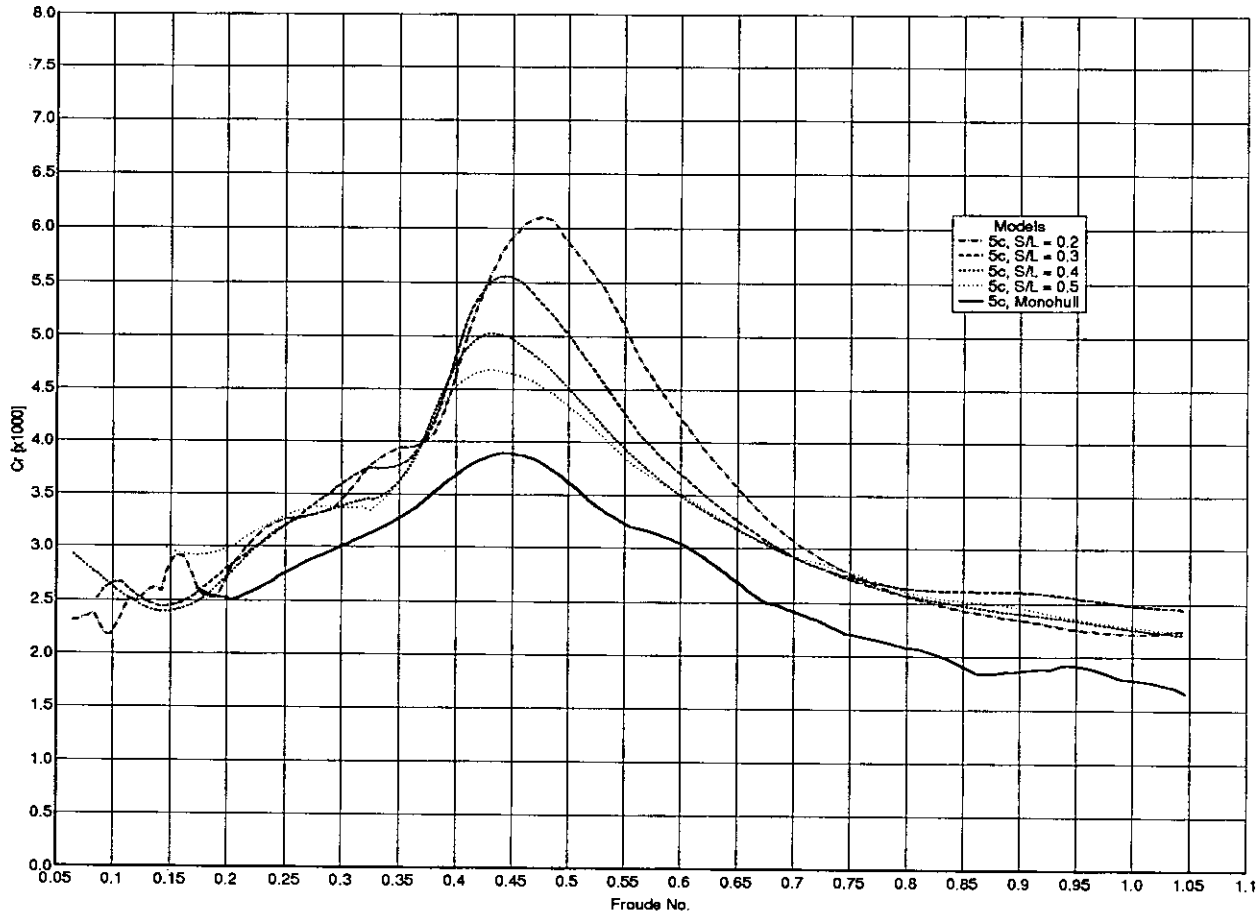

Fig 39. Residuary Resistance: Models: 5c

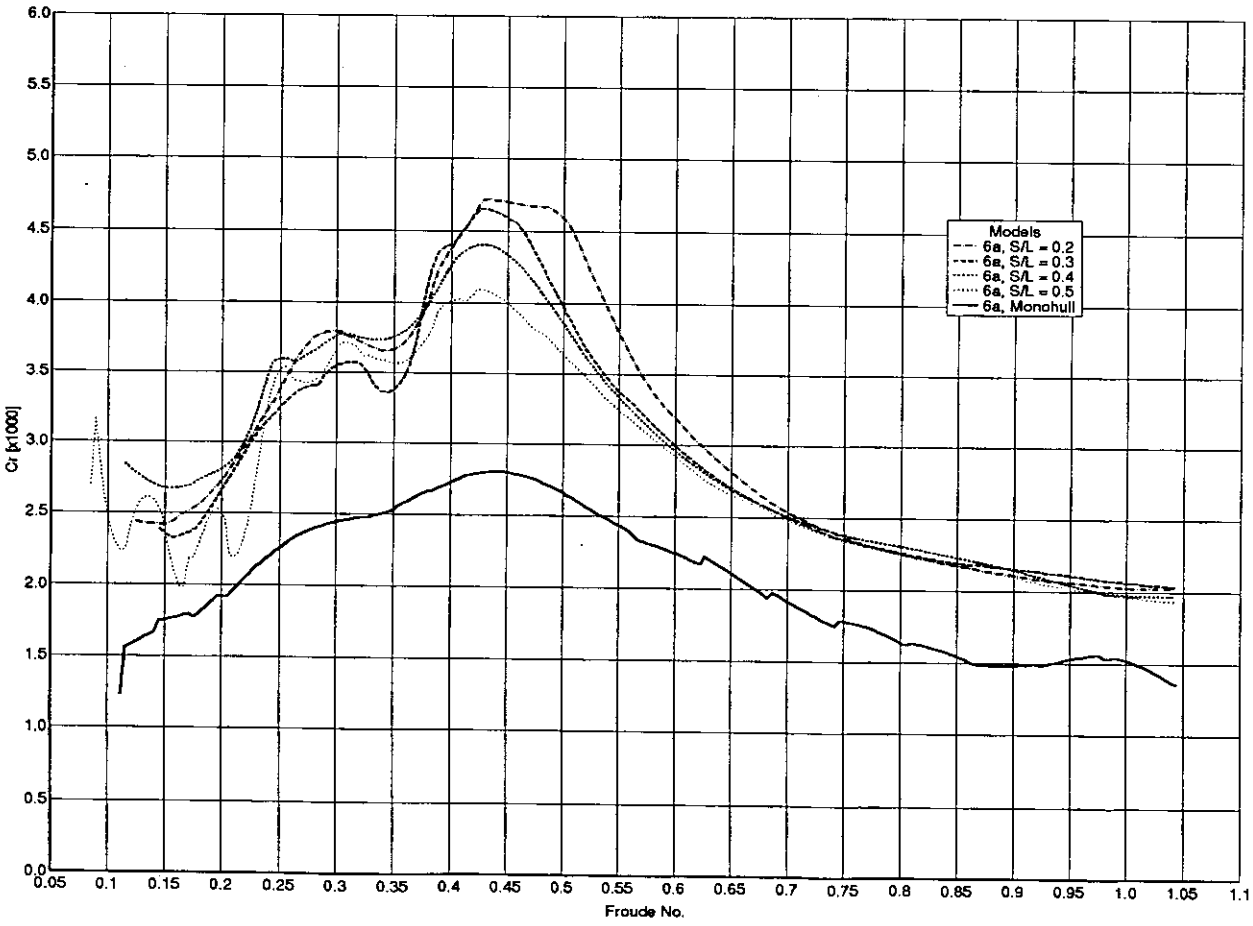

Fig 40. Residuary Resistance: Models: 6a

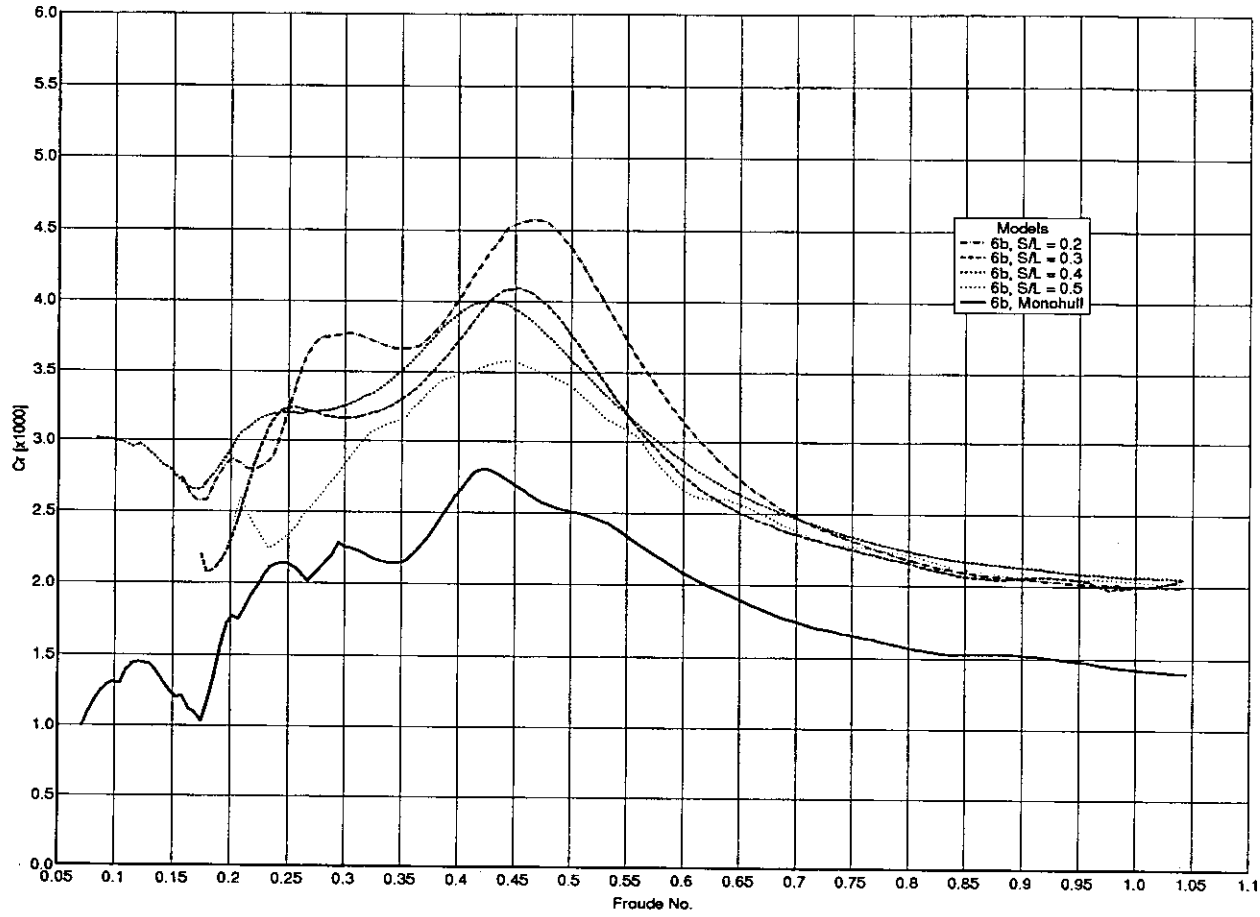

Fig 41. Residuary Resistance: Models: 6b

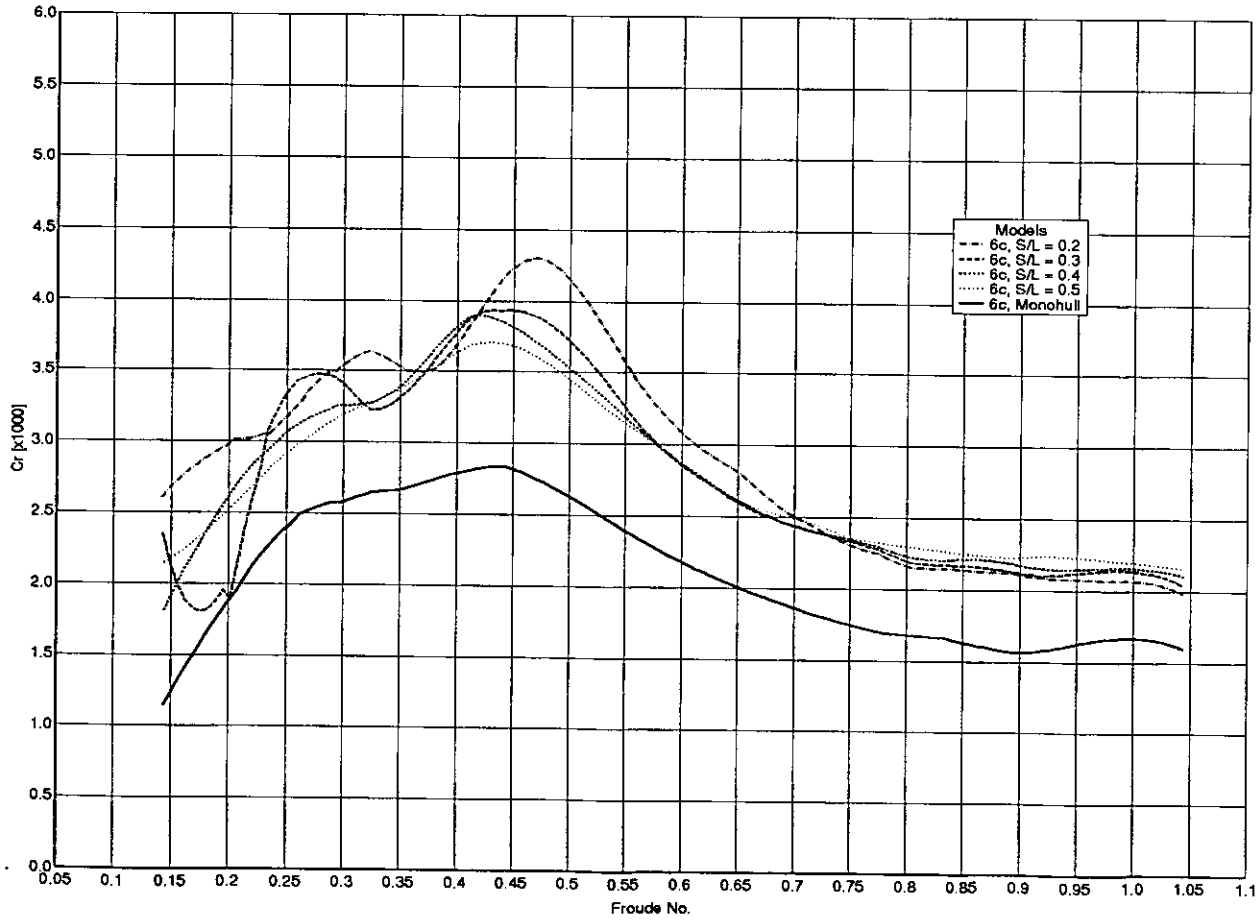

Fig 42. Residuary Resistance: Models: 6c

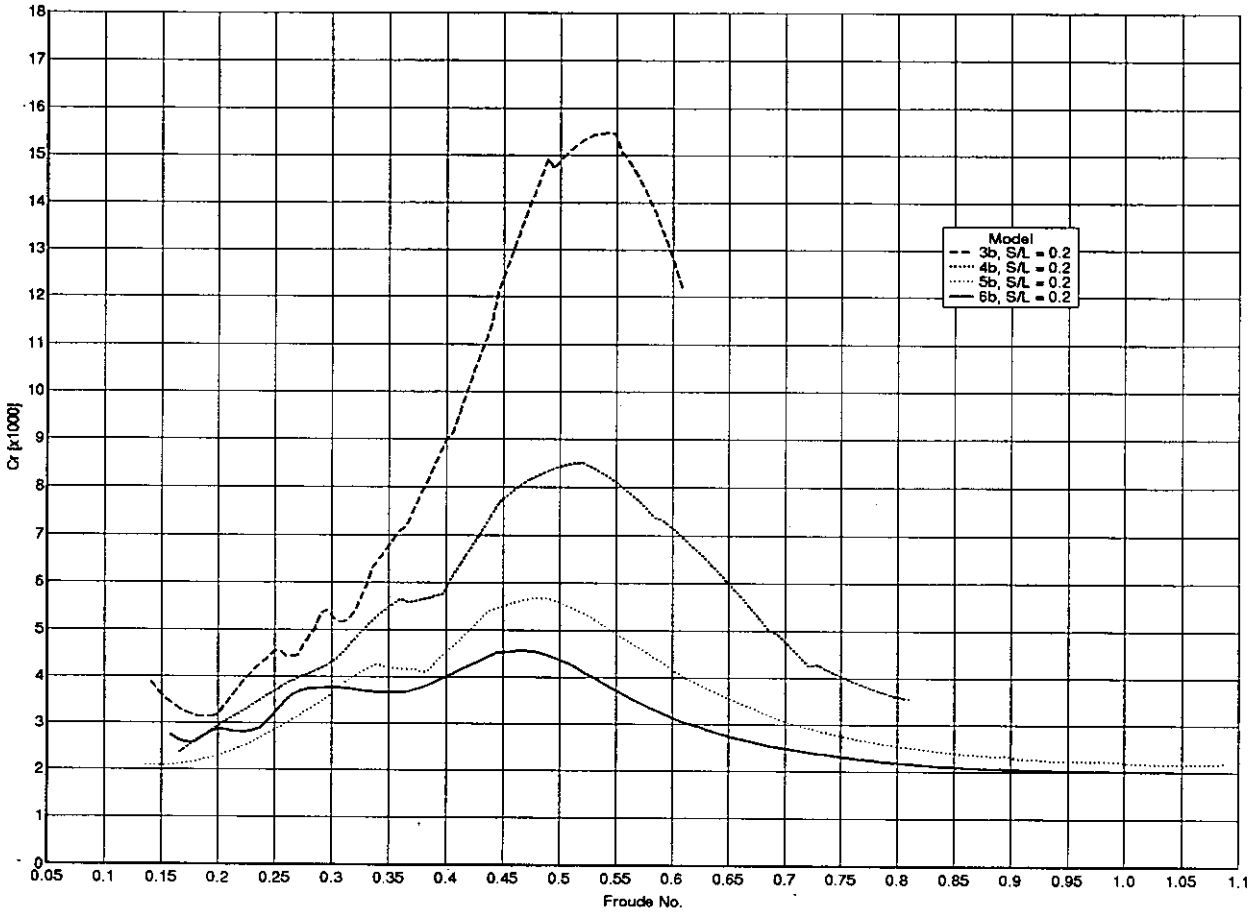

Fig 43a. Residuary Resistance: Models: 3b,4b,5b,6b (S/L = 0.2)

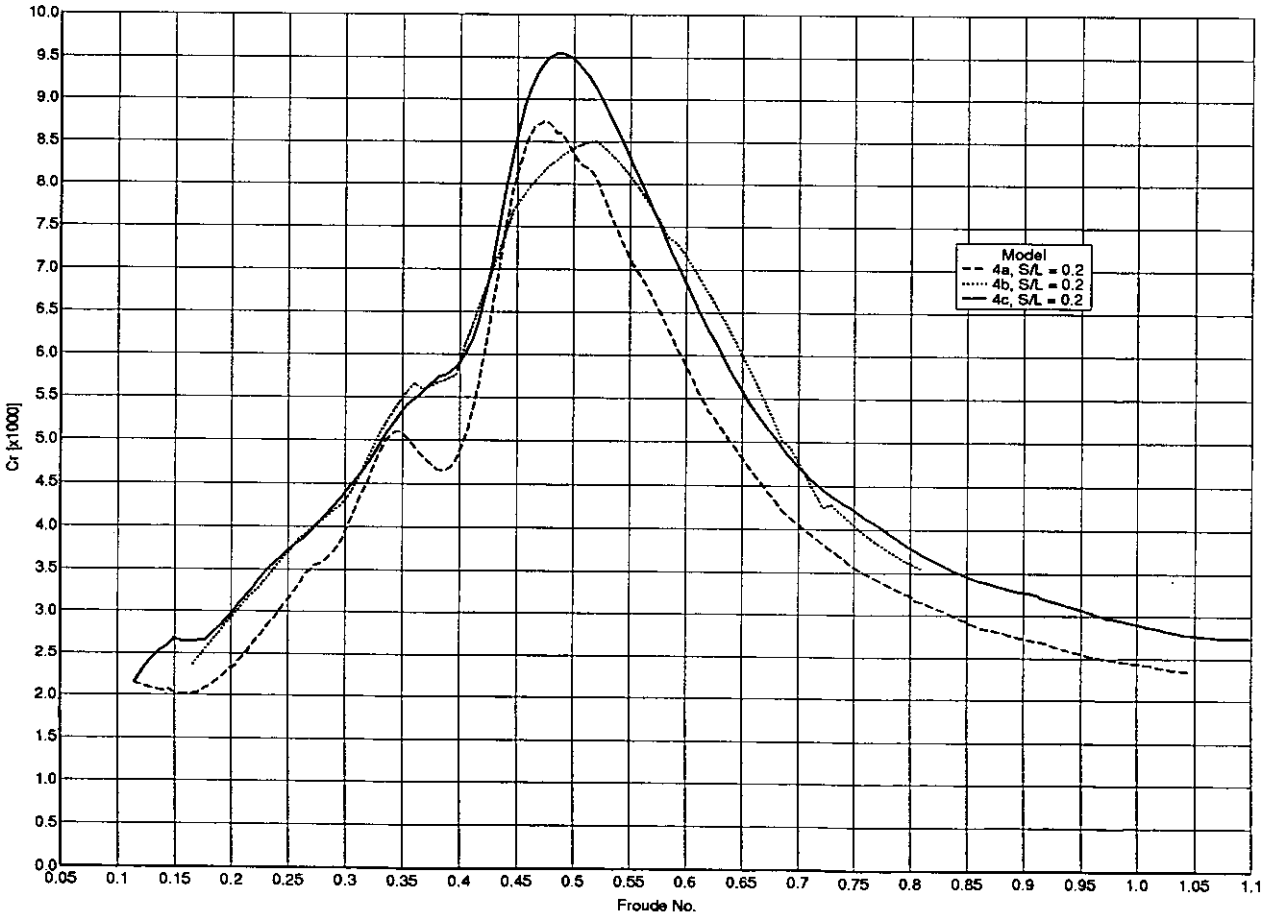

Fig 43b. Residuary Resistance: Models: 4a,4b,4c (S/L = 0.2)

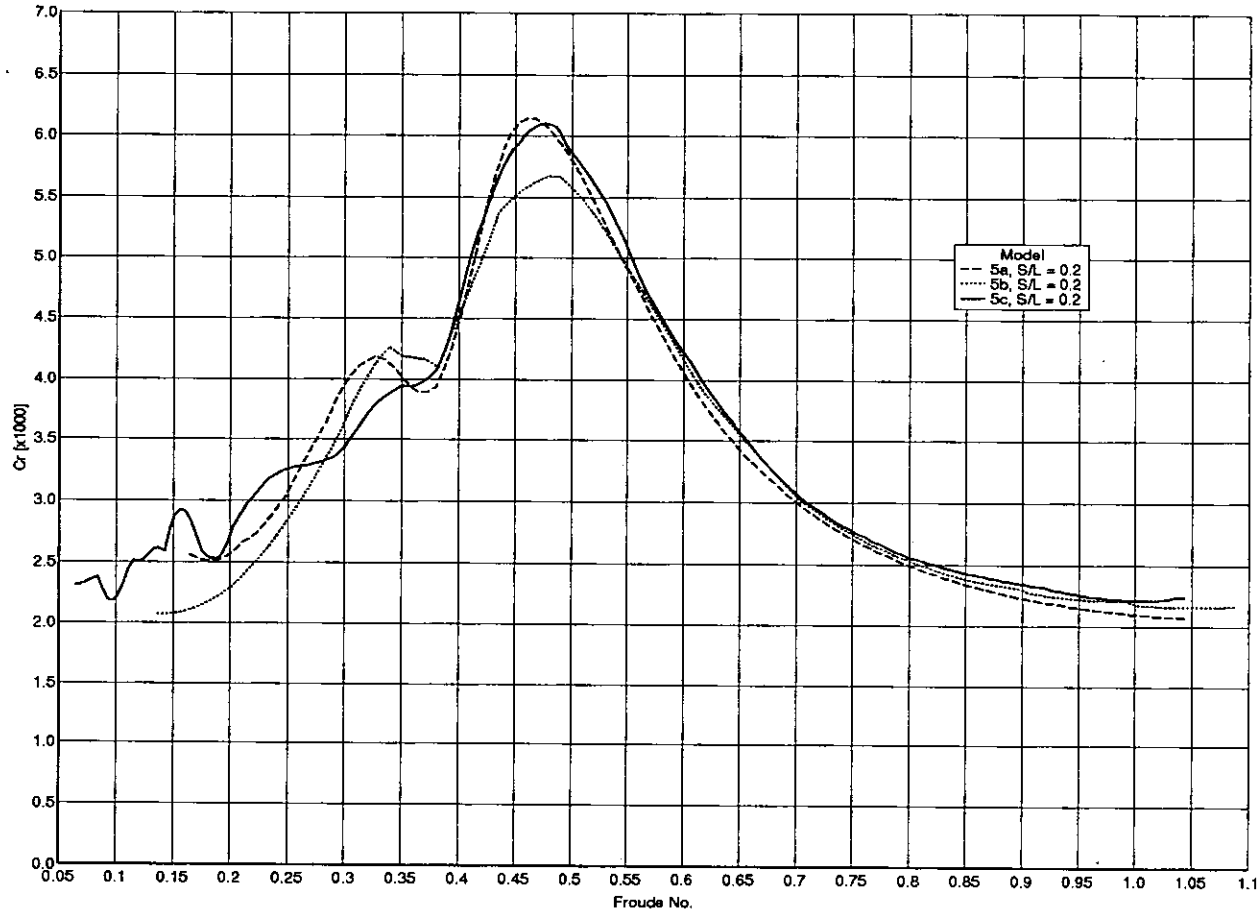

Fig 43c. Residuary Resistance: Models: 5a,5b,5c (S/L = 0.2)

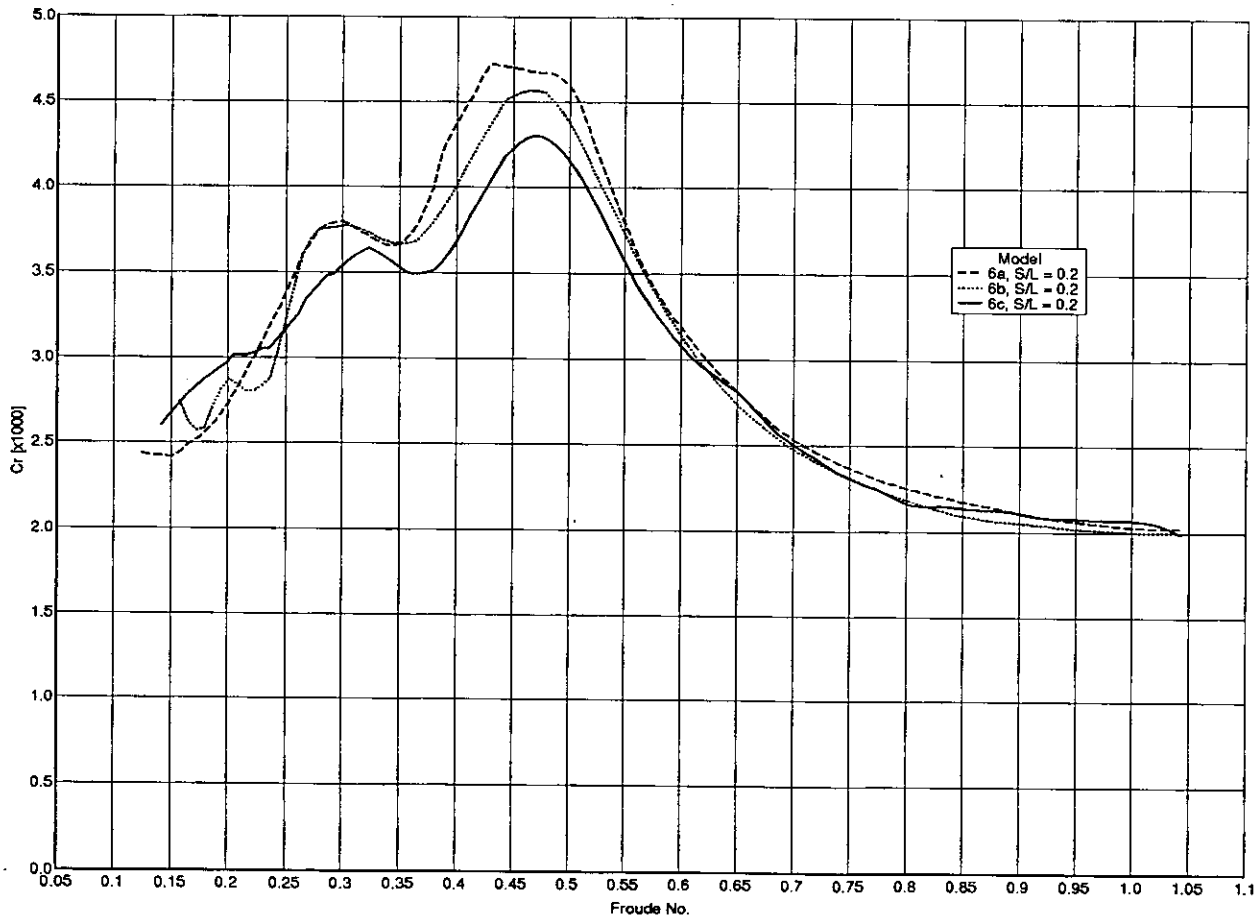

Fig 43d. Residuary Resistance: Models: 6a,6b,6c (S/L = 0.2)

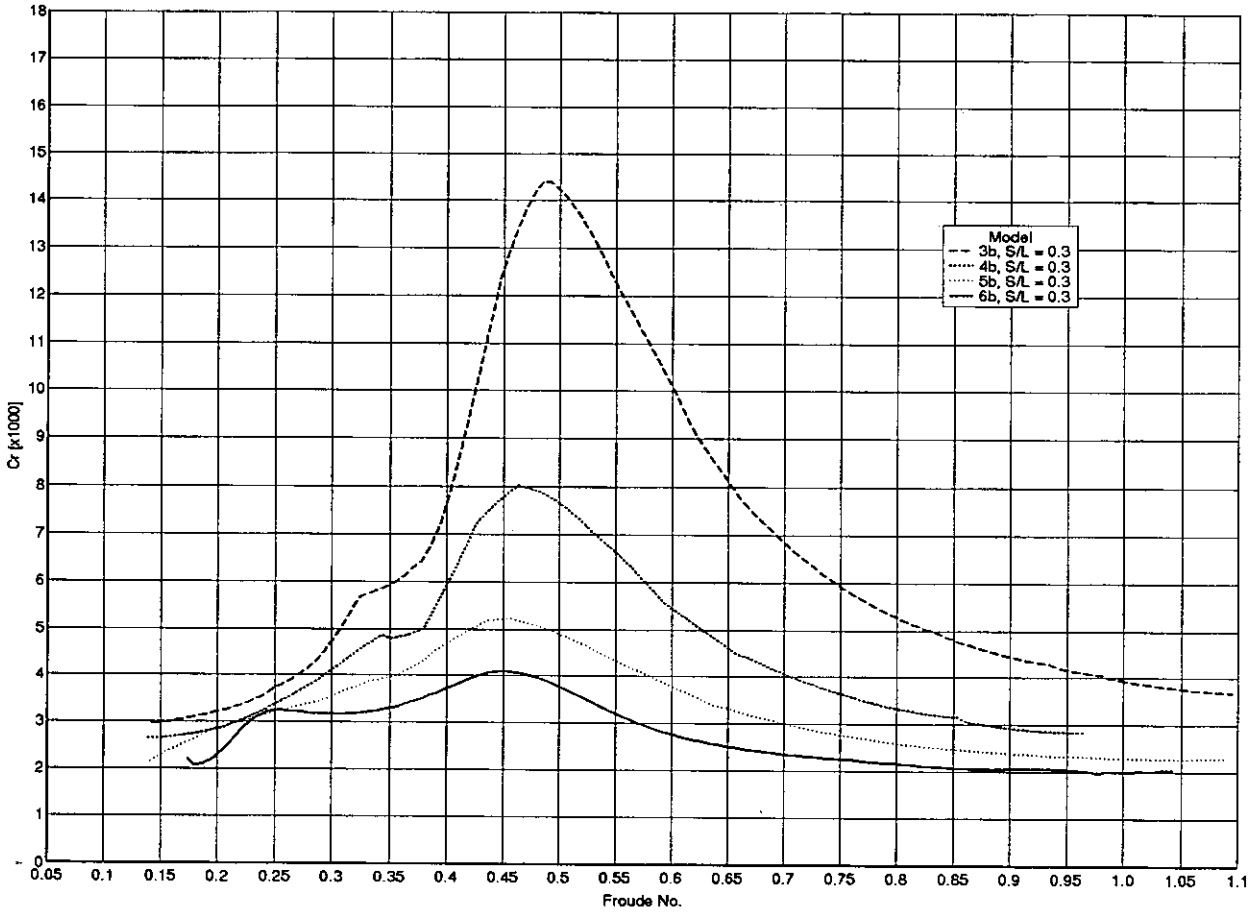

Fig 44a. Residuary Resistance: Models: 3b,4b,5b,6b (S/L = 0.3)

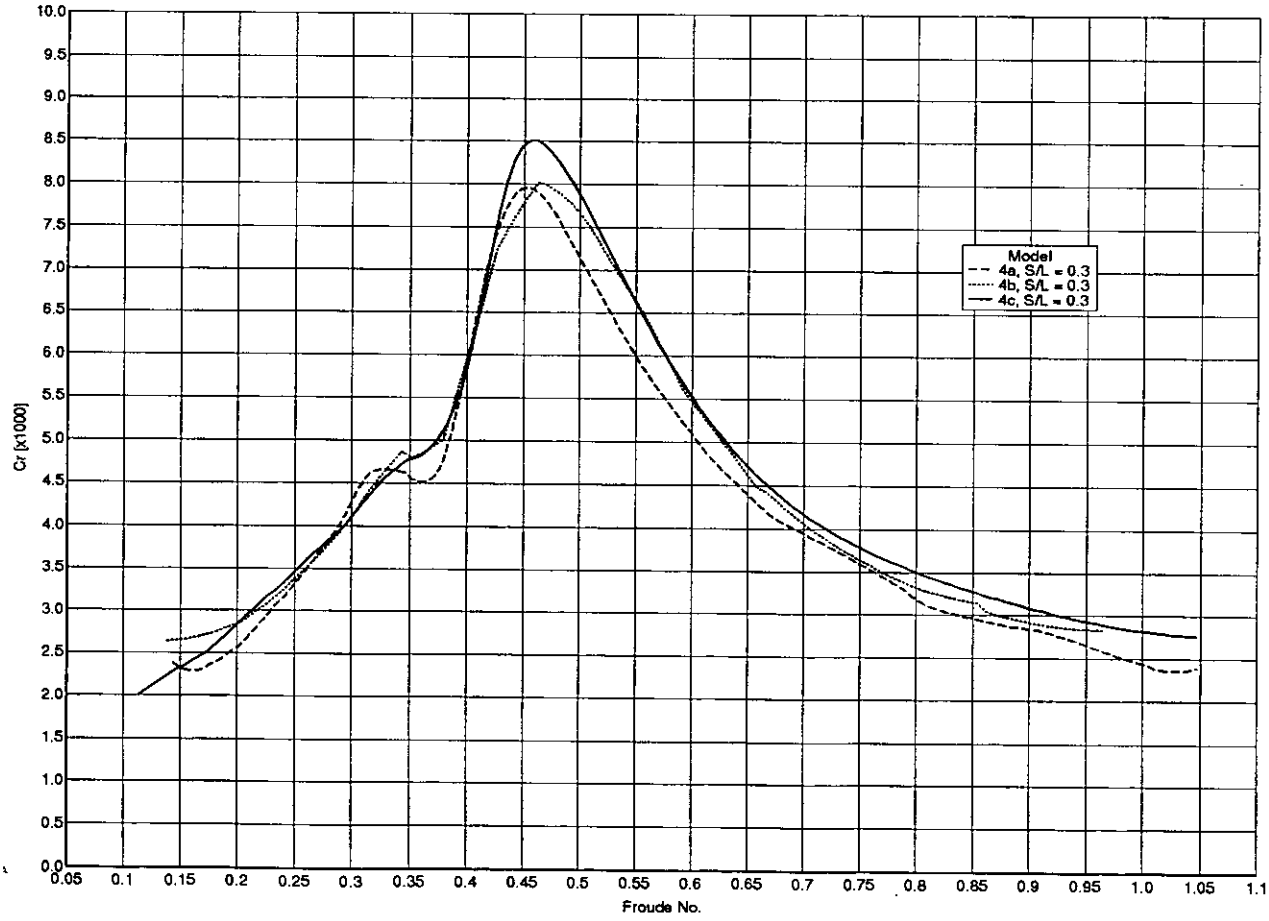

Fig 44b. Residuary Resistance: Models: 4a,4b,4c (S/L = 0.3)

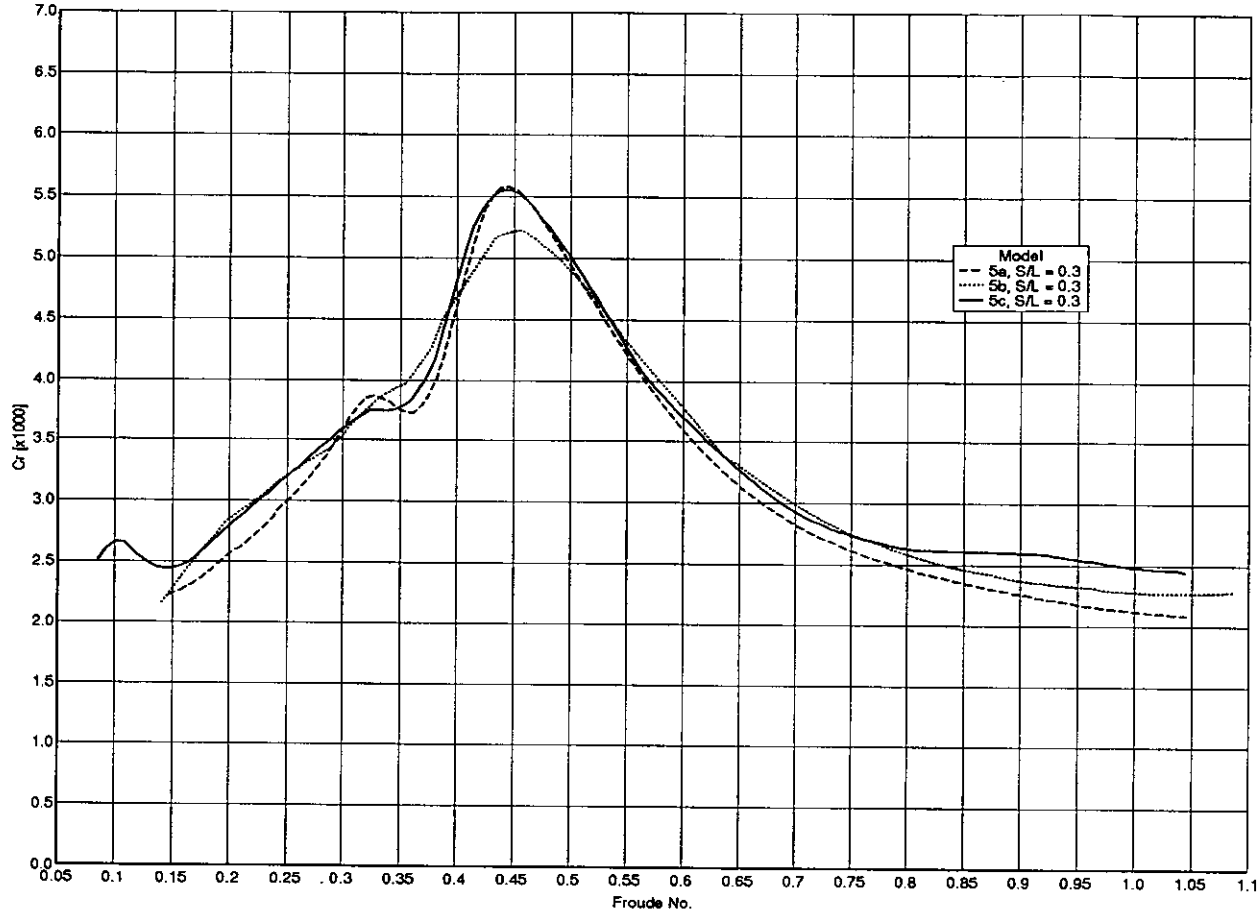

Fig 44c. Residuary Resistance: Models: 5a,5b,5c (S/L = 0.3)

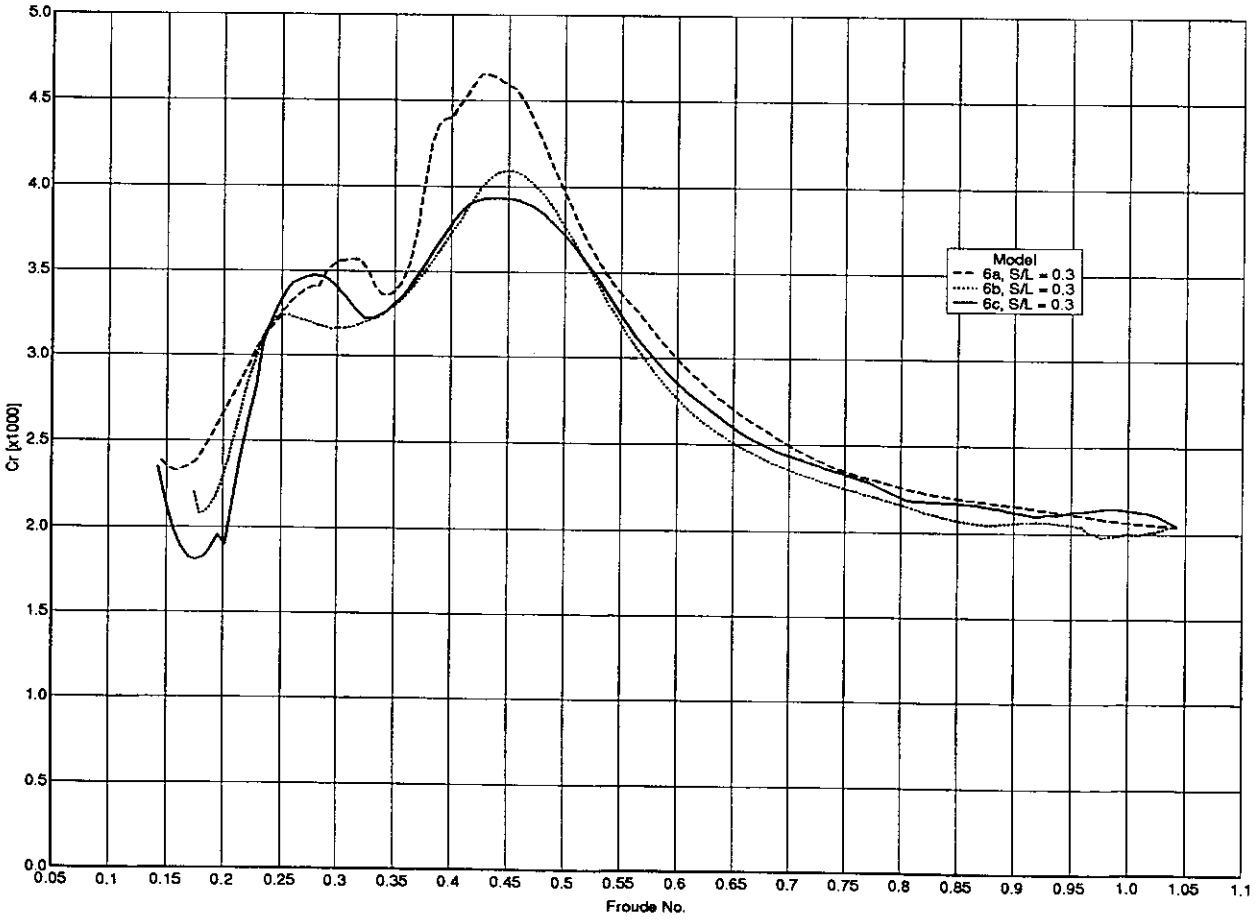

Fig 44d. Residuary Resistance: Models: 6a,6b,6c (S/L = 0.3)

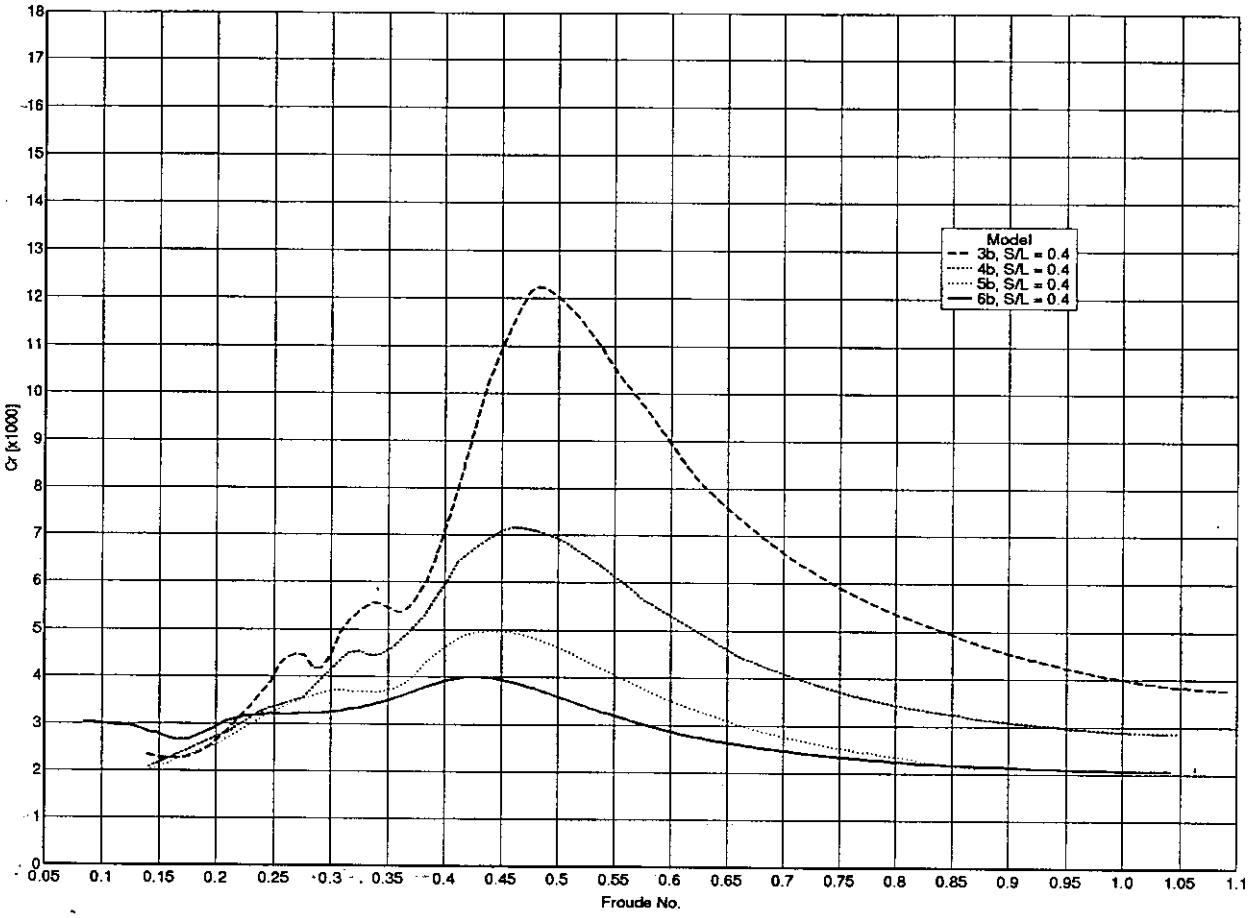

Fig 45a: Residuary Resistance: Models: 3b,4b,5b,6b (S/L = 0.4)

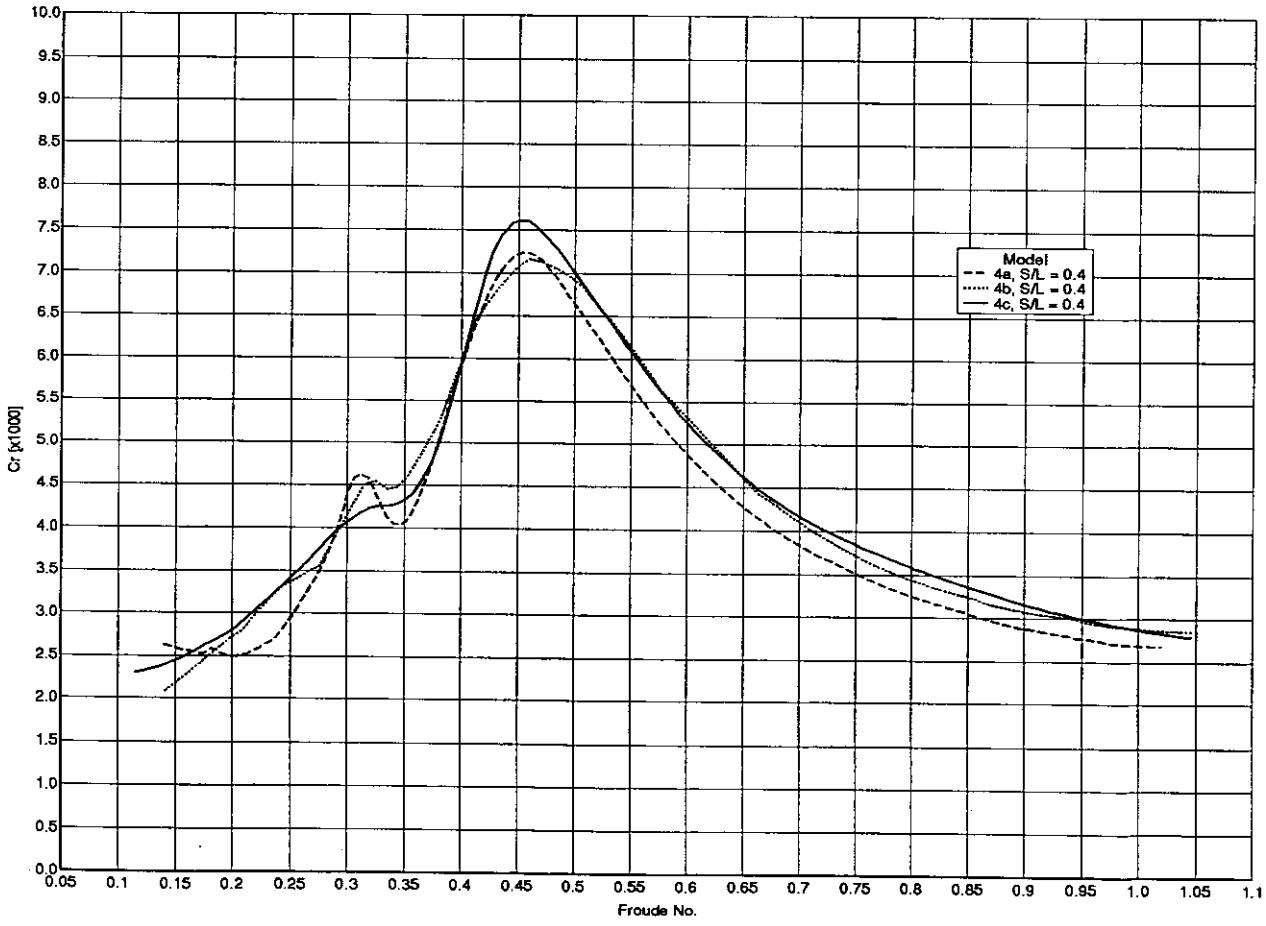

Fig 45b. Residuary Resistance: Models: 4a,4b,4c (S/L = 0.4)

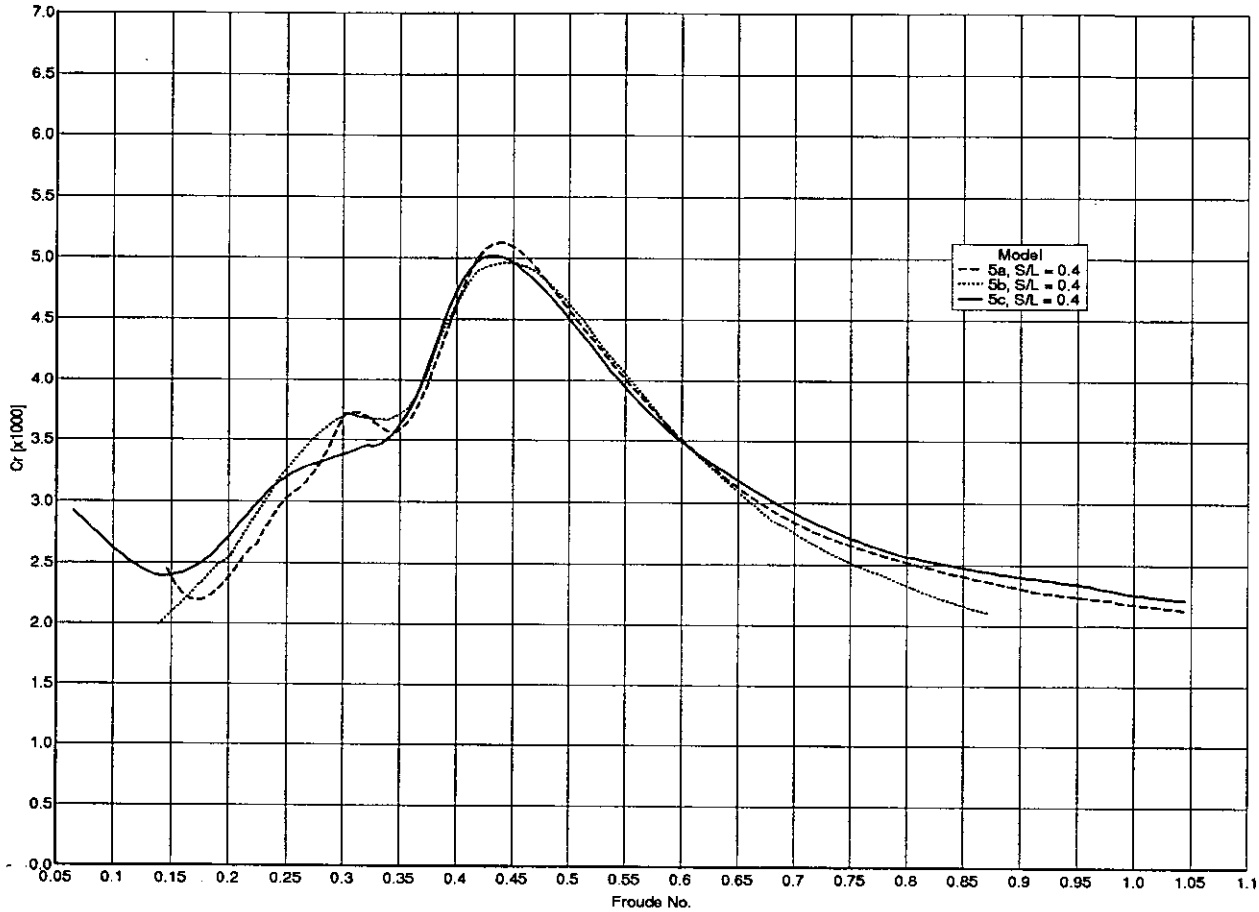

Fig 45c. Residuary Resistance: Models: 5a,5b,5c (S/L = 0.4)

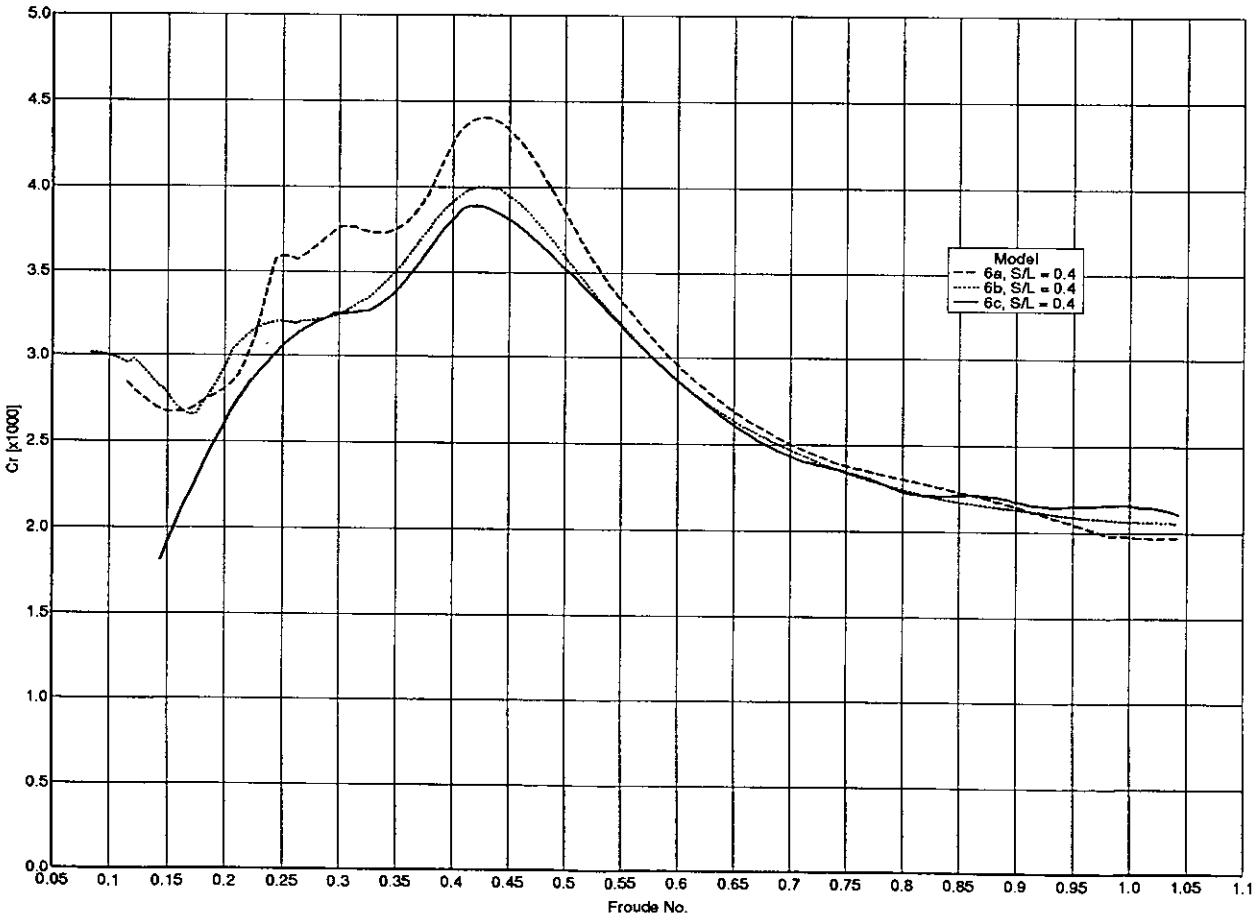

Fig 45d. Residuary Resistance: Models: 6a,6b,6c (S/L = 0.4)

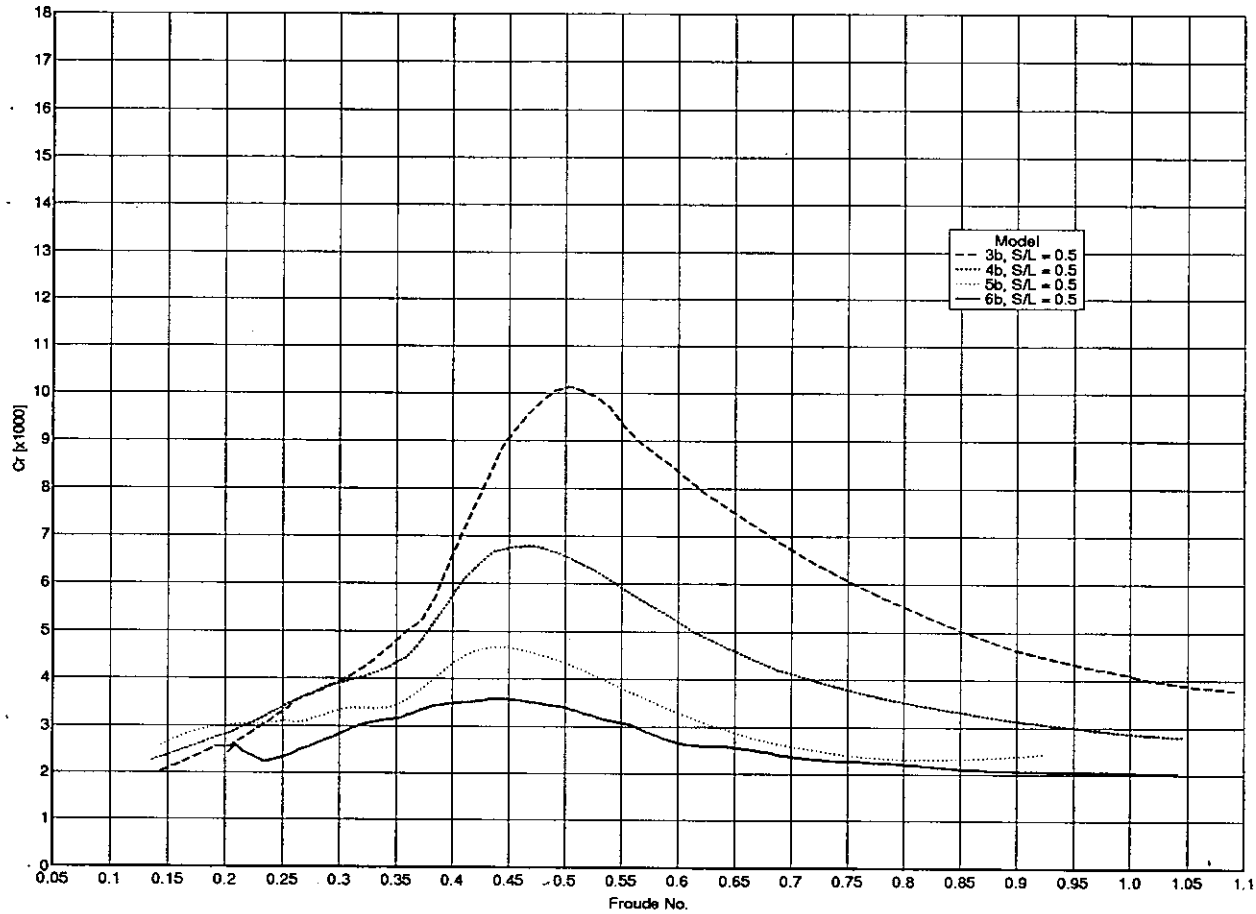

Fig 46a. Residuary Resistance: Models: 3b,4b,5b,6b (S/L = 0.5)

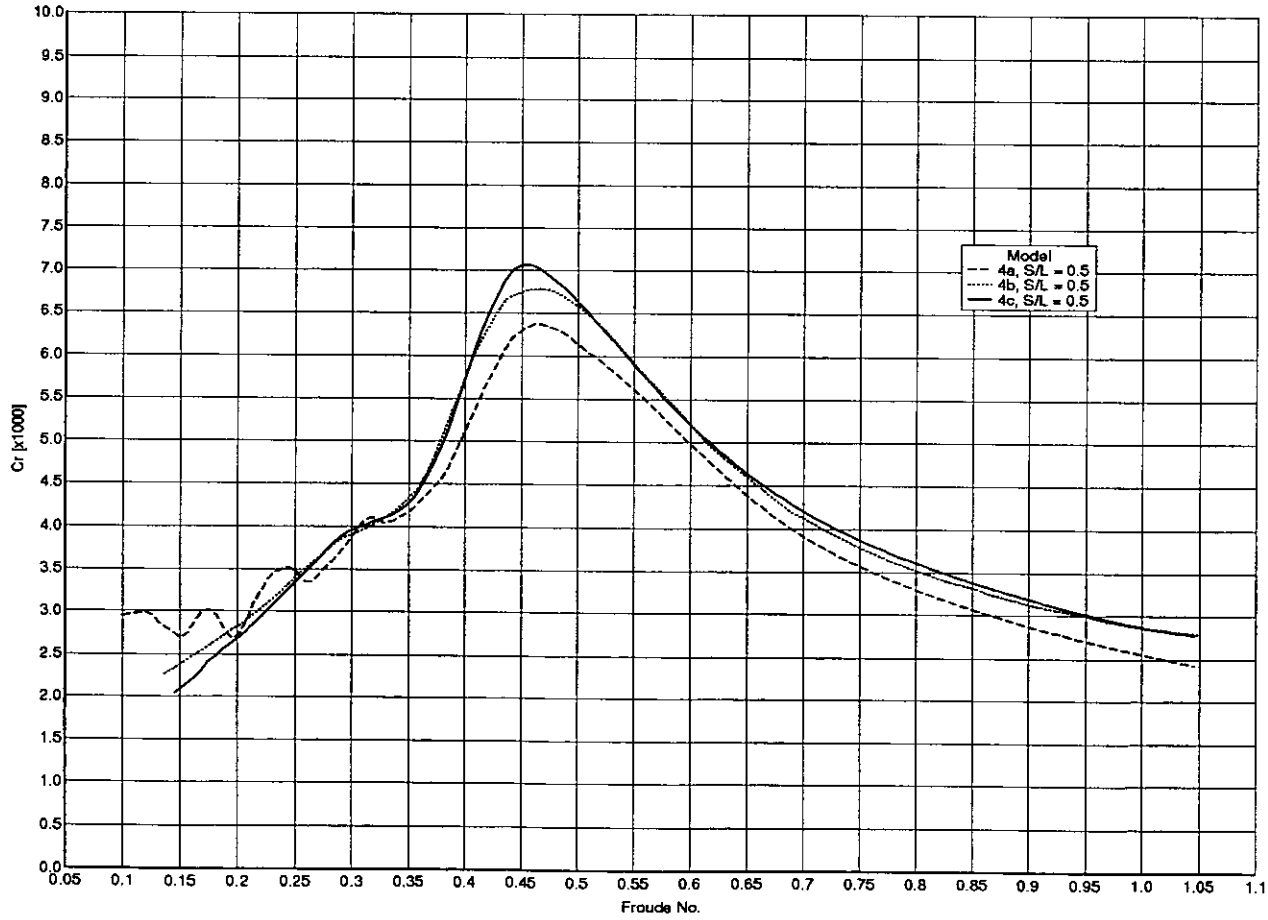

Fig 46b. Residuary Resistance: Models: 4a,4b,4c (S/L = 0.5)

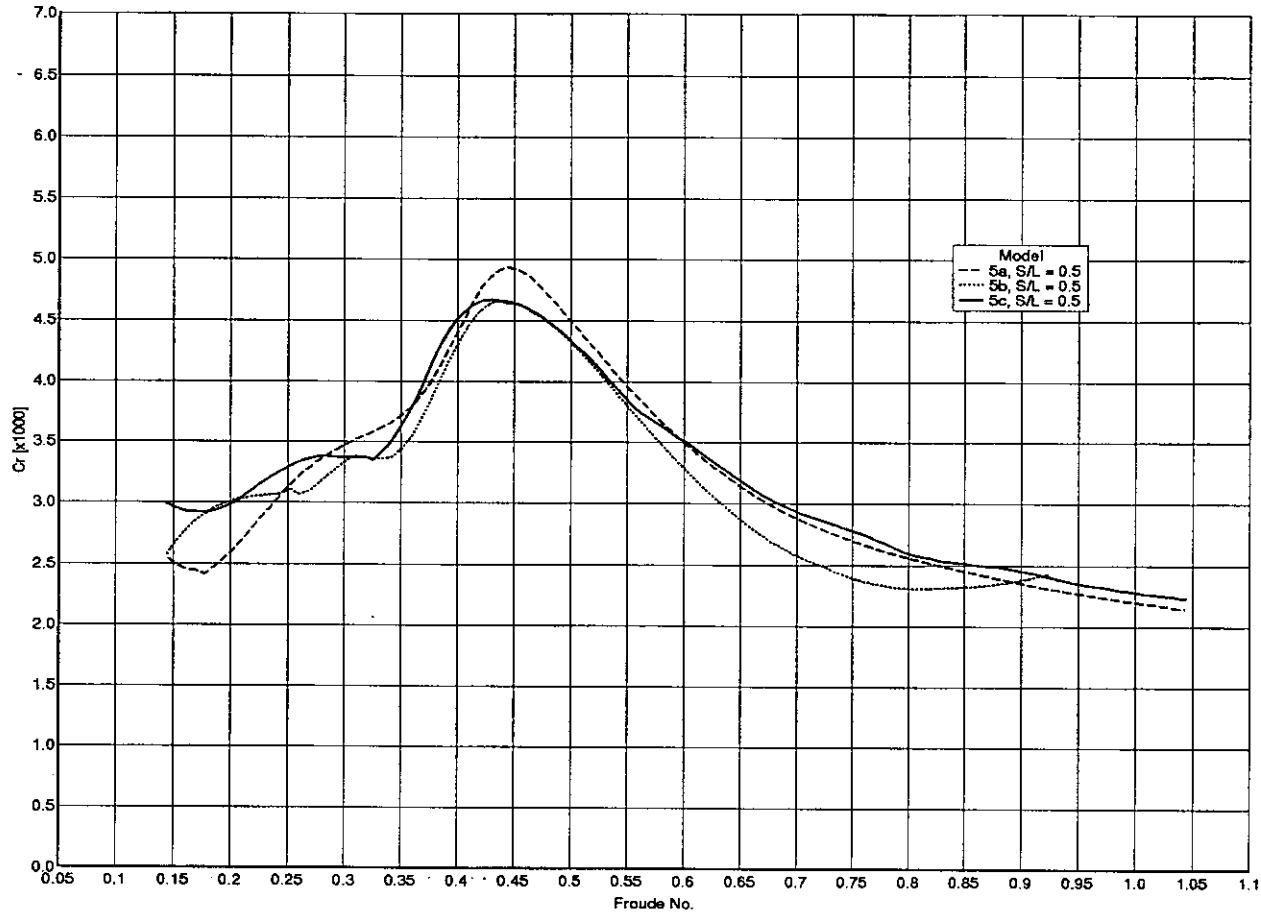

Fig 46c. Residuary Resistance: Models: 5a,5b,5c (S/L = 0.5)

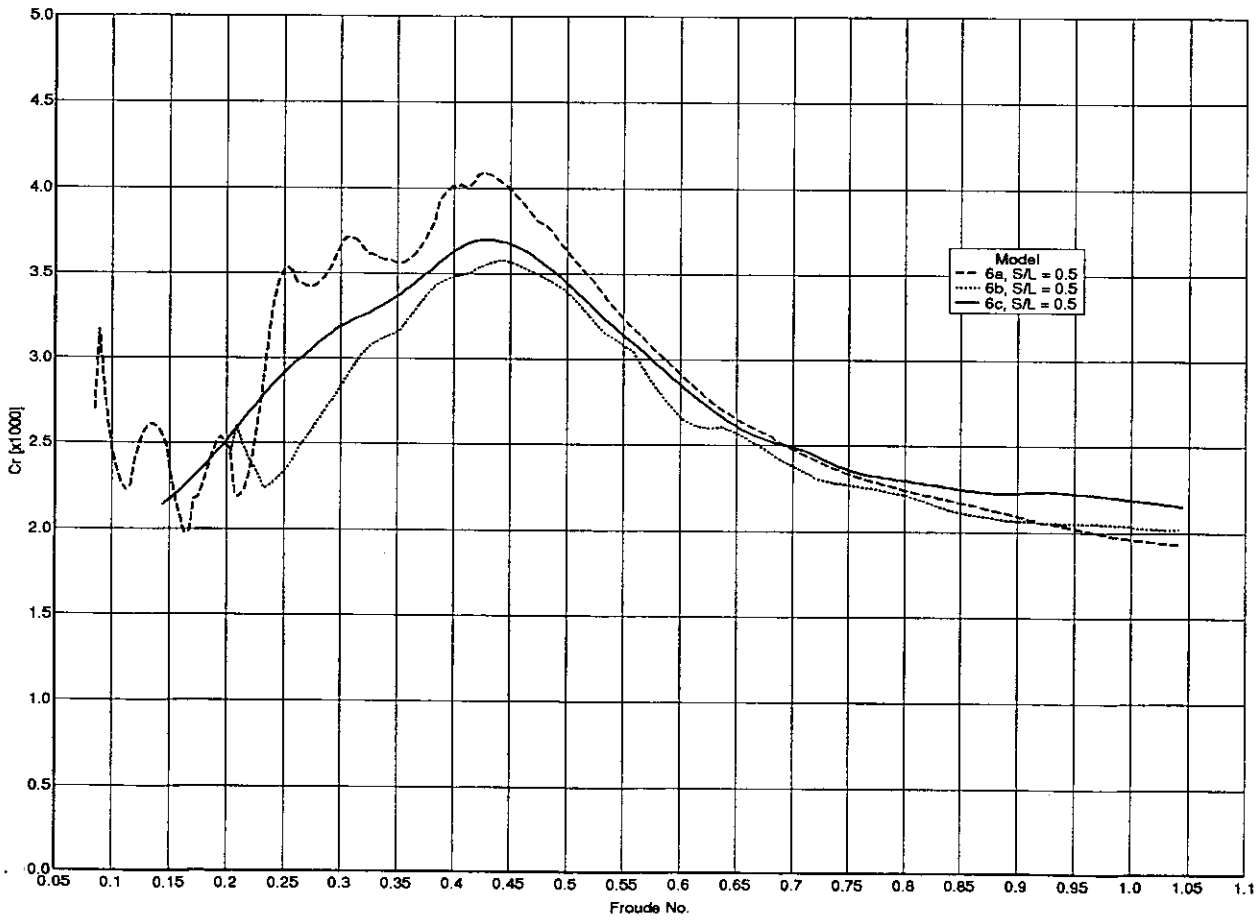

Fig 46d. Residuary Resistance: Models: 6a,6b,6c (S/L = 0.5)

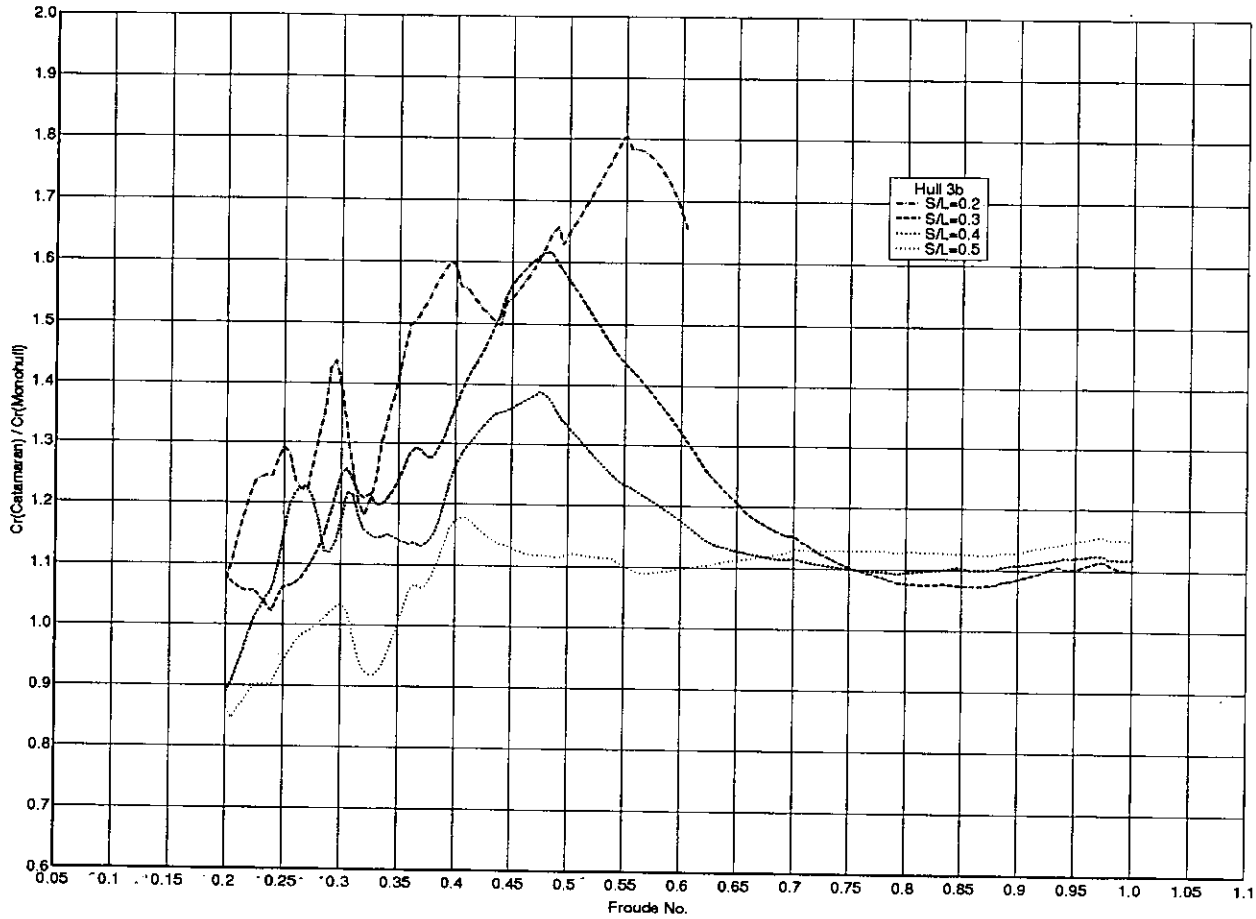

Fig 47. Residuary Resistance Interference Factor: Models 3b

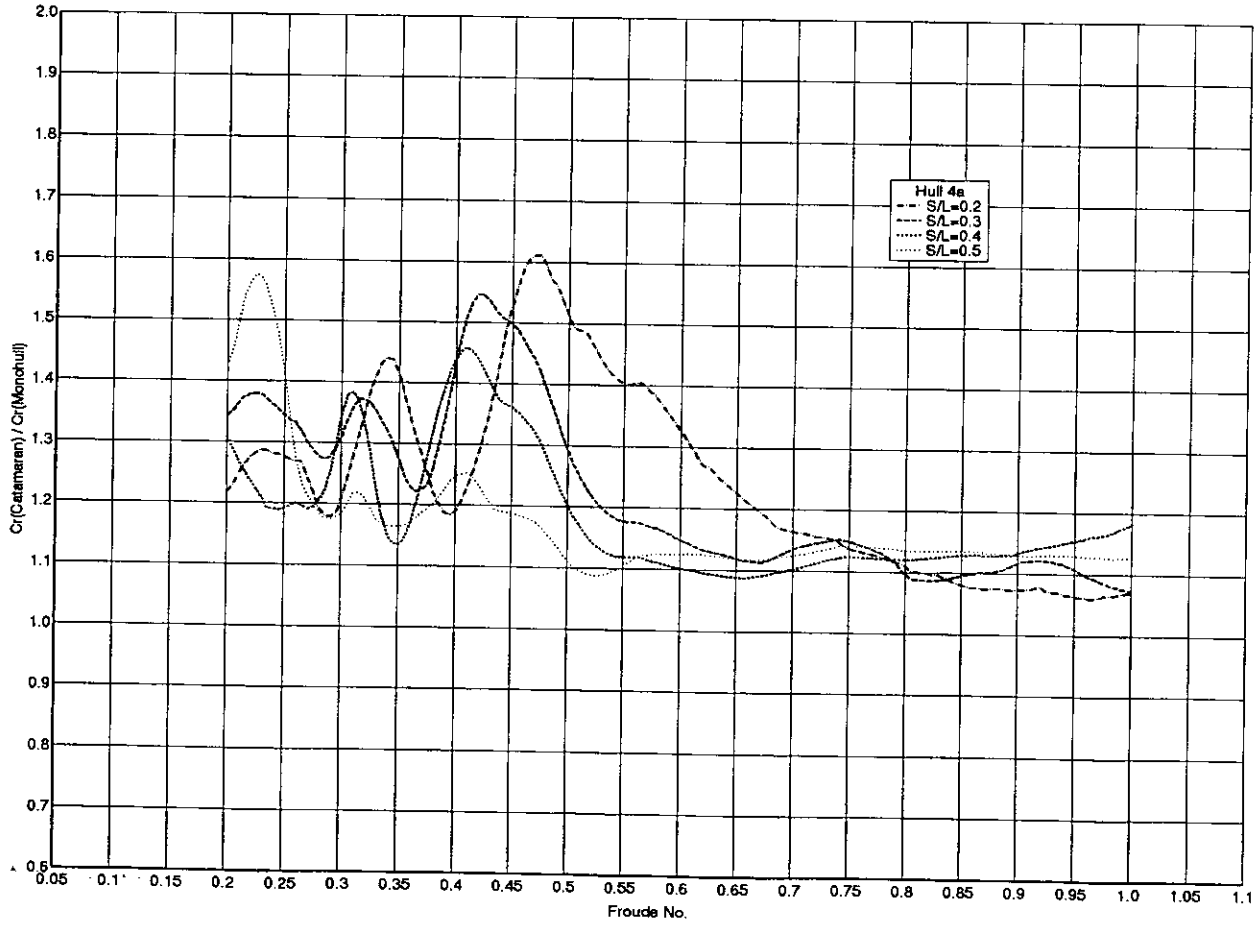

Fig 48. Residuary Resistance Interference Factor: Models 4a

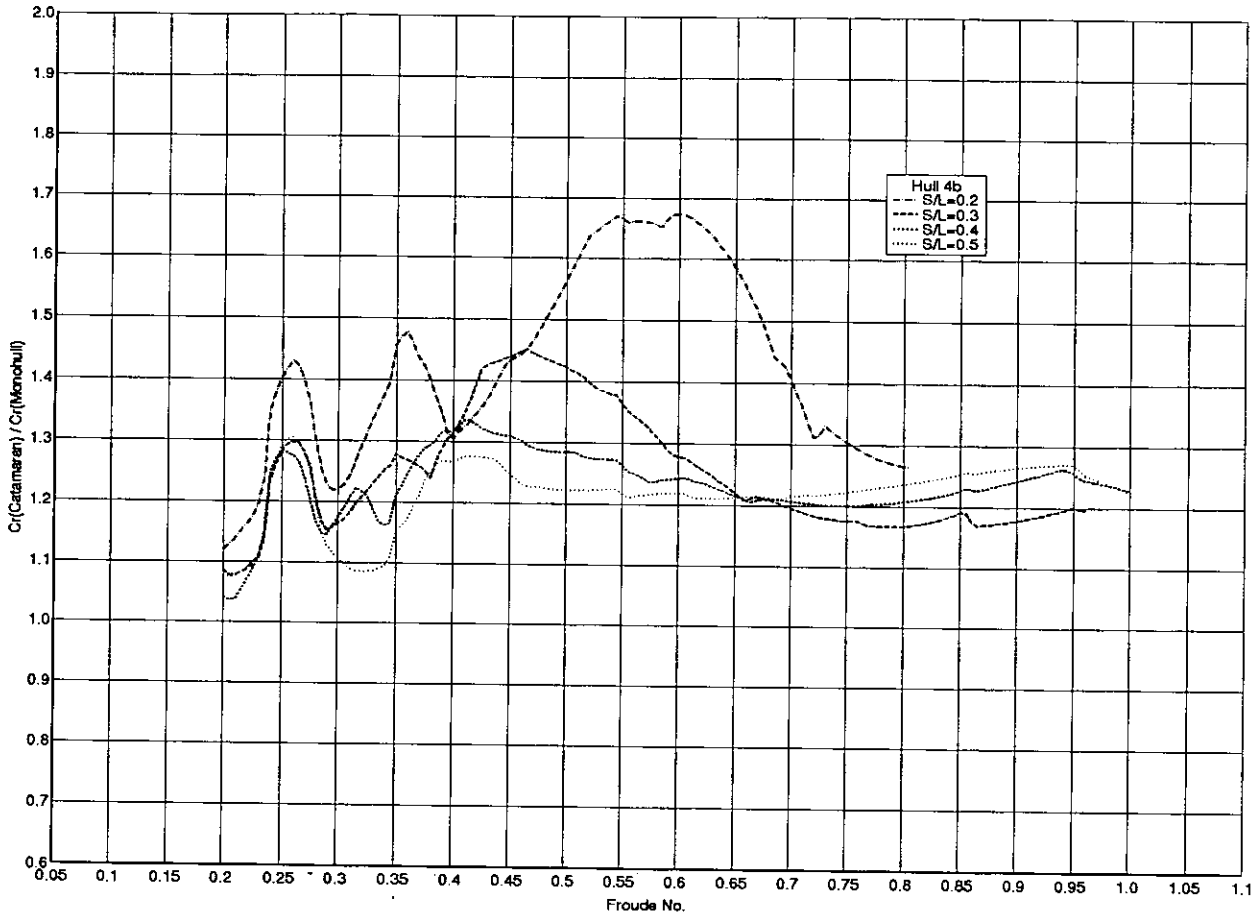

Fig 49. Residuary Resistance Interference Factor: Models 4b

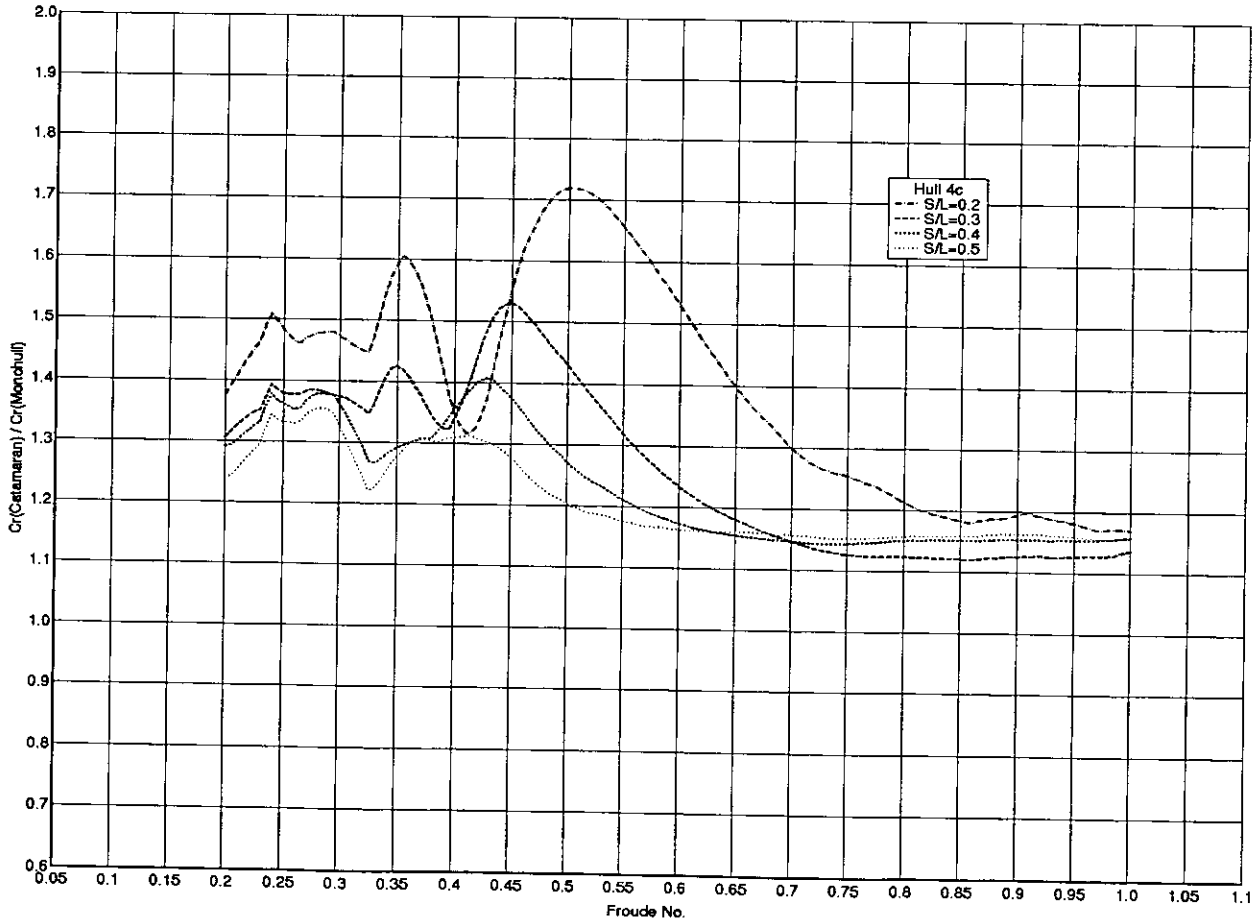

Fig 50. Residuary Resistance Interference Factor: Models 4c

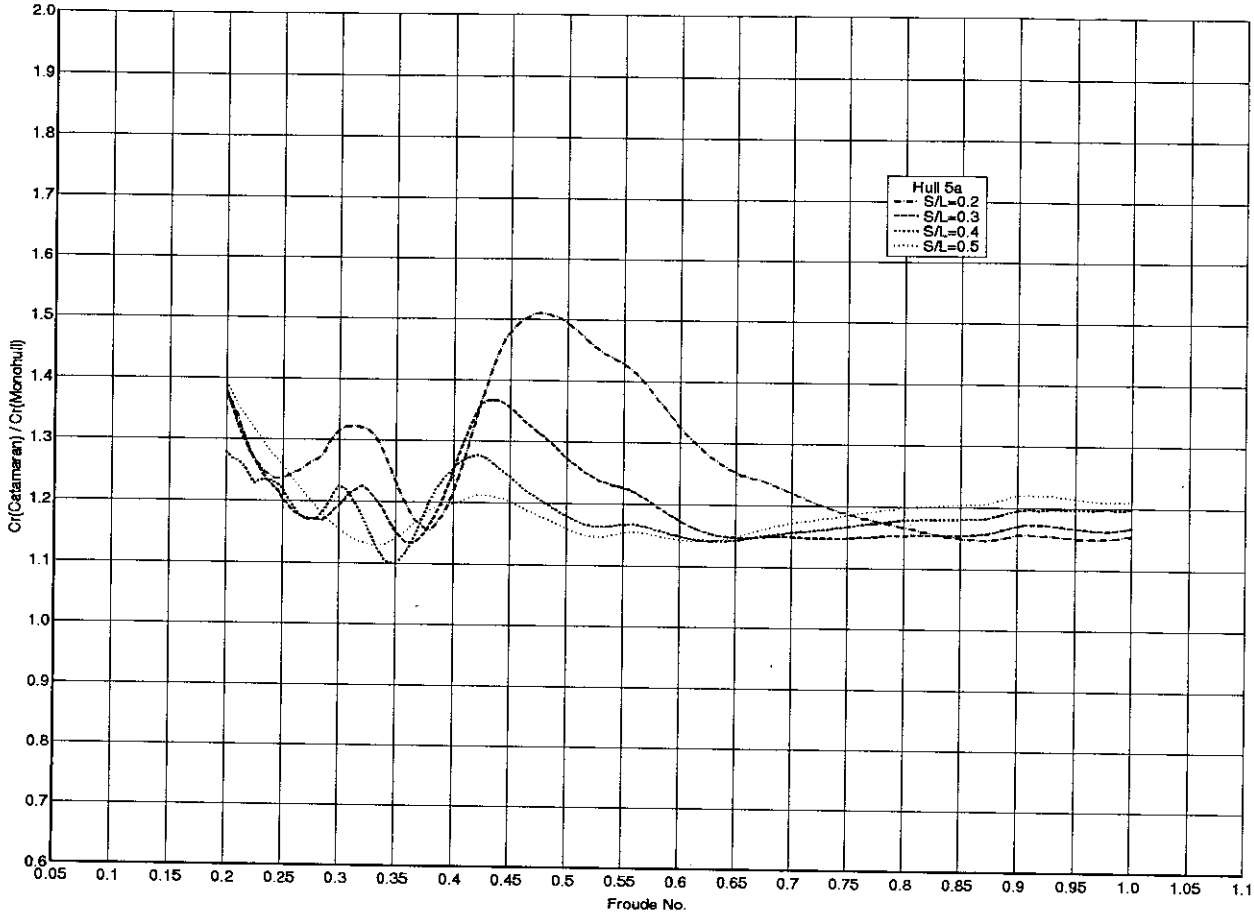

Fig 51. Residuary Resistance Interference Factor: Models 5a

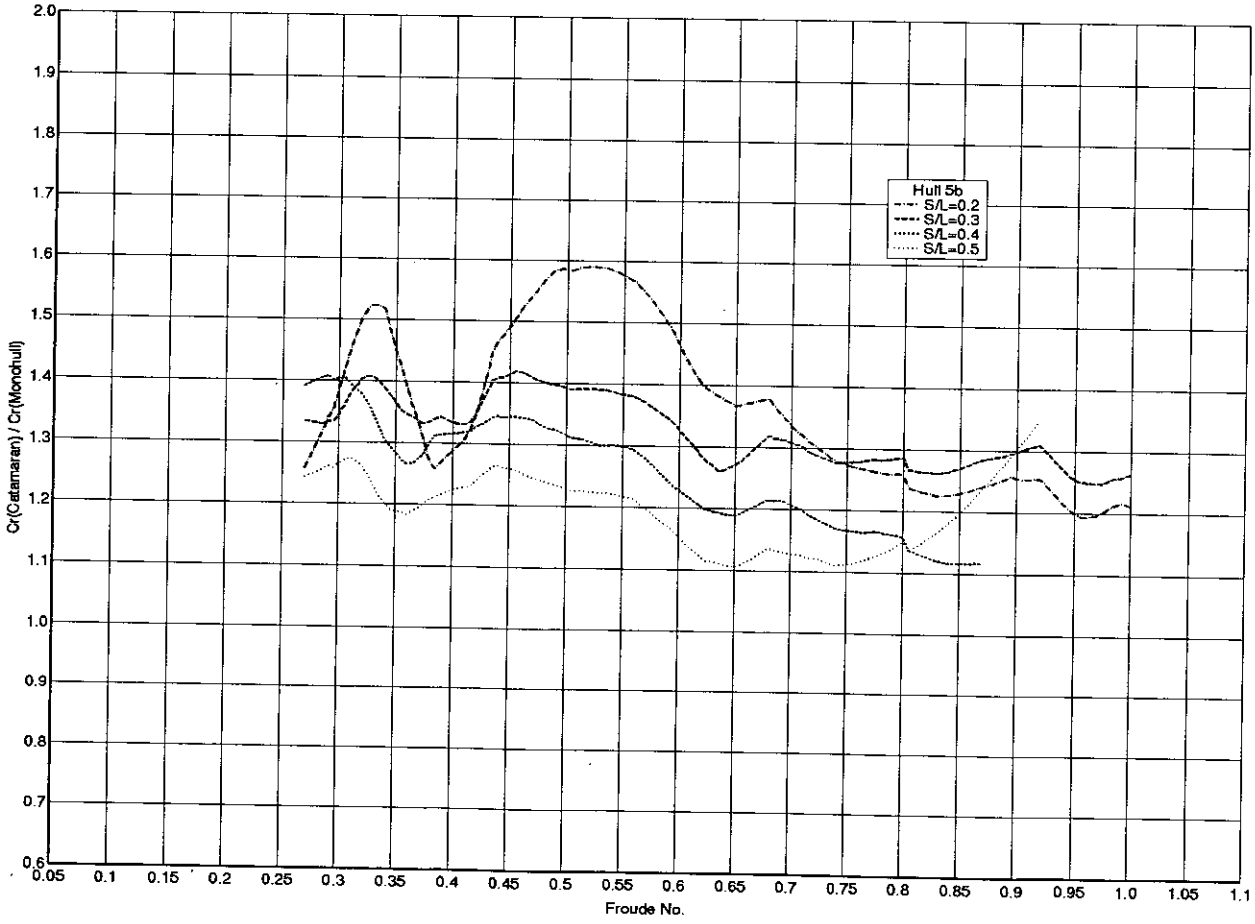

Fig 52. Residuary Resistance Interference Factor: Models 5b

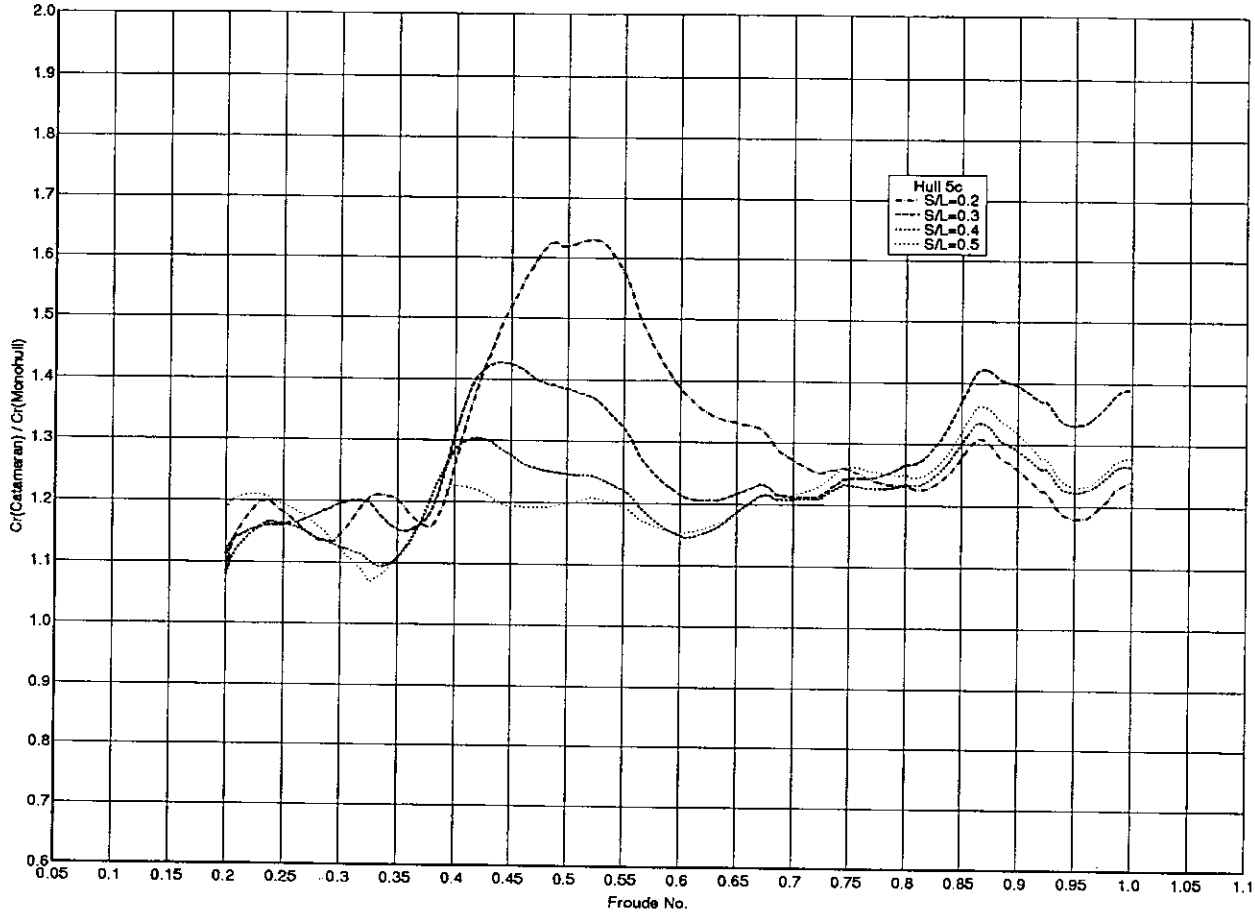

Fig 53. Residuary Resistance Interference Factor: Models 5c

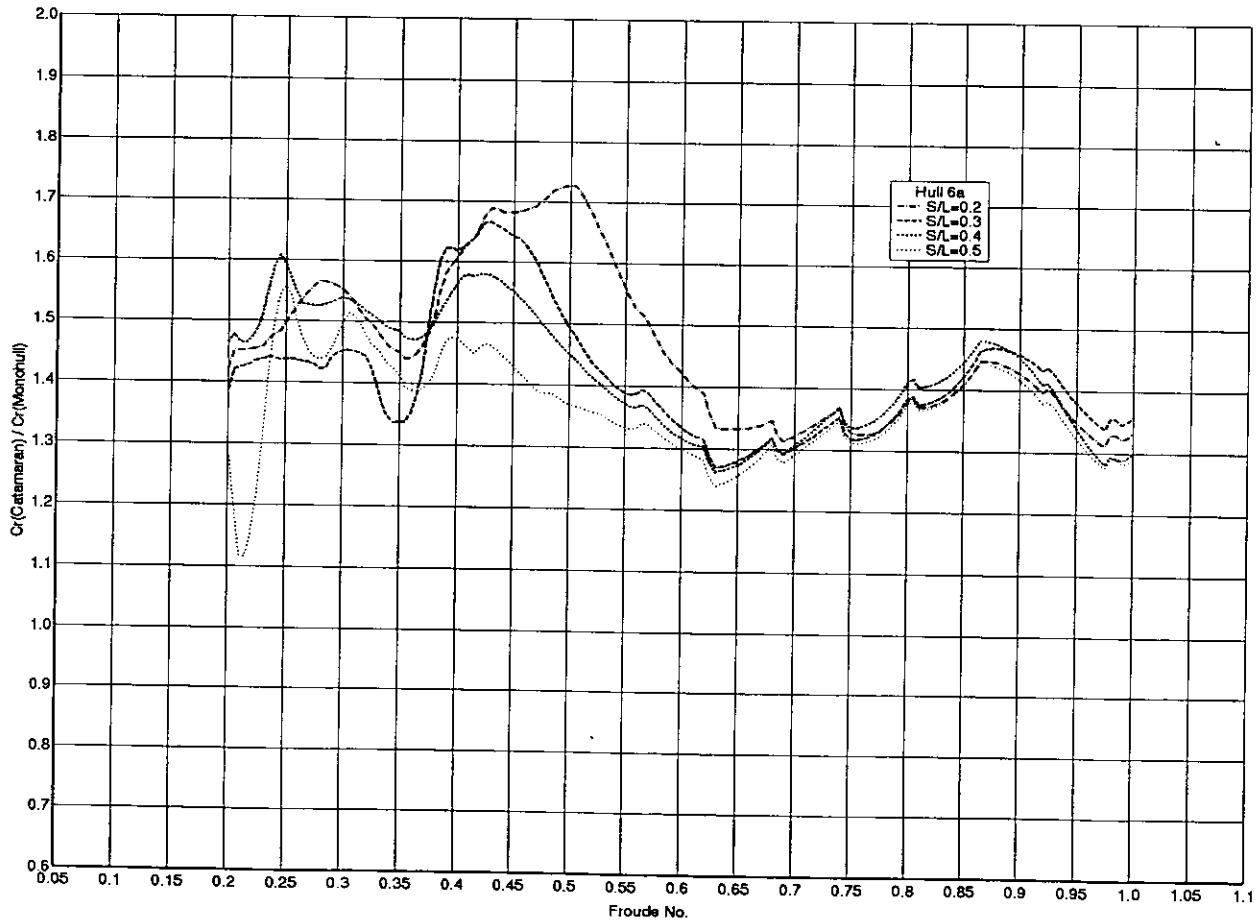

Fig 54. Residuary Resistance Interference Factor: Models 6a

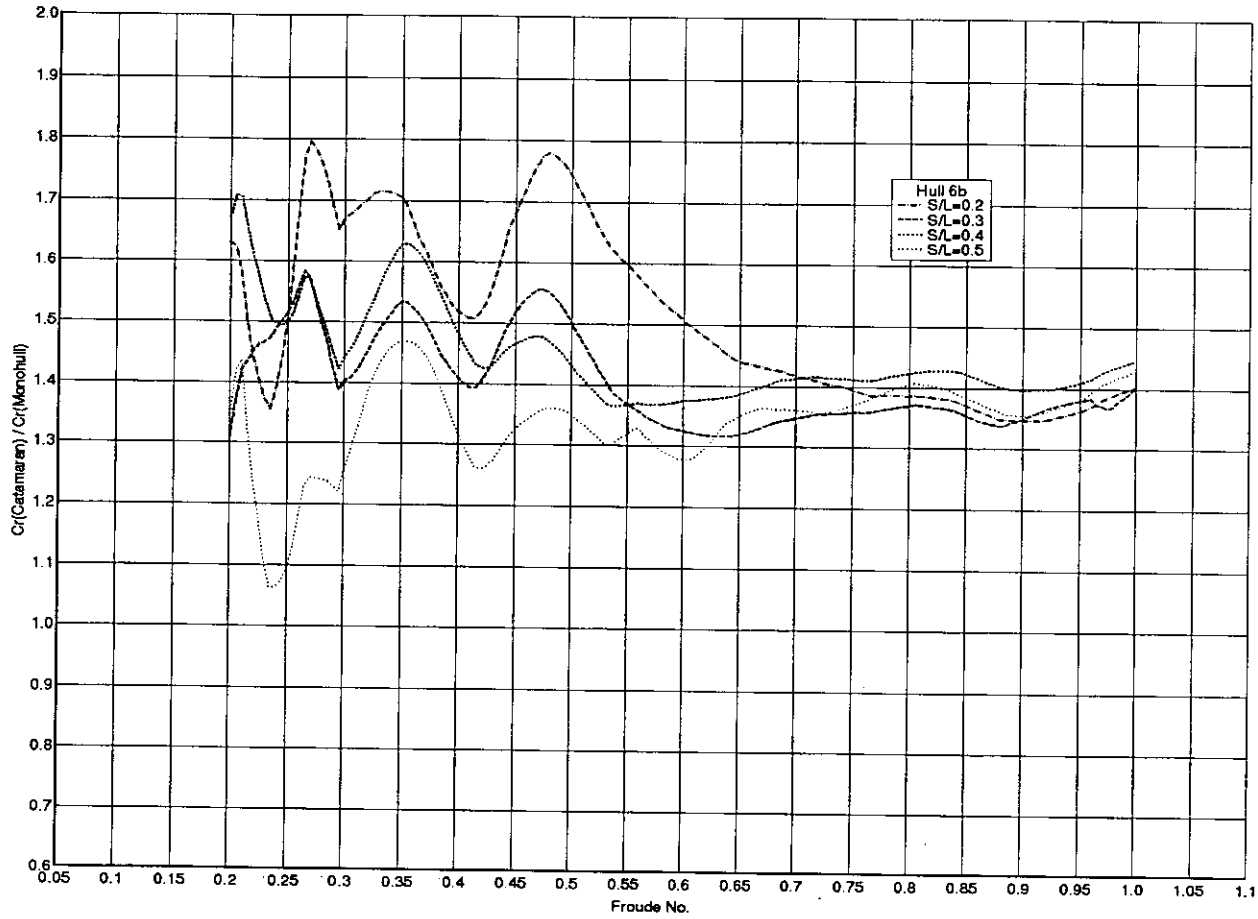

Fig 55. Residuary Resistance Interference Factor: Models 6b

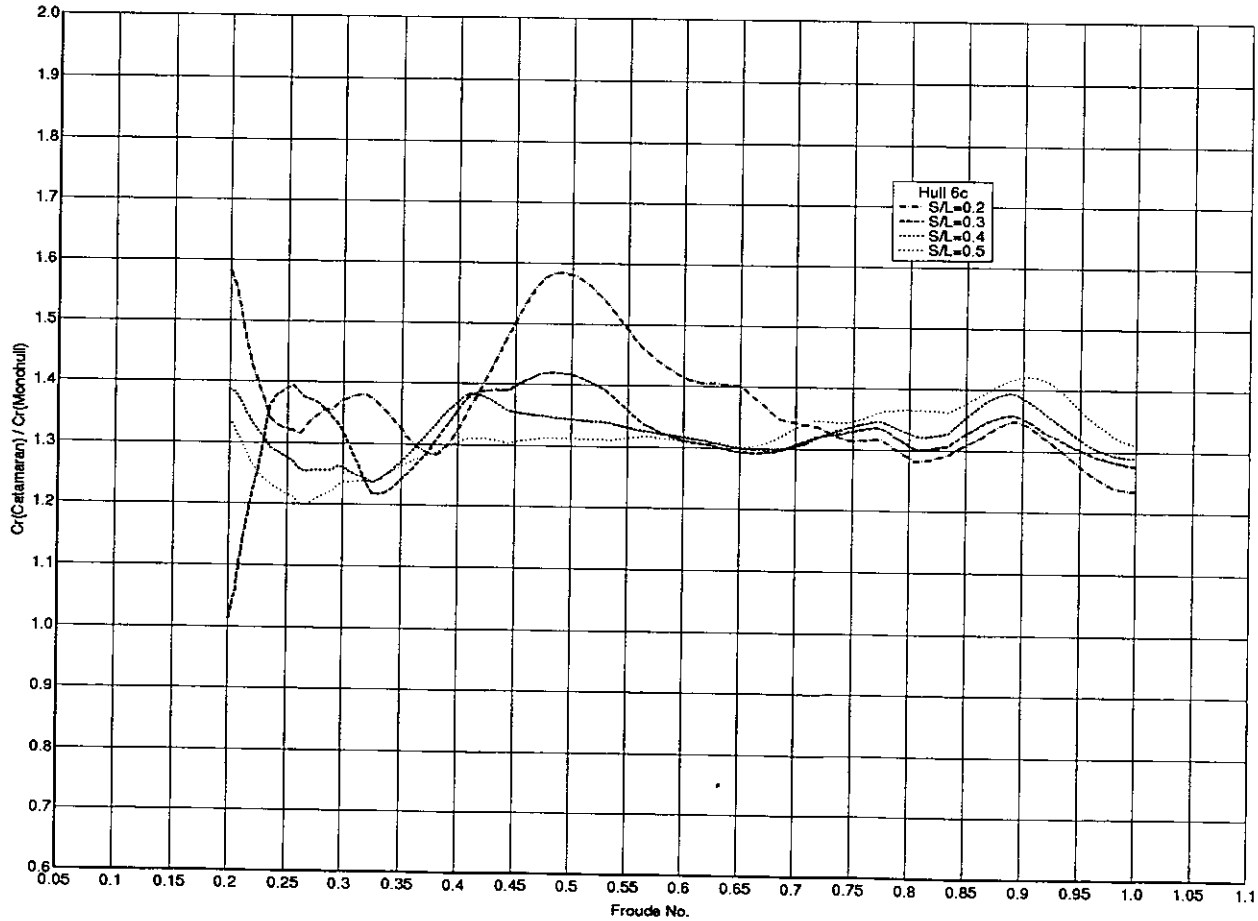

Fig 56. Residuary Resistance Interference Factor: Models 6c

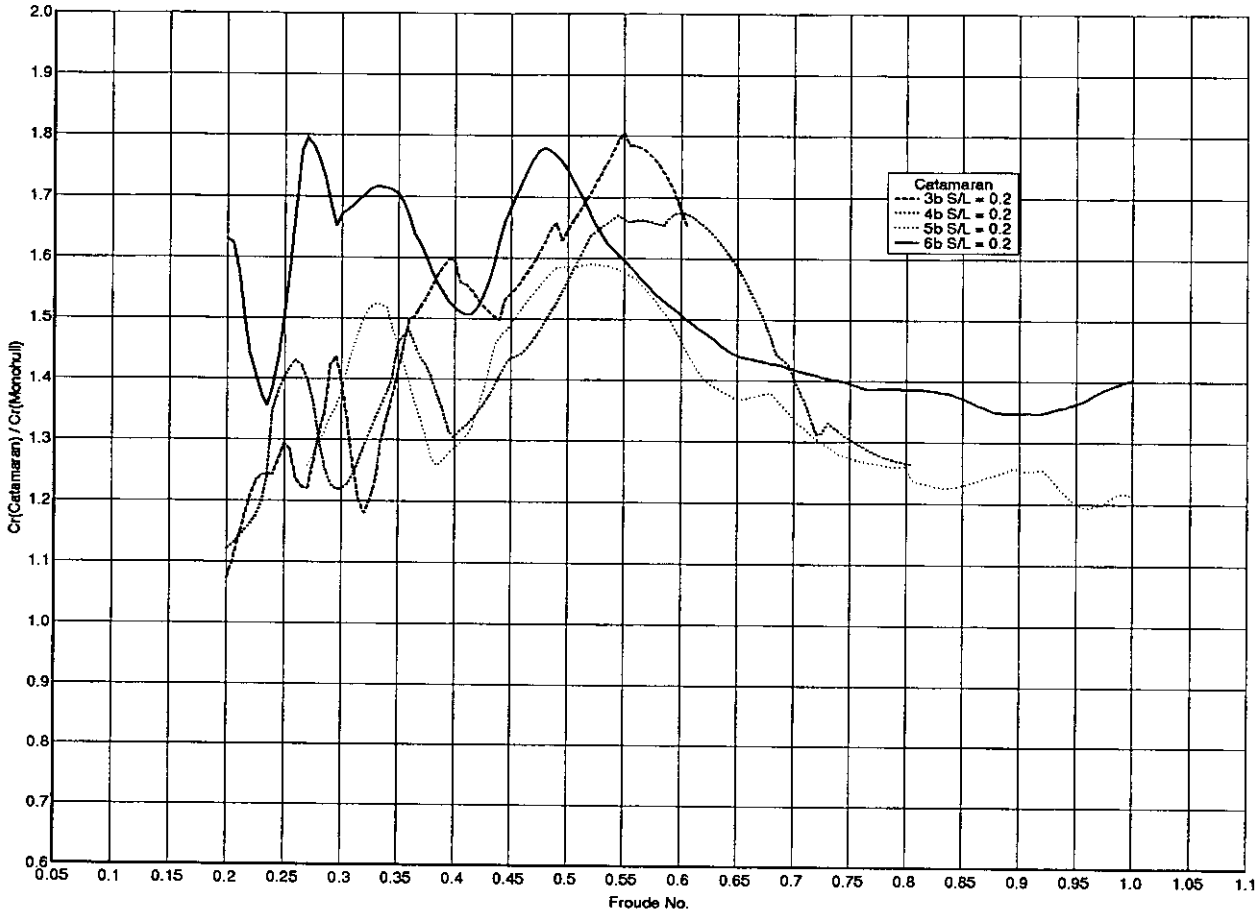

Fig 57. Residuary Resistance Interference Factor: S/L = 0.2

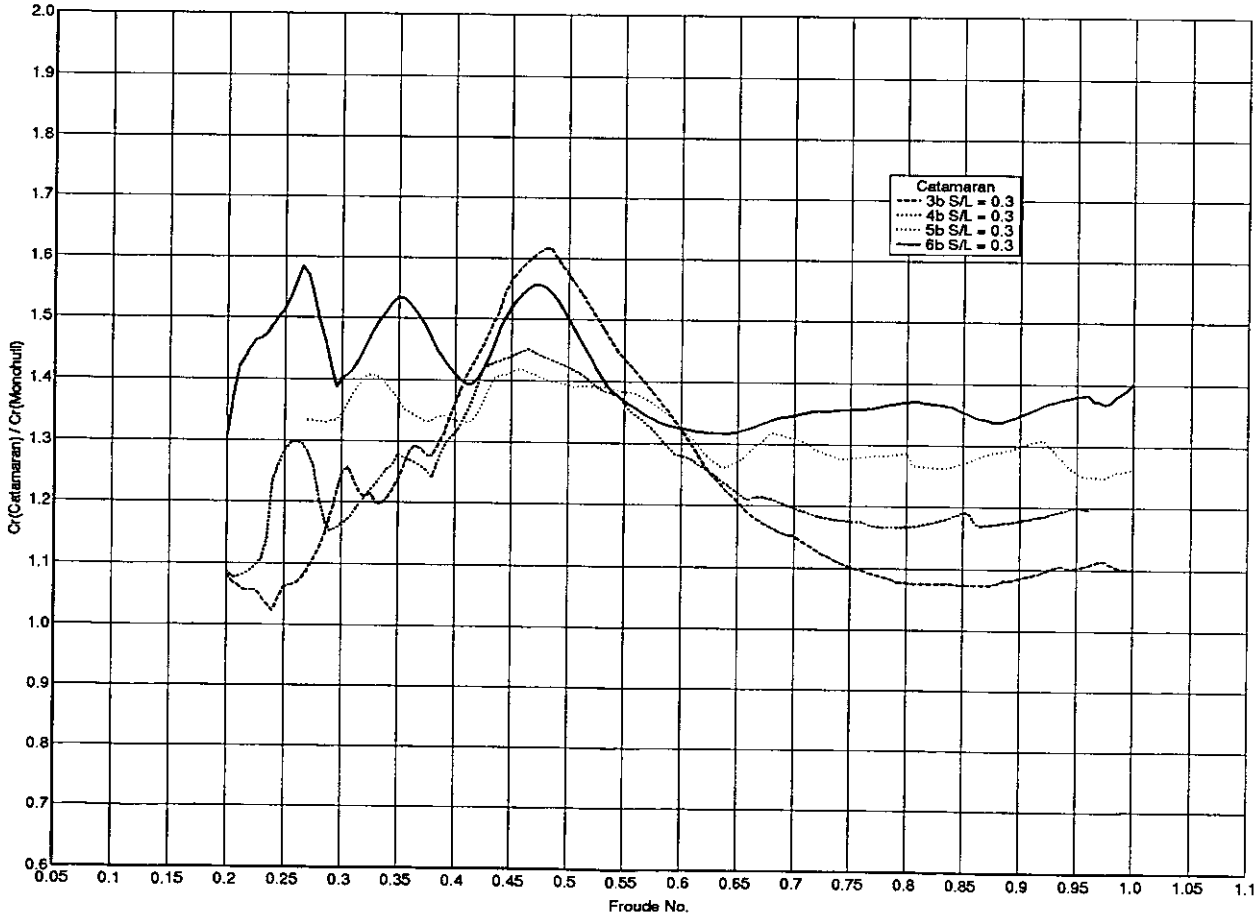

Fig 58. Residuary Resistance Interference Factor: S/L = 0.3

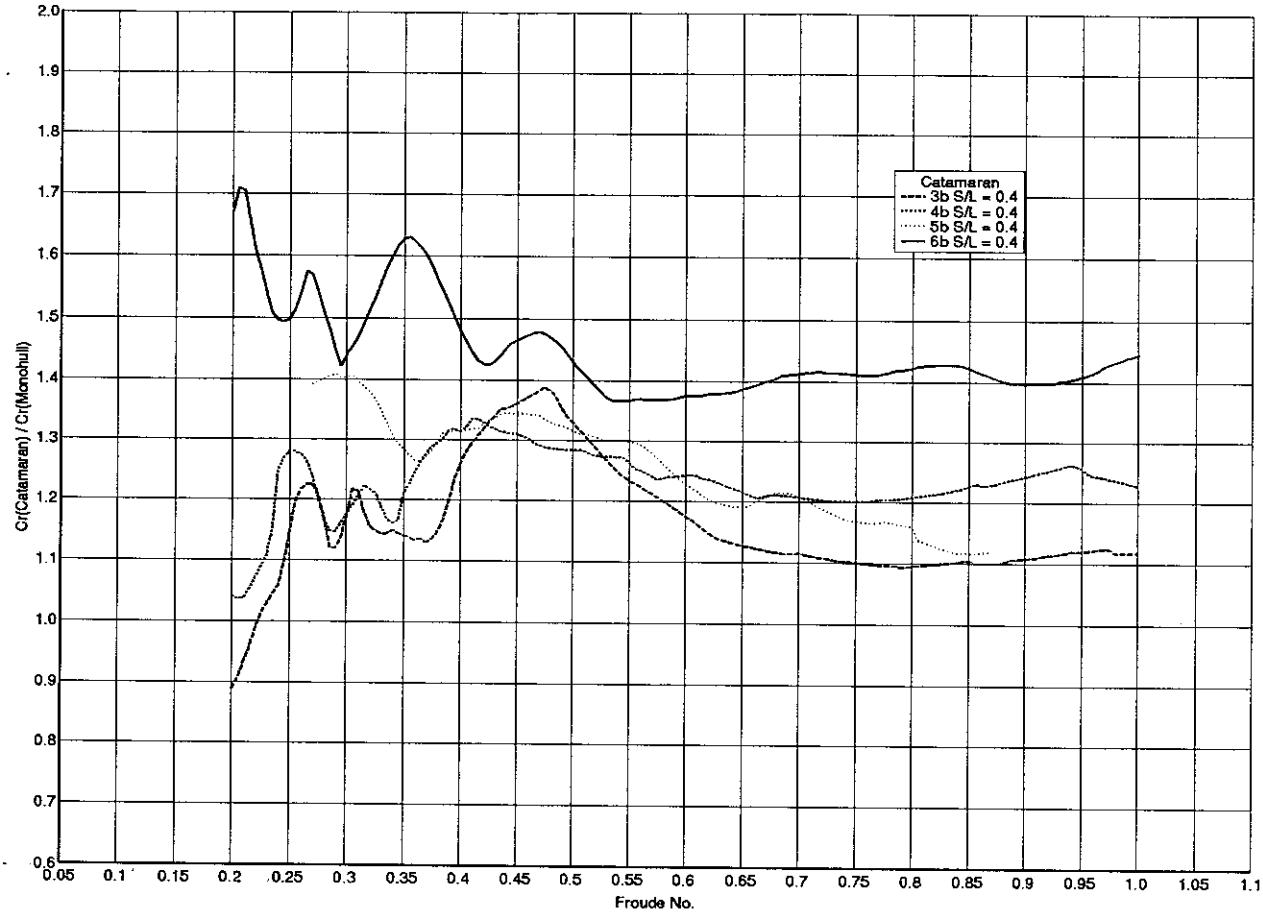

Fig 59. Residuary Resistance Interference Factor: S/L = 0.4

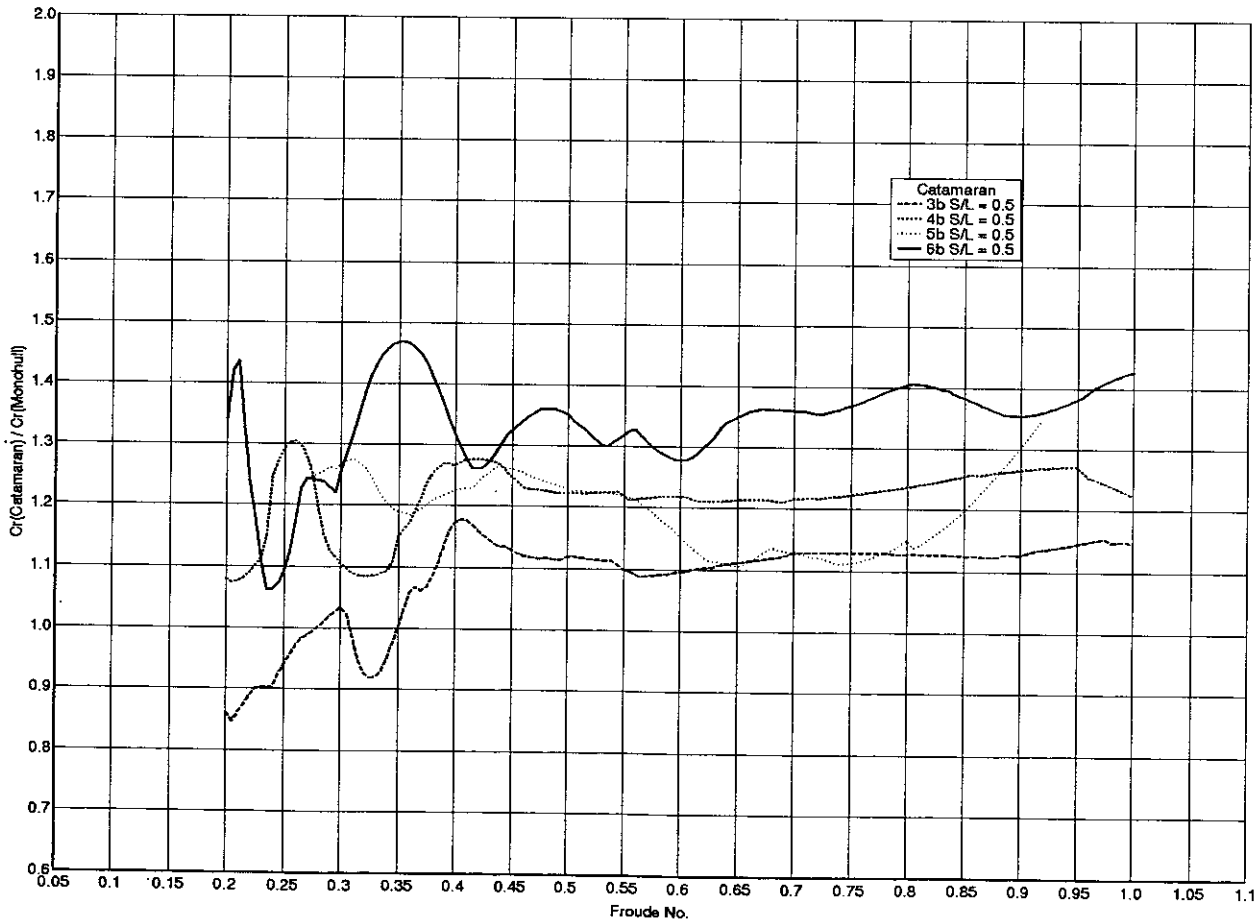

Fig 60. Residuary Resistance Interference Factor: S/L = 0.5

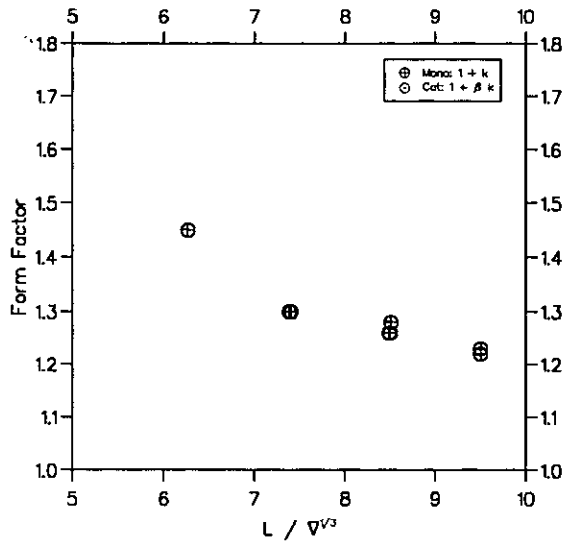

Fig 61a. Monohull

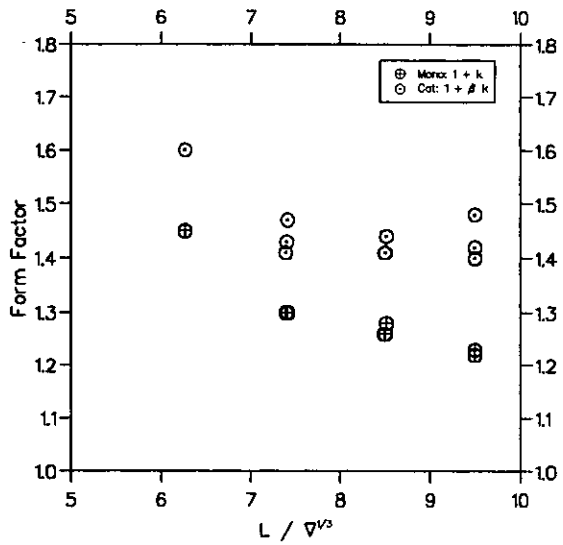

Fig 61b. Form Factors: S/L = 0.2

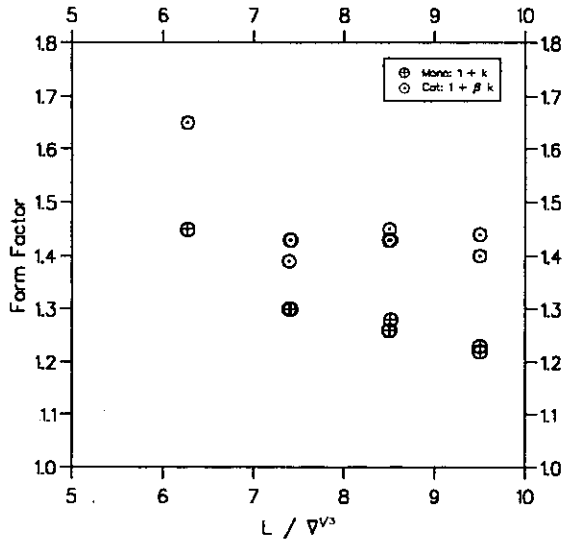

Fig 61c. Form Factors: S/L = 0.3

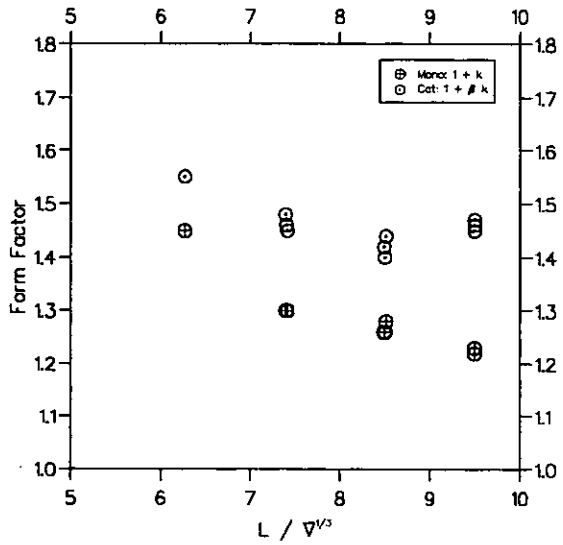

Fig 61d. Form Factors: S/L = 0.4

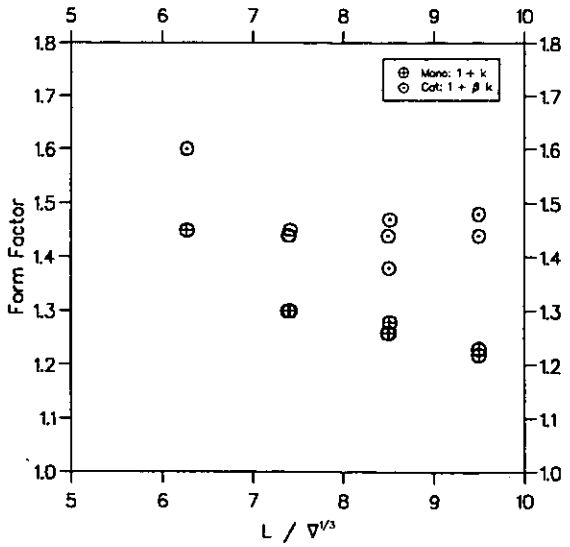

Fig 61e. Form Factors: S/L = 0.5

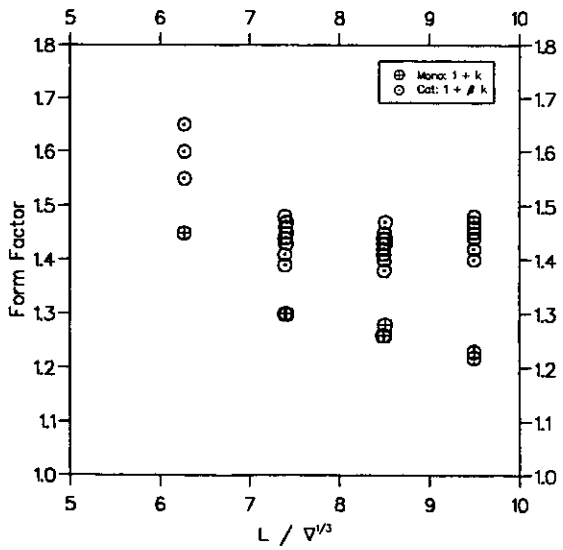

Fig 61f. Form Factors: All Models

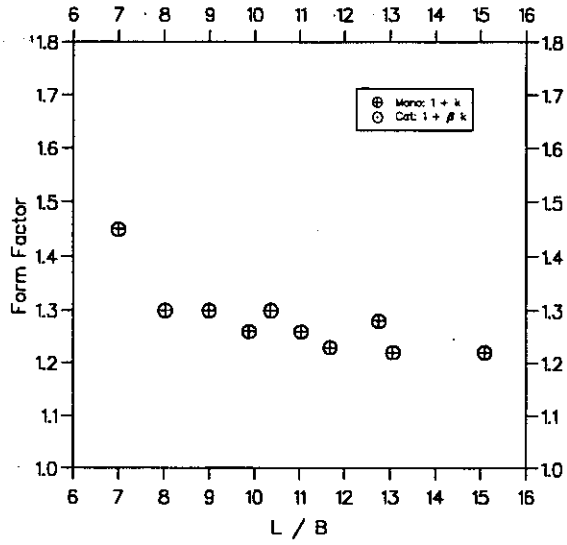

Fig 62a. Form Factors: Monohull

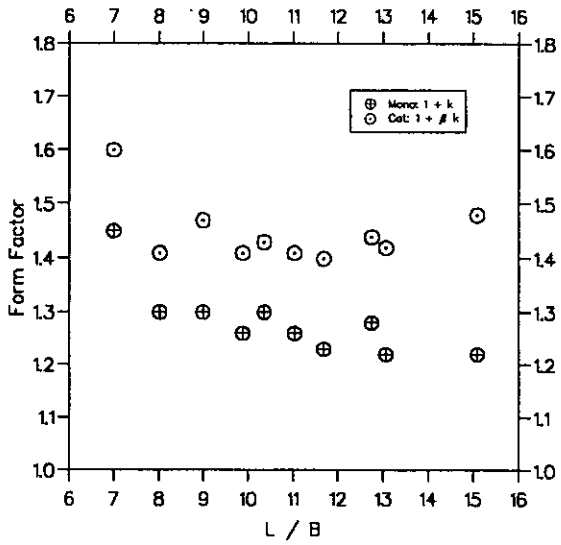

Fig 62b. Form Factors: S/L = 0.2

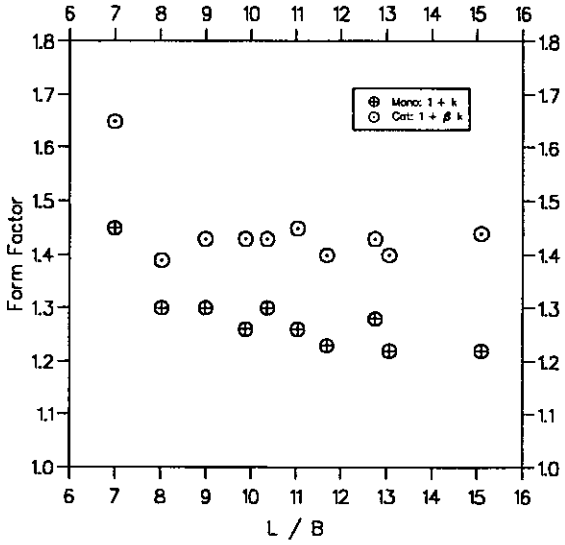

Fig 62c. Form Factors: S/L = 0.3

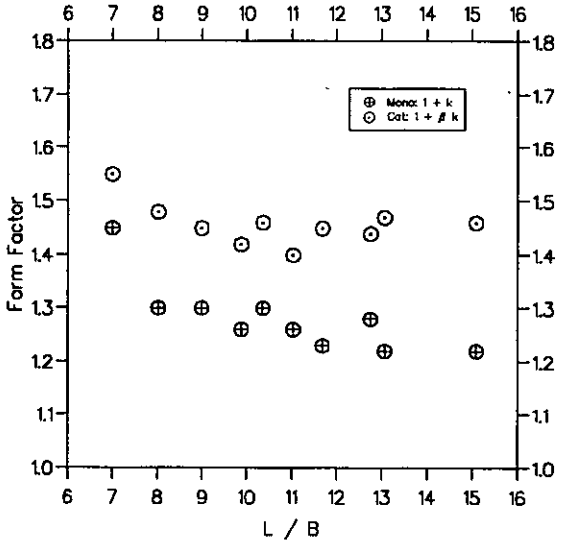

Fig 62b. Form Factors: S/L = 0.4

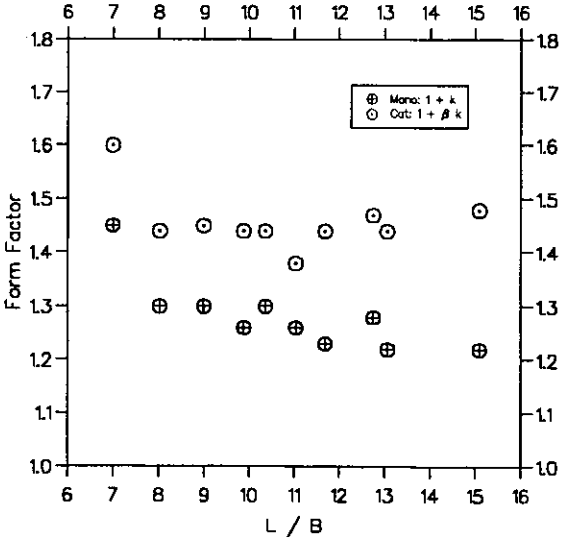

Fig 62e. Form Factors: S/L = 0.5

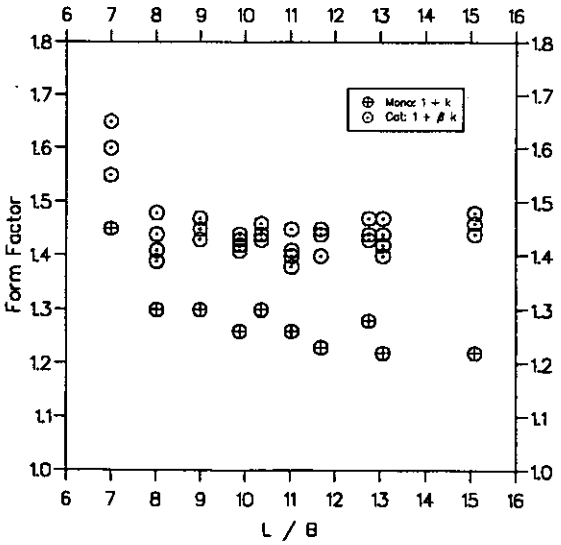

Fig 62f. Form Factors: All Models

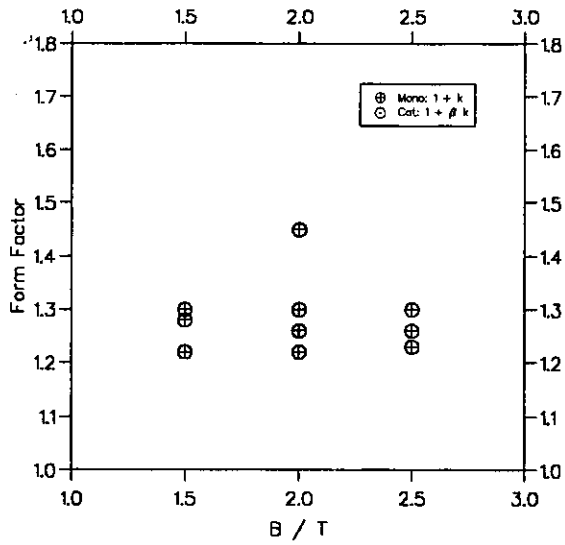

Fig 63a. Form Factors: Monohull

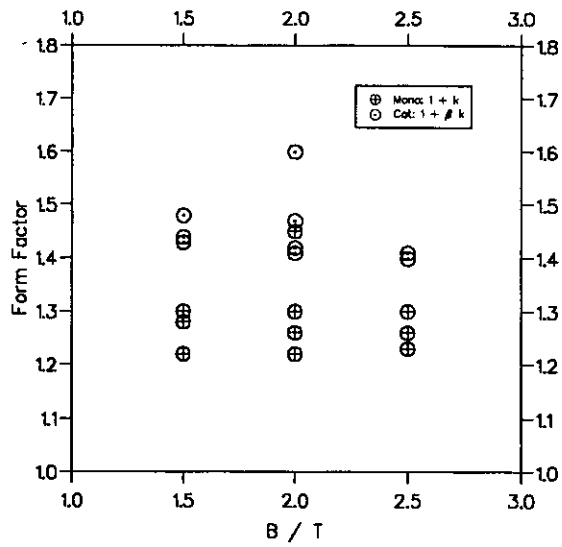

Fig 63b. Form Factors: S/L = 0.2

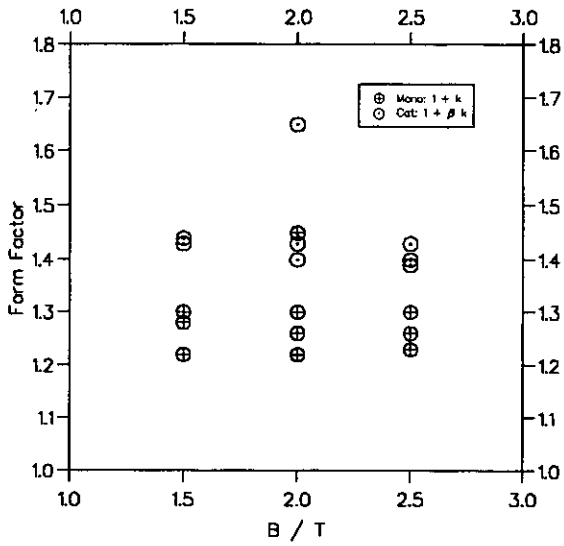

Fig 63c. Form Factors: S/L = 0.3

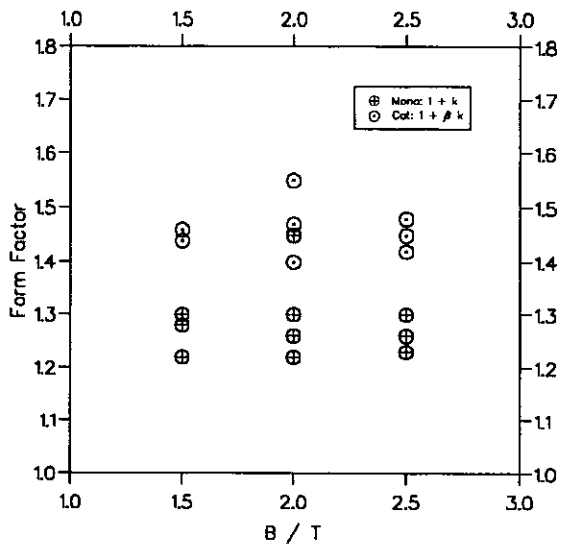

Fig 63d. Form Factors: S/L = 0.4

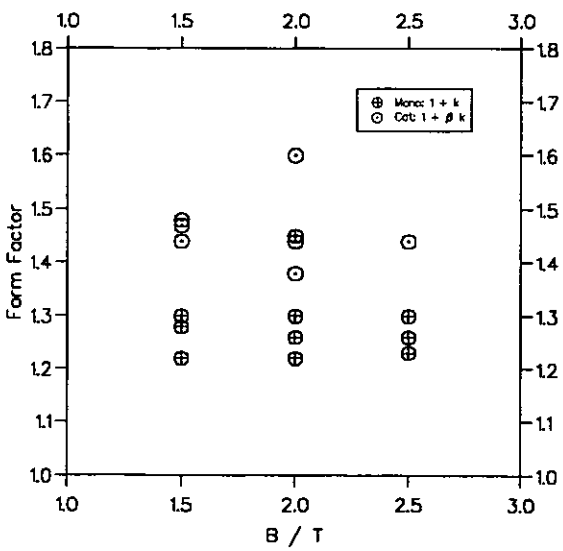

Fig 63e. Form Factors: S/L = 0.5

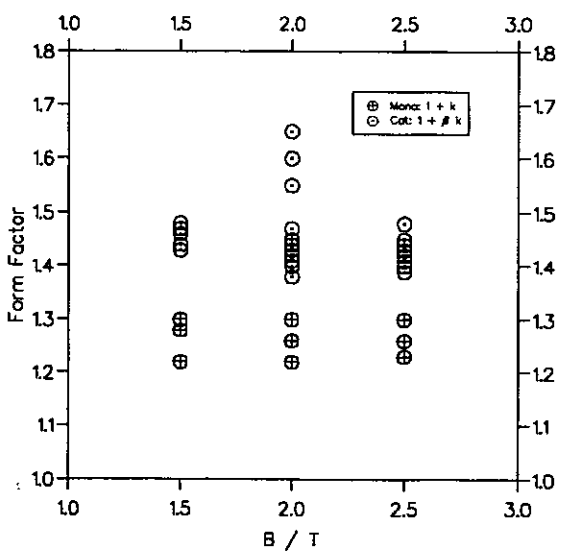

Fig 63f. Form Factors: All Models

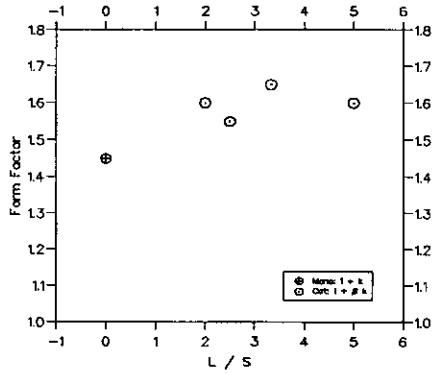

Fig 64. Form Factors: Model:3b

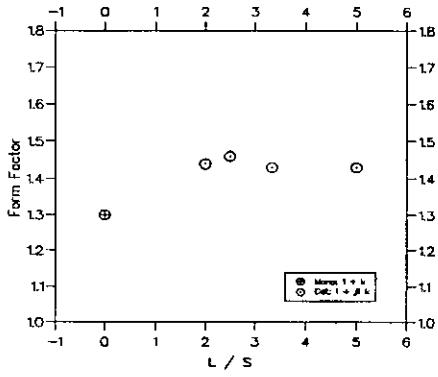

Fig 65a. Form Factors: Model:4a

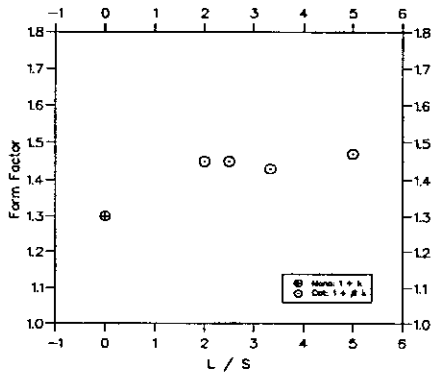

Fig 65b. Form Factors: Model:4b

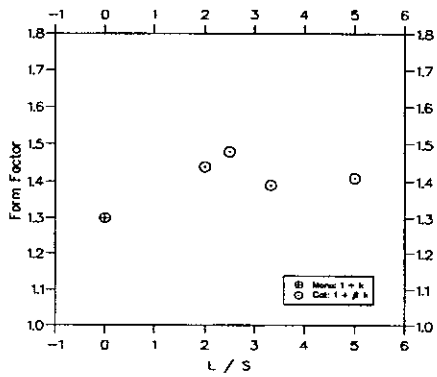

Fig 65c. Form Factors: Model:4c

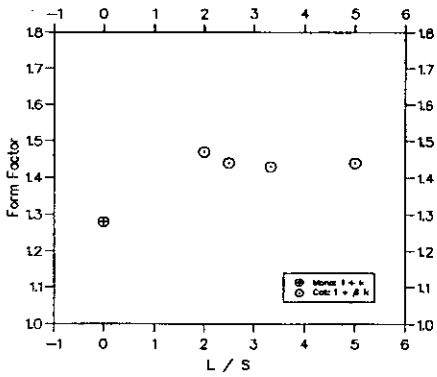

Fig 66a. Form Factors: Model:5a

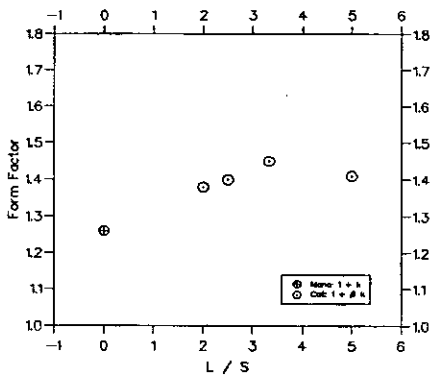

Fig 66b. Form Factors: Model:5b

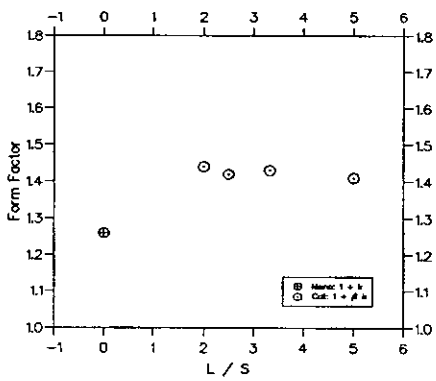

Fig 66c. Form Factors: Model:5c

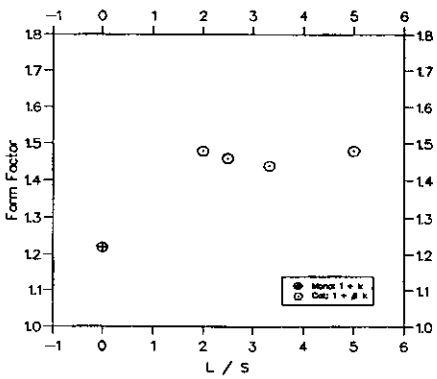

Fig 67a. Form Factors: Model:6a

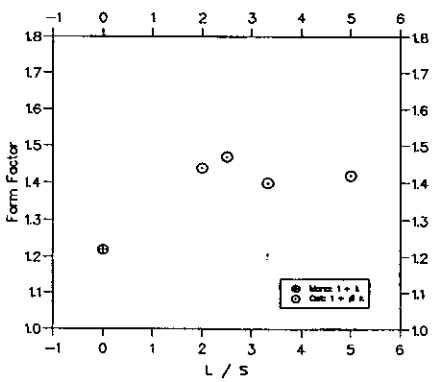

Fig 67b. Form Factors: Model:6b

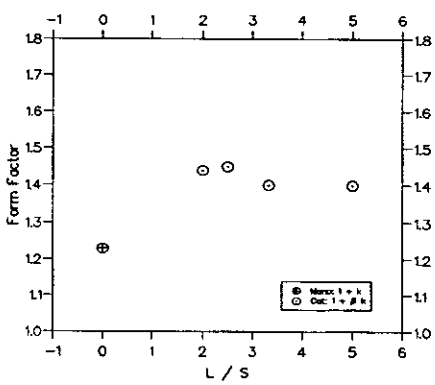

Fig 67c. Form Factors: Model:6c

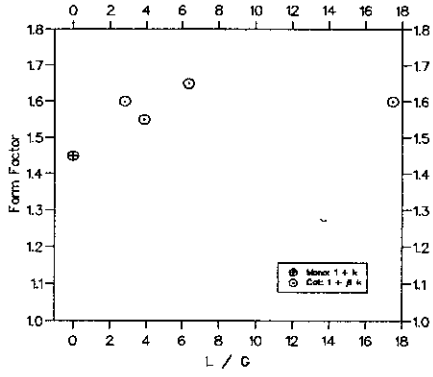

Fig 68. Form Factors: Model:3b

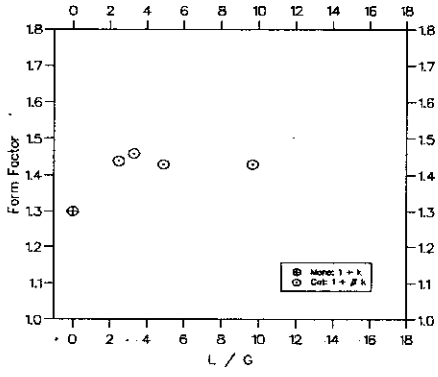

Fig 69a. Form Factors: Model:4a

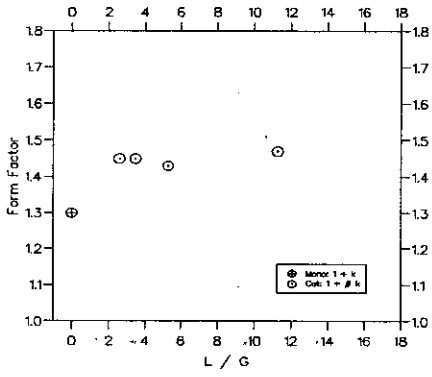

Fig 69b. Form Factors: Model:4b

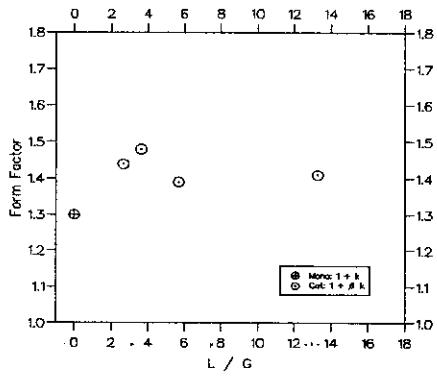

Fig 69c. Form Factors: Model:4c

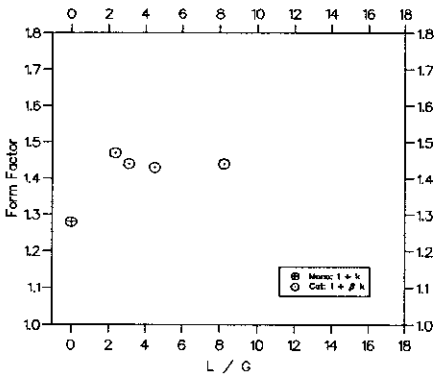

Fig 70a. Form Factors: Model:5a

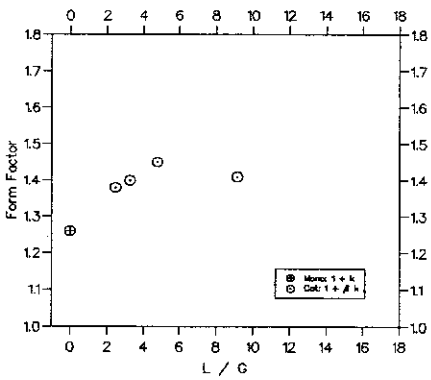

Fig 70b. Form Factors: Model:5b

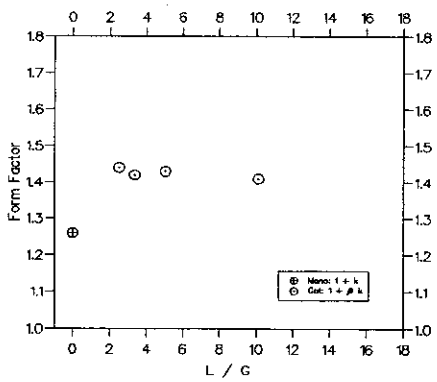

Fig 70c. Form Factors: Model:5c

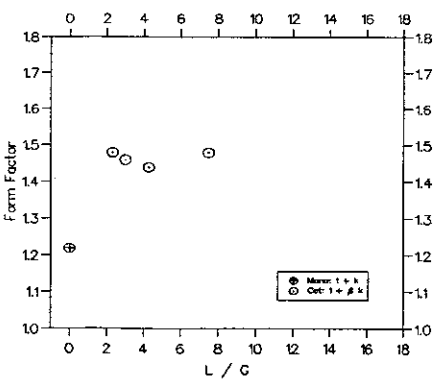

Fig 71a. Form Factors: Model:6a

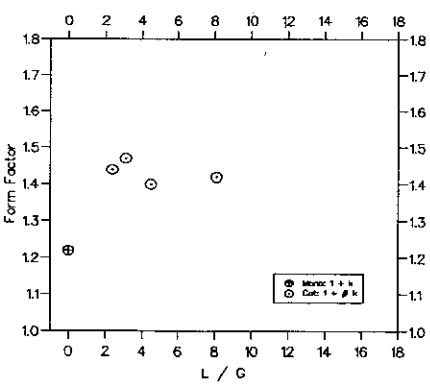

Fig 71b. Form Factors: Model:6b

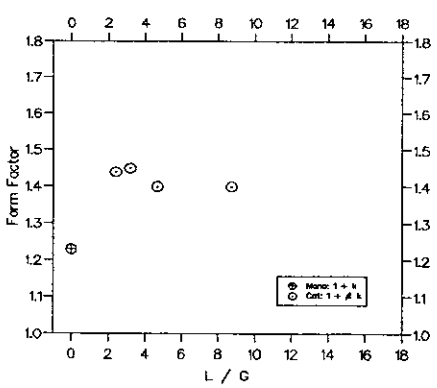

Fig 71c. Form Factors: Model:6c

TABLE III: Form Factors from C_{WP} Measurements

			Monohull	S/L = 0.2		S/L = 0.3		S/L = 0.4		S/L = 0.5	
$L/\nabla^{\frac{1}{3}}$	B/T	Model:	$1+k$	$1+\beta k$	β	$1+\beta k$	β	$1+\beta k$	β	$1+\beta k$	β
6.3	2.0	3b	1.45	1.60	1.33	1.65	1.44	1.55	1.22	1.60	1.33
7.4	1.5	4a	1.30	1.43	1.43	1.43	1.43	1.46	1.53	1.44	1.47
7.4	2.0	4b	1.30	1.47	1.57	1.43	1.43	1.45	1.50	1.45	1.50
7.4	2.5	4c	1.30	1.41	1.37	1.39	1.30	1.48	1.60	1.44	1.47
8.5	1.5	5a	1.28	1.44	1.57	1.43	1.54	1.44	1.57	1.47	1.68
8.5	2.0	5b	1.26	1.41	1.58	1.45	1.73	1.40	1.54	1.38	1.46
8.5	2.5	5c	1.26	1.41	1.58	1.43	1.65	1.42	1.62	1.44	1.69
9.5	1.5	6a	1.22	1.48	2.18	1.44	2.00	1.46	2.09	1.48	2.18
9.5	2.0	6b	1.22	1.42	1.91	1.40	1.82	1.47	2.14	1.44	2.00
9.5	2.5	6c	1.23	1.40	1.74	1.40	1.74	1.45	1.96	1.44	1.91

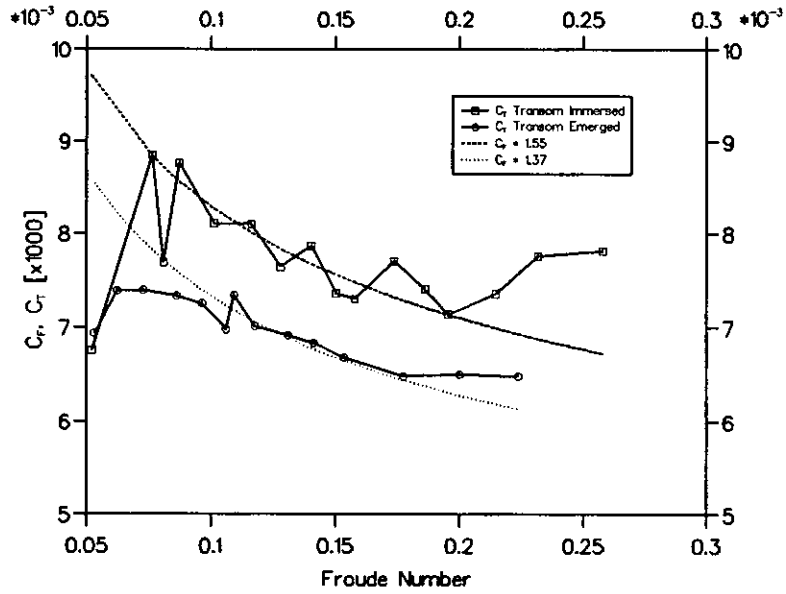

Fig 72a. Form Factor from SlowSpeed Tests

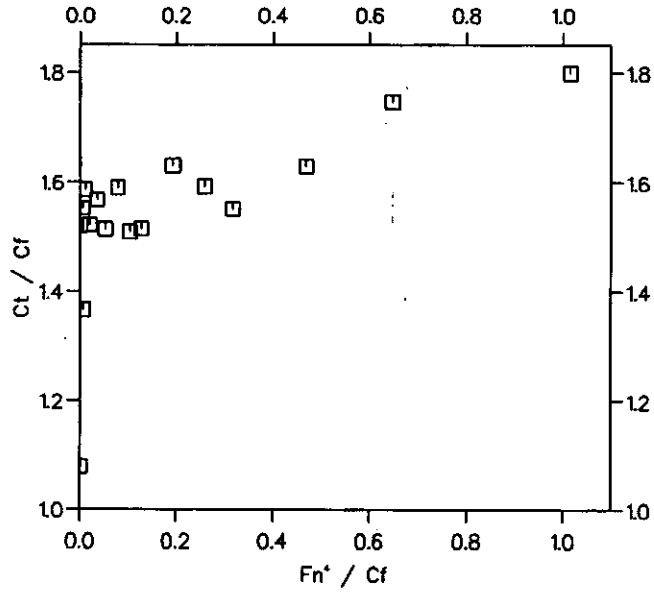

Fig 72b. Form Factor from Prohaska's Method: Transom Immeresd

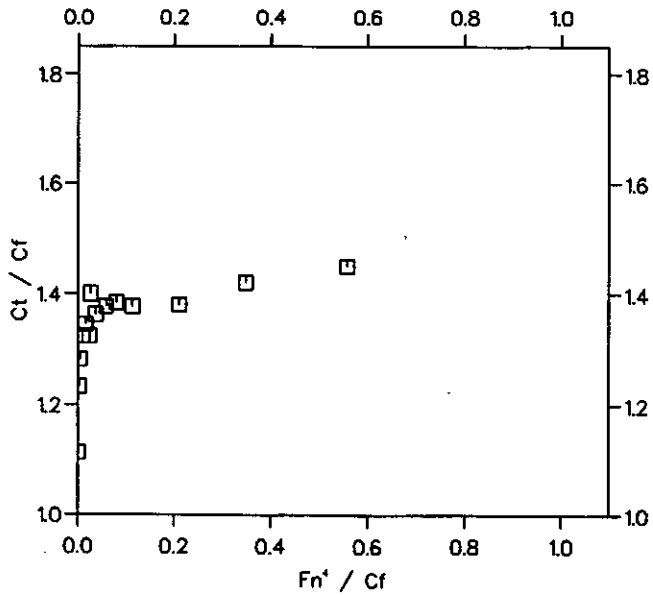

Fig 72c. Form Factor from Prohaska's Method: Transom Emerged

TABLE 1: Model 3b Experimental Results

	Monohull		S/L = 0.2		S/L = 0.3		S/L = 0.4		S/L = 0.5	
Fn	C_T	C_{WP}	C_T	C_{WP}	C_T	C_{WP}	C_T	C_{WP}	C_T	C_{WP}
0.200	7.553	0.076	7.774	0.052	7.800	0.054	7.224	0.047	7.148	0.131
0.250	7.880	0.259	8.910	0.216	8.095	0.201	8.389	0.219	7.672	0.433
0.300	8.016	0.722	9.510	0.439	8.958	0.688	8.672	0.508	8.142	0.651
0.350	8.878	1.199	10.848	0.877	10.020	1.408	9.549	0.940	8.879	1.060
0.400	9.590	1.633	12.941	1.392	11.617	1.483	11.054	1.294	10.558	2.341
0.450	11.913	3.530	16.271	3.644	16.447	4.691	14.812	4.389	12.942	4.686
0.500	12.836	5.229	18.672	6.265	18.035	8.293	15.825	7.187	13.910	6.336
0.550	12.271	6.393	19.145	8.468	16.004	8.462	14.266	6.983	13.122	6.340
0.600	11.292	6.067	16.484	8.800	13.756	7.240	12.628	6.325	12.028	5.684
0.650	10.347	5.175	11.983	6.218	11.733	5.640	11.203	5.557	11.099	4.963
0.700	9.514	4.474	9.514	4.474	10.412	4.432	10.202	4.797	10.286	4.294
0.750	8.897	4.024	8.897	4.024	9.448	3.436	9.435	3.976	9.592	3.599
0.800	8.383	3.484	8.383	3.484	8.761	2.923	8.845	3.245	9.009	2.961
0.850	7.917	2.838	7.917	2.838	8.247	2.622	8.382	2.719	8.478	2.473
0.900	7.498	2.253	7.498	2.253	7.848	2.446	7.939	2.600	8.020	2.065
0.950	7.148	1.711	7.148	1.711	7.535	2.250	7.599	2.229	7.698	1.870
1.000	6.910	1.282	6.910	1.282	7.267	1.985	7.327	1.903	7.430	1.677

(Coefficients $\times 10^3$)

TABLE 2: Model 4a Experimental Results

	Monohull		S/L = 0.2		S/L = 0.3		S/L = 0.4		S/L = 0.5	
Fn	C_T	C_{WP}	C_T	C_{WP}	C_T	C_{WP}	C_T	C_{WP}	C_T	C_{WP}
0.200	6.491	0.039	6.908	0.073	7.145	0.024	7.078	0.025	7.302	0.145
0.250	6.835	0.265	7.518	0.174	7.685	0.283	7.307	0.218	7.854	0.756
0.300	7.481	0.632	8.162	0.575	8.491	0.797	8.604	0.847	8.083	0.731
0.350	7.663	0.849	9.150	1.032	8.653	0.835	8.142	0.670	8.250	0.729
0.400	8.069	1.256	8.843	0.976	9.840	1.236	9.870	1.676	9.079	1.467
0.450	9.183	2.143	11.989	2.707	11.831	2.994	11.098	3.330	10.177	3.193
0.500	9.324	2.846	12.163	4.784	10.948	4.125	10.448	3.660	9.939	3.651
0.550	8.814	2.836	10.867	4.454	9.719	3.642	9.420	3.160	9.343	3.180
0.600	8.098	2.551	9.544	3.844	8.756	2.953	8.546	2.745	8.648	2.764
0.650	7.535	2.337	8.425	3.111	8.003	2.409	7.880	2.392	7.998	2.442
0.700	7.037	2.061	7.607	2.563	7.509	2.147	7.394	2.092	7.471	2.061
0.750	6.642	1.883	7.070	2.257	7.108	1.919	7.027	1.836	7.084	1.769
0.800	6.376	1.764	6.696	1.763	6.659	1.548	6.724	1.601	6.768	1.649
0.850	6.139	1.649	6.356	1.388	6.399	1.418	6.487	1.387	6.502	1.468
0.900	5.941	1.434	6.126	1.164	6.236	1.440	6.278	1.207	6.270	1.283
0.950	5.761	1.263	5.913	0.987	6.020	1.221	6.130	1.147	6.070	1.146
1.000	5.604	1.087	5.764	0.881	5.769	0.865	6.019	1.093	5.890	1.062

(Coefficients $\times 10^3$)

TABLE 3: Model 4b Experimental Results

	Monohull		S/L = 0.2		S/L = 0.3		S/L = 0.4		S/L = 0.5	
Fn	C_T	C_{WP}	C_T	C_{WP}	C_T	C_{WP}	C_T	C_{WP}	C_T	C_{WP}
0.200	7.196	0.049	7.516	0.025	7.426	0.072	7.307	0.043	7.406	0.091
0.250	6.999	0.295	8.056	0.142	7.744	0.185	7.734	0.171	7.765	0.223
0.300	7.740	0.605	8.519	0.458	8.321	0.641	8.357	0.767	8.110	0.454
0.350	7.841	0.868	9.560	1.054	8.894	0.907	8.635	0.787	8.406	0.702
0.400	8.489	1.183	9.866	1.087	9.904	1.025	9.910	1.408	9.686	1.462
0.450	9.280	2.587	11.627	2.700	11.655	3.040	10.956	2.941	10.619	2.618
0.500	9.187	3.376	12.219	4.085	11.467	4.421	10.721	3.749	10.380	3.059
0.550	8.593	3.186	11.828	4.713	10.368	4.585	9.874	3.686	9.649	2.950
0.600	7.942	2.749	10.825	4.478	9.137	3.966	8.981	3.230	8.875	2.672
0.650	7.398	2.508	9.618	3.840	8.231	3.226	8.215	2.703	8.204	2.390
0.700	6.954	2.406	8.328	2.994	7.621	2.633	7.658	2.280	7.685	2.182
0.750	6.612	2.175	7.554	2.473	7.154	2.086	7.232	1.941	7.300	2.024
0.800	6.320	1.885	7.076	2.090	6.797	1.921	6.911	1.767	6.992	1.852
0.850	6.080	1.584	6.080	1.584	6.586	1.816	6.680	1.618	6.752	1.682
0.900	5.872	1.338	5.872	1.338	6.312	1.618	6.474	1.505	6.527	1.461
0.950	5.724	1.172	5.724	1.172	6.197	1.600	6.330	1.300	6.361	1.245
1.000	5.678	1.134	5.678	1.134	5.678	1.134	6.213	1.063	6.201	1.071

(Coefficients $\times 10^3$)

TABLE 4: Model 4c Experimental Results

	Monohull		S/L = 0.2		S/L = 0.3		S/L = 0.4		S/L = 0.5	
Fn	C_T	C_{WP}	C_T	C_{WP}	C_T	C_{WP}	C_T	C_{WP}	C_T	C_{WP}
0.200	6.751	0.0	7.565	0.081	7.412	0.027	7.382	0.0	7.272	0.091
0.250	6.876	0.310	8.088	0.221	7.829	0.348	7.782	0.404	7.707	0.281
0.300	7.195	0.654	8.609	0.609	8.318	0.576	8.275	0.878	8.168	0.701
0.350	7.426	0.962	9.413	1.231	8.855	0.978	8.399	0.615	8.353	0.881
0.400	8.340	1.483	9.875	1.301	9.819	1.192	9.889	1.411	9.692	1.651
0.450	9.402	2.810	12.445	3.252	12.331	3.156	11.482	3.773	10.938	3.426
0.500	9.310	3.206	13.272	5.552	11.691	5.250	10.812	4.444	10.431	3.845
0.550	8.749	3.373	12.044	6.059	10.354	4.434	9.815	3.725	9.636	3.396
0.600	8.139	3.097	10.511	5.143	9.189	3.805	8.916	3.135	8.870	3.076
0.650	7.605	2.721	9.194	4.248	8.331	3.312	8.227	2.739	8.248	2.730
0.700	7.192	2.548	8.278	3.467	7.728	2.755	7.725	2.400	7.764	2.348
0.750	6.874	2.324	7.731	2.791	7.299	2.102	7.359	2.092	7.385	2.084
0.800	6.591	2.058	7.256	2.082	6.975	1.827	7.059	1.826	7.079	1.942
0.850	6.355	1.846	6.892	1.599	6.709	1.680	6.797	1.596	6.819	1.751
0.900	6.140	1.633	6.673	1.331	6.486	1.548	6.562	1.430	6.586	1.567
0.950	5.966	1.455	6.439	1.157	6.297	1.424	6.366	1.258	6.380	1.371
1.000	5.813	1.278	6.235	1.039	6.152	1.254	6.207	1.176	6.207	1.183

(Coefficients $\times 10^3$)

TABLE 5: Model 5a Experimental Results

	Monohull		S/L = 0.2		S/L = 0.3		S/L = 0.4		S/L = 0.5	
Fn	C_T	C_{WP}	C_T	C_{WP}	C_T	C_{WP}	C_T	C_{WP}	C_T	C_{WP}
0.200	6.436	0.094	7.148	0.052	7.147	0.061	6.964	0.061	7.175	0.109
0.250	6.857	0.281	7.444	0.168	7.361	0.161	7.401	0.299	7.493	0.289
0.300	7.215	0.532	8.167	0.655	7.797	0.666	7.894	0.736	7.681	0.543
0.350	7.340	0.647	8.096	0.946	7.833	0.693	7.666	0.549	7.793	0.668
0.400	7.644	0.931	8.441	0.815	8.573	0.847	8.586	1.139	8.372	1.119
0.450	7.982	1.534	9.945	2.339	9.440	2.359	8.977	2.114	8.807	1.927
0.500	7.682	1.783	9.603	3.145	8.748	2.576	8.379	2.231	8.299	2.042
0.550	7.168	1.728	8.642	2.900	7.949	2.234	7.743	2.052	7.695	1.885
0.600	6.729	1.557	7.731	2.436	7.262	1.878	7.182	1.749	7.166	1.676
0.650	6.348	1.401	7.039	1.937	6.749	1.573	6.737	1.453	6.751	1.420
0.700	6.021	1.261	6.564	1.531	6.387	1.325	6.405	1.231	6.442	1.167
0.750	5.793	1.148	6.219	1.280	6.129	1.135	6.172	1.073	6.213	1.021
0.800	5.608	1.043	5.966	1.081	5.937	0.988	5.991	0.959	6.031	0.976
0.850	5.473	0.970	5.775	0.903	5.784	0.878	5.839	0.874	5.886	0.937
0.900	5.326	0.893	5.627	0.784	5.657	0.820	5.704	0.827	5.751	0.859
0.950	5.233	0.809	5.516	0.714	5.546	0.788	5.601	0.803	5.635	0.748
1.000	5.152	0.745	5.432	0.691	5.456	0.771	5.510	0.807	5.533	0.659

(Coefficients $\times 10^3$)

TABLE 6: Model 5b Experimental Results

	Monohull		S/L = 0.2		S/L = 0.3		S/L = 0.4		S/L = 0.5	
Fn	C_T	C_{WP}	C_T	C_{WP}	C_T	C_{WP}	C_T	C_{WP}	C_T	C_{WP}
0.200	5.987	0.017	6.874	0.146	7.435	0.070	7.124	0.059	7.593	0.098
0.250	6.733	0.302	7.212	0.211	7.569	0.237	7.629	0.283	7.463	0.265
0.300	6.840	0.404	7.851	0.545	7.747	0.590	7.901	0.602	7.538	0.584
0.350	6.968	0.617	8.271	1.122	8.030	0.789	7.789	0.572	7.514	0.612
0.400	7.483	1.036	8.490	1.052	8.657	1.227	8.591	1.057	8.273	1.196
0.450	7.569	1.383	9.383	2.005	9.096	2.134	8.838	2.085	8.526	1.825
0.500	7.317	1.708	9.379	2.740	8.701	2.420	8.430	2.327	8.122	2.059
0.550	6.854	1.658	8.656	2.736	8.052	2.342	7.785	2.088	7.533	1.952
0.600	6.517	1.570	7.843	2.332	7.449	1.995	7.170	1.739	6.952	1.652
0.650	6.209	1.430	7.165	1.877	6.912	1.596	6.700	1.463	6.482	1.361
0.700	5.845	1.316	6.611	1.449	6.549	1.288	6.318	1.228	6.136	1.173
0.750	5.669	1.225	6.258	1.197	6.266	1.038	6.028	1.052	5.911	1.099
0.800	5.482	0.987	6.001	0.974	6.056	0.851	5.798	0.941	5.782	1.073
0.850	5.371	1.105	5.816	0.806	5.895	0.709	5.595	0.852	5.755	1.024
0.900	5.227	0.971	5.695	0.679	5.771	0.600	5.510	0.759	5.779	0.917
0.950	5.215	0.877	5.584	0.548	5.686	0.511	5.494	0.640	5.215	0.877
1.000	5.135	0.824	5.516	0.463	5.610	0.448	5.478	0.522	5.135	0.824

(Coefficients $\times 10^3$)

TABLE 7: Model 5c Experimental Results

	Monohull		S/L = 0.2		S/L = 0.3		S/L = 0.4		S/L = 0.5	
Fn	C_T	C_{WP}	C_T	C_{WP}	C_T	C_{WP}	C_T	C_{WP}	C_T	C_{WP}
0.200	7.099	0.013	7.313	0.020	7.383	0.042	7.301	0.071	7.565	0.098
0.250	7.125	0.298	7.626	0.345	7.569	0.291	7.573	0.261	7.660	0.294
0.300	7.218	0.598	7.653	0.428	7.807	0.642	7.594	0.628	7.579	0.597
0.350	7.350	0.760	8.015	0.977	7.856	0.791	7.700	0.676	7.702	0.731
0.400	7.656	1.187	8.605	1.106	8.782	1.184	8.700	1.527	8.488	1.409
0.450	7.768	1.769	9.785	2.514	9.420	2.700	8.846	2.523	8.521	2.114
0.500	7.419	2.003	9.662	3.531	8.814	2.985	8.311	2.758	8.138	2.246
0.550	6.960	1.896	8.824	3.329	8.003	2.552	7.674	2.498	7.583	2.046
0.600	6.714	1.802	7.897	2.738	7.370	2.036	7.162	2.029	7.178	1.867
0.650	6.295	1.629	7.187	2.161	6.877	1.675	6.793	1.665	6.797	1.591
0.700	5.977	1.561	6.634	1.723	6.490	1.423	6.481	1.448	6.496	1.386
0.750	5.719	1.338	6.285	1.447	6.255	1.180	6.231	1.270	6.293	1.265
0.800	5.547	1.213	6.030	1.171	6.103	1.030	6.035	1.143	6.065	1.149
0.850	5.336	1.121	5.866	0.964	6.040	0.971	5.909	1.059	5.947	1.078
0.900	5.260	1.001	5.742	0.867	5.996	0.889	5.800	0.956	5.850	1.007
0.950	5.278	0.939	5.622	0.771	5.913	0.764	5.705	0.875	5.721	0.886
1.000	5.116	0.816	5.544	0.726	5.813	0.657	5.588	0.777	5.613	0.791

(Coefficients $\times 10^3$)

TABLE 8: Model 6a Experimental Results

	Monohull		S/L = 0.2		S/L = 0.3		S/L = 0.4		S/L = 0.5	
Fn	C_T	C_{WP}	C_T	C_{WP}	C_T	C_{WP}	C_T	C_{WP}	C_T	C_{WP}
0.200	6.499	0.0	7.309	0.054	7.242	0.187	7.389	0.004	7.066	0.023
0.250	6.627	0.184	7.750	0.241	7.615	0.482	7.965	0.531	7.886	0.255
0.300	6.651	0.439	7.999	0.535	7.756	0.683	7.969	0.486	7.872	0.354
0.350	6.605	0.577	7.743	0.607	7.459	0.482	7.832	0.526	7.643	0.477
0.400	6.693	0.739	8.346	0.681	8.373	0.860	8.226	0.888	7.979	0.772
0.450	6.674	0.998	8.581	1.624	8.470	1.803	8.217	1.546	7.875	1.209
0.500	6.456	1.264	8.390	2.040	7.772	1.862	7.653	1.517	7.434	1.283
0.550	6.163	1.181	7.527	1.803	7.110	1.731	7.067	1.320	6.971	1.197
0.600	5.912	1.045	6.859	1.519	6.660	1.504	6.622	1.140	6.583	0.989
0.650	5.722	0.872	6.423	1.134	6.313	1.111	6.299	0.969	6.262	0.859
0.700	5.477	0.755	6.094	0.905	6.056	0.909	6.065	0.807	6.035	0.739
0.750	5.295	0.748	5.881	0.768	5.862	0.829	5.893	0.703	5.850	0.687
0.800	5.105	0.698	5.725	0.648	5.733	0.778	5.775	0.683	5.715	0.662
0.850	4.977	0.659	5.609	0.637	5.627	0.762	5.663	0.704	5.604	0.610
0.900	4.875	0.598	5.506	0.598	5.551	0.705	5.542	0.637	5.490	0.547
0.950	4.891	0.768	5.425	0.522	5.473	0.635	5.410	0.568	5.384	0.481
1.000	4.853	0.964	5.359	0.549	5.395	0.547	5.307	0.482	5.294	0.421

(Coefficients $\times 10^3$)

TABLE 9: Model 6b Experimental Results

	Monohull		S/L = 0.2		S/L = 0.3		S/L = 0.4		S/L = 0.5	
Fn	C_T	C_{WP}	C_T	C_{WP}	C_T	C_{WP}	C_T	C_{WP}	C_T	C_{WP}
0.200	6.337	0.032	7.446	0.070	6.880	0.016	7.516	0.075	6.935	0.110
0.250	6.506	0.182	7.587	0.204	7.605	0.123	7.573	0.295	6.705	0.234
0.300	6.463	0.437	7.977	0.540	7.370	0.474	7.459	0.495	7.041	0.492
0.350	6.228	0.557	7.745	0.622	7.377	0.554	7.580	0.586	7.236	0.586
0.400	6.608	0.828	7.976	0.928	7.691	0.879	7.883	0.956	7.449	0.937
0.450	6.573	1.156	8.412	1.809	7.970	1.629	7.827	1.383	7.448	1.303
0.500	6.308	1.221	8.177	2.114	7.569	1.687	7.390	1.489	7.192	1.386
0.550	6.067	1.185	7.463	1.855	6.930	1.432	6.924	1.336	6.813	1.228
0.600	5.751	1.105	6.810	1.541	6.428	1.202	6.533	1.105	6.328	1.124
0.650	5.511	0.953	6.349	1.335	6.118	0.989	6.245	0.893	6.176	0.984
0.700	5.308	0.845	6.037	1.121	5.915	0.795	6.028	0.784	5.938	0.728
0.750	5.170	0.758	5.825	0.872	5.763	0.657	5.853	0.737	5.783	0.685
0.800	5.047	0.716	5.656	0.667	5.630	0.609	5.713	0.693	5.686	0.656
0.850	4.960	0.764	5.526	0.558	5.501	0.675	5.605	0.645	5.545	0.691
0.900	4.920	0.727	5.448	0.572	5.453	0.656	5.526	0.607	5.461	0.674
0.950	4.845	0.719	5.383	0.595	5.409	0.386	5.452	0.571	5.411	0.545
1.000	4.758	0.750	5.333	0.625	5.332	0.533	5.394	0.527	5.367	0.411

(Coefficients $\times 10^3$)

TABLE 10: Model 6c Experimental Results

	Monohull		S/L = 0.2		S/L = 0.3		S/L = 0.4		S/L = 0.5	
Fn	C_T	C_{WP}	C_T	C_{WP}	C_T	C_{WP}	C_T	C_{WP}	C_T	C_{WP}
0.200	6.466	0.093	7.562	0.204	6.492	0.146	7.191	0.071	7.098	0.067
0.250	6.764	0.327	7.538	0.374	7.699	0.248	7.427	0.275	7.281	0.264
0.300	6.789	0.574	7.747	0.600	7.609	0.627	7.459	0.676	7.399	0.591
0.350	6.743	0.742	7.609	0.906	7.387	0.738	7.462	0.698	7.444	0.676
0.400	6.754	0.923	7.653	0.904	7.743	0.852	7.782	1.030	7.598	1.034
0.450	6.693	1.194	8.107	1.521	7.809	1.636	7.691	1.498	7.554	1.468
0.500	6.424	1.418	7.952	2.137	7.517	1.839	7.325	1.531	7.244	1.488
0.550	6.122	1.347	7.302	2.029	6.984	1.531	6.915	1.647	6.873	1.302
0.600	5.844	1.122	6.747	1.654	6.521	1.177	6.532	1.399	6.517	1.196
0.650	5.617	0.930	6.420	1.346	6.206	0.978	6.219	0.956	6.218	1.012
0.700	5.426	0.862	6.064	1.068	5.998	0.911	5.992	0.804	6.047	0.863
0.750	5.268	0.808	5.819	0.851	5.845	0.766	5.859	0.778	5.872	0.725
0.800	5.154	0.755	5.637	0.773	5.671	0.631	5.703	0.662	5.769	0.677
0.850	5.066	0.720	5.571	0.651	5.600	0.614	5.643	0.648	5.681	0.672
0.900	4.965	0.702	5.505	0.611	5.517	0.585	5.570	0.628	5.623	0.703
0.950	4.991	0.692	5.441	0.669	5.484	0.532	5.512	0.572	5.590	0.655
1.000	5.003	0.681	5.398	0.685	5.466	0.477	5.488	0.563	5.524	0.561

(Coefficients $\times 10^3$)

TABLE 11: Model 3b Running Trim and Sinkage

	Monohull		S/L = 0.2		S/L = 0.3		S/L = 0.4		S/L = 0.5	
Fn	Sink.	Trim	Sink.	Trim	Sink.	Trim	Sink.	Trim	Sink.	Trim
0.200	1.517	0.062	1.885	0.215	1.917	0.121	1.855	0.124	1.432	0.077
0.250	2.358	0.113	2.790	0.309	2.708	0.165	2.584	0.184	2.311	0.002
0.300	2.990	0.143	4.534	0.479	4.157	0.173	4.048	0.252	3.722	0.079
0.350	4.572	0.175	6.550	0.378	5.534	0.109	4.936	0.201	5.608	0.592
0.400	6.685	0.809	9.416	1.322	9.767	1.736	8.219	1.437	7.369	1.538
0.450	8.264	1.976	12.225	3.286	10.961	3.448	8.883	2.816	8.312	2.537
0.500	8.222	2.827	12.043	4.776	9.273	4.804	7.992	3.664	8.349	3.302
0.550	7.413	3.422	9.281	5.368	6.695	5.128	6.318	4.049	6.481	3.858
0.600	6.423	3.734	4.135	5.281	4.481	5.075	4.710	4.119	4.786	3.889
0.650	5.319	3.893	5.319	3.893	1.591	4.658	3.207	4.085	3.742	3.898
0.700	4.258	3.936	4.258	3.936	-0.159	4.256	1.862	4.044	2.747	3.909
0.750	3.397	3.925	3.397	3.925	-1.256	4.035	0.733	4.032	1.809	3.912
0.800	2.592	3.892	2.592	3.892	-2.386	3.876	-0.437	4.035	0.961	3.902
0.850	1.774	3.845	1.774	3.845	-3.408	3.785	-2.107	3.969	0.232	3.875
0.900	0.974	3.785	0.974	3.785	-4.255	3.749	-2.525	3.838	-0.380	3.826
0.950	0.356	3.720	0.356	3.720	-5.178	3.776	-2.553	3.664	-0.912	3.759
1.000	0.160	3.662	0.160	3.662	-5.416	3.785	-2.341	3.432	-1.479	3.699

(Sinkage: Percent Draught [increase in draught +ve]
Trim: Degrees [bow up +ve])

TABLE 12: Model 4a Running Trim and Sinkage

	Monohull		S/L = 0.2		S/L = 0.3		S/L = 0.4		S/L = 0.5	
Fn	Sink.	Trim	Sink.	Trim	Sink.	Trim	Sink.	Trim	Sink.	Trim
0.200	1.304	0.030	1.729	-0.001	2.074	0.026	1.767	0.109	1.485	0.091
0.250	1.814	0.054	2.357	0.032	3.264	0.084	2.468	0.142	2.098	0.082
0.300	2.617	0.081	3.545	0.091	4.253	0.111	3.297	0.121	3.045	0.176
0.350	3.436	0.121	5.207	0.134	6.423	0.284	4.862	0.222	4.145	0.360
0.400	5.047	0.541	7.090	0.465	9.647	0.869	7.620	0.801	5.409	0.647
0.450	6.466	1.066	9.495	1.627	11.528	1.655	8.417	1.349	7.047	1.322
0.500	6.608	1.444	8.994	2.639	10.508	2.094	7.248	1.774	6.585	1.594
0.550	5.770	1.703	6.913	2.786	8.074	2.162	5.573	1.817	5.540	1.647
0.600	4.923	1.760	4.215	2.671	5.014	2.051	4.419	1.804	4.507	1.663
0.650	4.032	1.783	1.747	2.373	3.023	1.955	3.636	1.796	3.654	1.670
0.700	3.646	1.828	0.722	2.152	1.792	1.956	2.931	1.800	3.116	1.673
0.750	3.585	1.868	-0.037	2.010	0.974	1.931	2.145	1.814	2.766	1.672
0.800	3.610	1.912	-0.486	1.948	0.433	1.902	1.333	1.828	2.493	1.670
0.850	3.704	1.956	-0.959	1.897	-0.145	1.858	0.714	1.830	2.214	1.676
0.900	3.876	2.009	-1.844	1.837	-0.796	1.842	0.456	1.818	1.799	1.698
0.950	3.939	2.016	-3.025	1.784	-0.799	1.828	0.451	1.815	1.324	1.716
1.000	3.818	1.999	-3.443	1.774	-0.374	1.714	-0.232	1.828	0.864	1.729

(Sinkage: Percent Draught [increase in draught +ve]
Trim: Degrees [bow up +ve])

TABLE 13: Model 4b Running Trim and Sinkage

	Monohull		S/L = 0.2		S/L = 0.3		S/L = 0.4		S/L = 0.5	
Fn	Sink.	Trim	Sink.	Trim	Sink.	Trim	Sink.	Trim	Sink.	Trim
0.200	1.542	0.045	2.046	0.100	1.676	0.156	1.860	0.165	1.657	0.117
0.250	2.285	0.065	3.295	0.174	2.780	0.184	2.499	0.175	2.492	0.177
0.300	3.135	0.107	4.256	0.250	3.749	0.200	3.175	0.144	3.331	0.226
0.350	4.050	0.141	5.820	0.226	5.433	0.303	5.746	0.345	4.802	0.394
0.400	5.626	0.574	8.997	0.845	8.148	0.987	7.793	0.819	6.844	0.795
0.450	7.081	0.989	10.004	1.918	9.261	2.009	8.552	1.535	8.078	1.450
0.500	7.279	1.717	9.128	2.497	7.887	2.521	7.640	1.805	7.346	1.754
0.550	6.488	1.859	6.819	2.908	5.984	2.616	5.975	1.915	6.219	1.931
0.600	5.891	1.846	4.394	2.969	4.106	2.532	4.491	1.925	4.928	2.037
0.650	4.683	1.841	2.821	2.899	2.405	2.378	3.375	1.922	3.734	2.084
0.700	4.198	1.834	0.978	2.720	1.197	2.274	2.392	1.928	2.666	2.103
0.750	3.892	1.784	-2.116	2.341	0.211	2.227	1.486	1.953	1.666	2.135
0.800	3.994	1.883	-3.504	2.223	-0.774	2.235	0.645	1.998	0.836	2.185
0.850	3.844	1.952	3.844	1.952	-1.820	2.279	-0.197	2.053	0.070	2.253
0.900	3.554	1.965	3.554	1.965	-2.901	2.317	-1.065	2.104	-0.707	2.337
0.950	3.243	1.974	3.243	1.974	-3.998	2.346	-1.681	2.122	-1.327	2.384
1.000	3.566	1.931	3.566	1.931	3.566	1.931	-1.755	2.083	-1.601	2.338

(Sinkage: Percent Draught [increase in draught +ve]
Trim: Degrees [bow up +ve])

TABLE 14: Model 4c Running Trim and Sinkage

	Monohull		S/L = 0.2		S/L = 0.3		S/L = 0.4		S/L = 0.5	
Fn	Sink.	Trim	Sink.	Trim	Sink.	Trim	Sink.	Trim	Sink.	Trim
0.200	1.405	0.043	2.732	0.042	2.173	0.075	2.590	0.049	1.738	0.021
0.250	2.574	0.075	3.703	0.099	3.140	0.081	2.831	0.069	2.630	0.073
0.300	3.406	0.053	5.131	0.176	4.447	0.196	4.217	0.104	3.513	0.102
0.350	4.997	0.189	7.039	0.210	6.547	0.263	5.683	0.225	5.339	0.216
0.400	6.757	0.546	10.232	0.547	8.821	0.673	8.001	0.764	7.924	0.706
0.450	8.401	1.048	13.745	1.715	10.777	1.677	8.857	1.570	9.291	1.237
0.500	8.445	1.511	13.198	2.736	9.371	2.190	8.371	1.868	8.710	1.671
0.550	7.251	1.697	8.538	3.167	6.513	2.254	5.776	1.942	6.509	1.849
0.600	5.697	1.827	4.065	3.113	3.900	2.161	4.380	1.945	4.973	1.876
0.650	4.522	1.935	0.682	2.802	2.235	2.081	3.207	1.948	3.966	1.881
0.700	3.770	1.953	-1.108	2.502	0.813	2.022	2.182	1.955	3.023	1.895
0.750	3.418	2.000	-2.344	2.329	-0.461	1.995	1.320	1.968	2.150	1.926
0.800	3.564	2.043	-4.197	2.171	-1.615	1.983	0.586	1.984	1.308	1.960
0.850	3.662	2.087	-5.189	2.098	-2.527	1.955	-0.127	2.007	0.293	1.973
0.900	3.544	2.120	-6.140	2.034	-3.236	1.855	-1.047	2.045	-0.503	1.962
0.950	3.164	2.151	-7.046	1.972	-3.206	1.889	-1.245	2.055	-1.421	1.954
1.000	2.750	2.150	-7.914	1.901	-2.903	2.000	-1.094	2.047	-2.011	1.976

(Sinkage: Percent Draught [increase in draught +ve]
Trim: Degrees [bow up +ve])

TABLE 15: Model 5a Running Trim and Sinkage

	Monohull		S/L = 0.2		S/L = 0.3		S/L = 0.4		S/L = 0.5	
Fn	Sink.	Trim	Sink.	Trim	Sink.	Trim	Sink.	Trim	Sink.	Trim
0.200	1.860	0.096	2.594	0.071	1.443	0.047	1.550	0.038	1.766	0.017
0.250	2.305	0.097	3.359	0.085	2.032	0.109	2.267	0.113	2.253	0.035
0.300	2.963	0.100	4.126	0.087	3.101	0.182	2.945	0.170	2.938	0.071
0.350	3.887	0.160	4.476	0.030	4.042	0.130	3.872	0.173	3.970	0.116
0.400	5.201	0.409	6.531	0.352	5.644	0.744	6.210	0.638	5.945	0.450
0.450	6.270	0.777	9.086	1.327	6.320	1.331	7.140	1.157	6.968	0.988
0.500	6.170	1.023	8.842	1.897	5.607	1.444	6.197	1.346	6.407	1.233
0.550	5.363	1.091	6.585	1.987	4.484	1.446	4.820	1.374	5.002	1.327
0.600	4.638	1.148	4.480	1.874	3.389	1.426	3.705	1.367	3.949	1.341
0.650	4.078	1.204	2.646	1.702	2.593	1.394	2.926	1.388	3.284	1.347
0.700	3.835	1.249	1.288	1.539	1.992	1.357	2.470	1.441	2.896	1.358
0.750	4.024	1.276	0.527	1.437	1.634	1.340	2.322	1.482	2.773	1.369
0.800	4.352	1.308	0.003	1.375	1.429	1.350	2.286	1.495	2.805	1.381
0.850	4.539	1.351	-0.315	1.355	1.287	1.386	2.259	1.503	2.880	1.414
0.900	4.833	1.435	-0.495	1.355	1.218	1.444	2.232	1.538	2.909	1.469
0.950	5.556	1.456	-0.575	1.362	1.209	1.486	2.214	1.604	2.898	1.558
1.000	5.498	1.454	-0.631	1.397	1.290	1.574	2.144	1.652	2.886	1.538

(Sinkage: Percent Draught [increase in draught +ve]
Trim: Degrees [bow up +ve])

TABLE 16: Model 5b Running Trim and Sinkage

	Monohull		S/L = 0.2		S/L = 0.3		S/L = 0.4		S/L = 0.5	
Fn	Sink.	Trim	Sink.	Trim	Sink.	Trim	Sink.	Trim	Sink.	Trim
0.200	1.730	-0.009	1.314	0.082	1.491	0.390	2.161	0.146	2.074	0.232
0.250	2.298	0.036	2.231	0.123	2.391	0.386	3.052	0.199	2.795	0.379
0.300	3.067	0.073	3.200	0.139	3.376	0.333	3.929	0.245	3.760	0.478
0.350	4.073	0.128	4.962	0.213	5.114	0.401	5.231	0.309	5.788	0.573
0.400	5.721	0.354	7.601	0.579	7.494	0.730	7.403	0.961	7.198	0.719
0.450	6.880	0.672	9.272	1.142	8.156	1.190	7.290	1.340	8.466	1.134
0.500	6.607	0.799	8.673	1.541	6.624	1.354	6.426	1.545	8.231	1.300
0.550	5.625	0.913	6.360	1.670	5.128	1.388	5.069	1.641	6.453	1.457
0.600	4.905	0.961	3.700	1.605	3.640	1.372	3.823	1.671	4.585	1.499
0.650	4.080	1.009	1.683	1.492	2.484	1.335	2.949	1.658	3.561	1.510
0.700	4.241	1.030	0.250	1.387	1.718	1.299	2.361	1.620	2.831	1.514
0.750	4.005	1.053	-0.718	1.304	1.220	1.279	1.980	1.568	2.331	1.514
0.800	4.675	1.100	-1.205	1.254	1.421	1.345	1.722	1.515	2.069	1.511
0.850	5.455	1.139	-1.278	1.241	1.659	1.409	1.553	1.477	2.007	1.508
0.900	5.614	1.184	-1.048	1.259	1.903	1.480	1.447	1.465	2.089	1.508
0.950	4.997	1.214	-0.676	1.297	2.047	1.542	1.399	1.466	2.245	1.518
1.000	3.837	1.261	-0.375	1.337	1.914	1.554	1.477	1.463	2.082	1.515

(Sinkage: Percent Draught [increase in draught +ve]
Trim: Degrees [bow up +ve])

TABLE 17: Model 5c Running Trim and Sinkage

	Monohull		S/L = 0.2		S/L = 0.3		S/L = 0.4		S/L = 0.5	
Fn	Sink.	Trim	Sink.	Trim	Sink.	Trim	Sink.	Trim	Sink.	Trim
0.200	1.760	0.015	2.291	-0.034	2.186	0.009	1.844	0.014	1.952	-0.016
0.250	2.287	0.038	3.265	-0.017	2.855	0.061	2.571	0.040	2.731	0.014
0.300	3.063	0.058	4.607	0.060	3.917	0.085	3.639	0.037	3.940	0.052
0.350	4.439	0.140	6.323	0.099	5.754	0.112	5.288	0.148	5.366	0.141
0.400	6.132	0.381	9.464	0.518	8.726	0.562	7.649	0.567	8.186	0.543
0.450	7.097	0.702	11.431	1.114	9.859	1.173	8.673	0.921	8.611	0.869
0.500	6.844	0.955	10.501	1.879	8.410	1.456	7.674	1.236	7.848	1.124
0.550	5.710	1.079	7.148	2.003	5.609	1.464	5.931	1.291	6.428	1.244
0.600	4.658	1.127	3.609	1.904	3.313	1.404	3.927	1.295	4.781	1.280
0.650	3.886	1.154	1.064	1.742	1.795	1.345	2.512	1.288	3.426	1.290
0.700	3.251	1.182	-0.522	1.589	1.166	1.312	2.001	1.298	2.889	1.303
0.750	3.437	1.230	-1.164	1.483	1.008	1.312	1.873	1.332	2.957	1.352
0.800	3.914	1.267	-1.408	1.421	1.181	1.339	1.746	1.379	2.876	1.434
0.850	4.283	1.317	-1.649	1.397	1.126	1.388	1.702	1.453	2.561	1.515
0.900	4.406	1.366	-1.983	1.390	0.600	1.441	1.703	1.506	2.461	1.573
0.950	4.258	1.392	-2.519	1.373	0.287	1.487	1.430	1.553	2.279	1.617
1.000	3.578	1.419	-3.245	1.356	0.224	1.520	0.990	1.582	1.919	1.655

(Sinkage: Percent Draught [increase in draught +ve]
Trim: Degrees [bow up +ve])

TABLE 18: Model 6a Running Trim and Sinkage

	Monohull		S/L = 0.2		S/L = 0.3		S/L = 0.4		S/L = 0.5	
Fn	Sink.	Trim	Sink.	Trim	Sink.	Trim	Sink.	Trim	Sink.	Trim
0.200	1.469	-0.007	2.204	0.071	1.357	0.030	1.471	-0.002	-1.033	-0.037
0.250	2.137	0.060	2.737	0.109	1.962	0.050	1.999	0.042	1.603	0.001
0.300	2.960	0.030	2.941	0.163	2.597	0.063	2.712	0.079	2.706	0.032
0.350	3.641	0.078	3.329	0.093	3.371	0.119	3.628	0.157	3.694	0.081
0.400	5.058	0.299	5.514	0.443	5.215	0.476	5.651	0.534	5.190	0.292
0.450	5.541	0.573	7.061	1.121	6.211	0.968	6.001	0.777	5.815	0.603
0.500	5.477	0.689	6.047	1.419	5.553	1.122	5.379	0.926	5.402	0.705
0.550	4.737	0.771	4.321	1.450	4.202	1.141	3.967	0.980	3.828	0.848
0.600	3.982	0.808	2.445	1.326	2.458	1.071	2.760	0.976	2.913	0.891
0.650	3.530	0.834	1.034	1.093	1.612	0.994	1.978	0.969	2.266	0.917
0.700	3.496	0.854	0.797	1.055	1.583	0.987	1.794	0.972	2.006	0.942
0.750	3.953	0.867	0.726	1.047	1.755	1.018	2.229	0.986	2.166	0.967
0.800	4.610	0.893	0.699	1.049	1.934	1.066	2.914	1.014	2.500	1.002
0.850	5.420	1.031	0.708	1.058	2.178	1.129	3.264	1.067	2.722	1.056
0.900	5.505	1.117	0.969	1.116	2.671	1.221	2.945	1.180	2.666	1.130
0.950	5.426	1.146	0.679	1.161	3.488	1.373	2.315	1.271	2.502	1.219
1.000	5.200	1.148	0.252	1.212	3.393	1.456	2.013	1.329	2.474	1.252

(Sinkage: Percent Draught [increase in draught +ve]
Trim: Degrees [bow up +ve])

TABLE 19: Model 6b Running Trim and Sinkage

	Monohull		S/L = 0.2		S/L = 0.3		S/L = 0.4		S/L = 0.5	
Fn	Sink.	Trim	Sink.	Trim	Sink.	Trim	Sink.	Trim	Sink.	Trim
0.200	1.344	-0.132	2.062	0.006	2.295	-0.042	2.274	0.000	1.394	0.051
0.250	2.452	-0.093	3.420	0.014	2.981	-0.008	2.744	0.000	1.916	0.097
0.300	3.127	-0.074	4.264	0.008	3.441	-0.011	3.266	-0.002	2.687	0.096
0.350	3.736	-0.020	5.295	0.060	3.959	0.016	4.690	-0.023	3.973	0.178
0.400	5.092	0.183	7.505	0.374	6.182	0.386	6.808	0.156	5.480	0.417
0.450	5.852	0.451	9.404	0.916	6.267	0.826	7.586	0.455	6.269	0.705
0.500	5.414	0.556	8.842	1.320	5.596	0.897	6.773	0.598	5.651	0.907
0.550	4.469	0.640	6.045	1.394	4.881	0.943	5.086	0.650	4.569	0.958
0.600	3.742	0.685	3.778	1.303	3.453	0.977	3.937	0.648	3.451	0.973
0.650	3.395	0.707	1.973	1.152	2.024	0.928	3.200	0.651	2.650	0.966
0.700	3.101	0.715	1.035	1.029	1.758	0.894	2.981	0.645	2.549	0.974
0.750	3.215	0.729	0.583	0.970	2.516	0.926	3.109	0.677	2.983	0.994
0.800	4.262	0.782	0.185	0.936	2.847	0.950	3.632	0.712	3.264	1.035
0.850	5.277	0.869	0.257	0.917	3.004	0.965	4.222	0.758	3.670	1.092
0.900	5.905	0.960	1.020	0.938	3.306	1.020	4.485	0.829	4.076	1.150
0.950	6.689	1.039	1.595	0.975	3.899	1.074	4.275	0.813	3.910	1.235
1.000	7.363	1.092	1.728	1.062	4.039	1.006	3.843	0.766	3.287	1.309

(Sinkage: Percent Draught [increase in draught +ve]
Trim: Degrees [bow up +ve])

TABLE 20: Model 6c Running Trim and Sinkage

	Monohull		S/L = 0.2		S/L = 0.3		S/L = 0.4		S/L = 0.5	
Fn	Sink.	Trim	Sink.	Trim	Sink.	Trim	Sink.	Trim	Sink.	Trim
0.200	1.549	-0.075	1.423	0.016	2.498	0.029	2.440	-0.034	1.893	-0.017
0.250	1.997	-0.065	2.377	0.055	3.160	0.009	3.045	-0.013	2.485	0.005
0.300	2.932	-0.040	3.509	0.067	3.886	0.033	3.517	0.149	3.248	0.021
0.350	4.148	0.013	4.452	0.079	5.116	0.036	4.962	0.138	4.548	0.082
0.400	5.600	0.181	6.996	0.380	7.192	0.350	6.803	0.480	6.097	0.305
0.450	6.324	0.414	8.324	0.903	8.076	0.829	7.690	0.892	6.851	0.636
0.500	5.472	0.608	7.632	1.364	7.055	1.065	7.060	0.984	6.397	0.811
0.550	4.620	0.664	4.288	1.437	4.647	1.044	4.932	1.156	4.596	0.878
0.600	3.893	0.695	2.466	1.369	3.173	0.999	3.814	1.107	3.430	0.903
0.650	3.482	0.713	1.179	1.256	2.251	0.968	3.154	1.039	2.818	0.916
0.700	3.125	0.728	1.058	1.157	1.483	0.927	2.592	0.973	2.446	0.930
0.750	2.170	0.749	0.857	1.092	1.855	0.921	2.627	0.972	2.637	0.957
0.800	3.108	0.781	0.454	1.062	2.470	0.975	3.343	1.009	3.173	1.003
0.850	4.479	0.831	0.337	1.068	2.771	1.002	3.913	1.063	3.935	1.084
0.900	5.274	0.906	0.140	1.097	3.529	1.095	3.913	1.294	3.943	1.163
0.950	6.071	0.986	0.003	1.146	3.477	1.159	4.208	1.281	3.556	1.235
1.000	7.354	1.055	0.005	1.203	3.496	1.231	4.142	1.360	4.513	1.280

(Sinkage: Percent Draught [increase in draught +ve]
Trim: Degrees [bow up +ve])

TABLE 21: Model 3b Residuary Resistance ($C_T - C_{F_{ITTC}}$)

Fn	Monohull C_R	S/L = 0.2 C_R	S/L = 0.3 C_R	S/L = 0.4 C_R	S/L = 0.5 C_R
0.200	2.971	3.192	3.214	2.642	2.555
0.250	3.510	4.540	3.726	4.019	3.299
0.300	3.808	5.303	4.750	4.464	3.938
0.350	4.800	6.771	5.943	5.472	4.803
0.400	5.621	8.972	7.648	7.085	6.589
0.450	8.036	12.393	12.569	10.934	9.064
0.500	9.038	14.874	14.237	12.027	10.112
0.550	8.543	15.417	12.275	10.538	9.394
0.600	7.626	12.818	10.089	8.962	8.361
0.650	6.736	8.371	8.123	7.592	7.488
0.700	5.954	5.954	6.852	6.642	6.726
0.750	5.383	5.383	5.934	5.921	6.078
0.800	4.911	4.911	5.289	5.373	5.537
0.850	4.484	4.484	4.814	4.949	5.046
0.900	4.102	4.102	4.452	4.543	4.624
0.950	3.785	3.785	4.172	4.236	4.335
1.000	3.579	3.579	3.936	3.996	4.099

(Coefficients $\times 10^3$)

TABLE 22: Model 4a Residuary Resistance ($C_T - C_{F_{ITTC}}$)

Fn	Monohull C_R	S/L = 0.2 C_R	S/L = 0.3 C_R	S/L = 0.4 C_R	S/L = 0.5 C_R
0.200	1.909	2.327	2.564	2.495	2.719
0.250	2.465	3.148	3.315	2.937	3.484
0.300	3.273	3.954	4.283	4.396	3.875
0.350	3.585	5.073	4.576	4.064	4.173
0.400	4.100	4.874	5.871	5.900	5.109
0.450	5.305	8.111	7.953	7.220	6.299
0.500	5.526	8.365	7.150	6.650	6.140
0.550	5.086	7.138	5.990	5.692	5.615
0.600	4.431	5.878	5.090	4.880	4.981
0.650	3.924	4.815	4.392	4.269	4.387
0.700	3.477	4.047	3.949	3.834	3.911
0.750	3.128	3.556	3.594	3.512	3.570
0.800	2.904	3.224	3.187	3.252	3.296
0.850	2.706	2.923	2.966	3.054	3.070
0.900	2.544	2.729	2.839	2.881	2.873
0.950	2.398	2.550	2.657	2.767	2.707
1.000	2.272	2.433	2.437	2.687	2.558

(Coefficients $\times 10^3$)

TABLE 23: Model 4b Residuary Resistance ($C_T - C_{F_{ITTC}}$)

Fn	Monohull C_R	S/L = 0.2 C_R	S/L = 0.3 C_R	S/L = 0.4 C_R	S/L = 0.5 C_R
0.200	2.613	2.929	2.841	2.721	2.820
0.250	2.629	3.686	3.374	3.365	3.396
0.300	3.532	4.311	4.113	4.150	3.902
0.350	3.763	5.483	4.816	4.557	4.329
0.400	4.520	5.897	5.934	5.940	5.716
0.450	5.402	7.748	7.777	7.078	6.741
0.500	5.389	8.420	7.669	6.922	6.581
0.550	4.865	8.099	6.639	6.145	5.921
0.600	4.276	7.159	5.471	5.315	5.209
0.650	3.787	6.008	4.620	4.605	4.593
0.700	3.394	4.769	4.061	4.098	4.125
0.750	3.098	4.041	3.641	3.718	3.786
0.800	2.848	3.605	3.326	3.440	3.520
0.850	2.647	2.647	3.153	3.247	3.319
0.900	2.476	2.476	2.917	3.078	3.131
0.950	2.361	2.361	2.834	2.968	2.998
1.000	2.347	2.347	2.347	2.882	2.870

(Coefficients $\times 10^3$)

TABLE 24: Model 4c Residuary Resistance ($C_T - C_{F_{ITTC}}$)

Fn	Monohull C_R	S/L = 0.2 C_R	S/L = 0.3 C_R	S/L = 0.4 C_R	S/L = 0.5 C_R
0.200	2.169	2.983	2.830	2.801	2.690
0.250	2.506	3.718	3.459	3.412	3.336
0.300	2.987	4.401	4.110	4.067	3.960
0.350	3.349	5.336	4.777	4.321	4.275
0.400	4.371	5.905	5.850	5.919	5.722
0.450	5.525	8.567	8.454	7.605	7.061
0.500	5.512	9.474	7.892	7.013	6.633
0.550	5.021	8.316	6.625	6.087	5.907
0.600	4.473	6.845	5.522	5.249	5.204
0.650	3.995	5.584	4.720	4.617	4.637
0.700	3.632	4.718	4.167	4.165	4.203
0.750	3.360	4.216	3.785	3.845	3.871
0.800	3.119	3.784	3.503	3.587	3.608
0.850	2.922	3.459	3.276	3.364	3.387
0.900	2.743	3.276	3.089	3.165	3.190
0.950	2.603	3.076	2.934	3.003	3.017
1.000	2.481	2.904	2.821	2.875	2.875

(Coefficients $\times 10^3$)

TABLE 25: Model 5a Residuary Resistance ($C_T - C_{F_{ITTC}}$)

Fn	Monohull C_R	S/L = 0.2 C_R	S/L = 0.3 C_R	S/L = 0.4 C_R	S/L = 0.5 C_R
0.200	1.862	2.565	2.565	2.381	2.592
0.250	2.485	3.074	2.991	3.031	3.123
0.300	3.009	3.959	3.589	3.686	3.473
0.350	3.260	4.018	3.756	3.589	3.716
0.400	3.677	4.472	4.604	4.616	4.403
0.450	4.103	6.068	5.563	5.099	4.929
0.500	3.884	5.805	4.950	4.581	4.501
0.550	3.442	4.914	4.221	4.015	3.966
0.600	3.063	4.065	3.596	3.516	3.499
0.650	2.736	3.429	3.138	3.126	3.140
0.700	2.461	3.004	2.827	2.845	2.882
0.750	2.278	2.705	2.615	2.658	2.699
0.800	2.138	2.494	2.465	2.519	2.559
0.850	2.038	2.342	2.351	2.406	2.453
0.900	1.931	2.231	2.260	2.308	2.354
0.950	1.871	2.153	2.183	2.238	2.272
1.000	1.818	2.100	2.124	2.179	2.201

(Coefficients $\times 10^3$)

TABLE 26: Model 5b Residuary Resistance ($C_T - C_{F_{ITTC}}$)

Fn	Monohull C_R	S/L = 0.2 C_R	S/L = 0.3 C_R	S/L = 0.4 C_R	S/L = 0.5 C_R
0.200	1.406	2.288	2.849	2.538	3.006
0.250	2.362	2.843	3.200	3.260	3.093
0.300	2.632	3.643	3.539	3.693	3.330
0.350	2.890	4.194	3.952	3.711	3.437
0.400	3.514	4.520	4.687	4.622	4.303
0.450	3.691	5.506	5.218	4.960	4.648
0.500	3.518	5.581	4.903	4.632	4.324
0.550	3.125	4.927	4.323	4.057	3.804
0.600	2.851	4.177	3.783	3.504	3.286
0.650	2.599	3.555	3.302	3.090	2.872
0.700	2.285	3.051	2.989	2.759	2.576
0.750	2.155	2.744	2.752	2.515	2.396
0.800	2.010	2.529	2.584	2.327	2.310
0.850	1.938	2.383	2.462	2.163	2.322
0.900	1.830	2.298	2.375	2.111	2.382
0.950	1.852	2.221	2.324	2.128	1.852
1.000	1.803	2.186	2.279	2.145	1.803

(Coefficients $\times 10^3$)

TABLE 27: Model 5c Residuary Resistance ($C_T - C_{F_{ITTC}}$)

Fn	Monohull C_R	S/L = 0.2 C_R	S/L = 0.3 C_R	S/L = 0.4 C_R	S/L = 0.5 C_R
0.200	2.517	2.731	2.801	2.718	2.983
0.250	2.756	3.256	3.199	3.203	3.290
0.300	3.010	3.445	3.599	3.386	3.371
0.350	3.273	3.937	3.779	3.623	3.625
0.400	3.687	4.635	4.813	4.731	4.519
0.450	3.891	5.908	5.543	4.969	4.644
0.500	3.621	5.864	5.016	4.513	4.340
0.550	3.232	5.095	4.274	3.945	3.855
0.600	3.048	4.231	3.703	3.495	3.512
0.650	2.685	3.576	3.267	3.183	3.187
0.700	2.417	3.074	2.930	2.920	2.936
0.750	2.205	2.771	2.741	2.717	2.779
0.800	2.076	2.558	2.632	2.564	2.594
0.850	1.903	2.434	2.607	2.476	2.514
0.900	1.863	2.346	2.599	2.404	2.454
0.950	1.915	2.259	2.550	2.341	2.358
1.000	1.785	2.213	2.481	2.256	2.281

(Coefficients $\times 10^3$)

TABLE 28: Model 6a Residuary Resistance ($C_T - C_{F_{ITTC}}$)

Fn	Monohull C_R	S/L = 0.2 C_R	S/L = 0.3 C_R	S/L = 0.4 C_R	S/L = 0.5 C_R
0.200	1.916	2.727	2.660	2.807	2.484
0.250	2.257	3.379	3.244	3.595	3.515
0.300	2.443	3.792	3.548	3.761	3.665
0.350	2.527	3.665	3.381	3.754	3.566
0.400	2.723	4.377	4.403	4.257	4.009
0.450	2.796	4.703	4.593	4.339	3.998
0.500	2.658	4.592	3.974	3.855	3.635
0.550	2.434	3.799	3.382	3.338	3.243
0.600	2.246	3.193	2.994	2.955	2.916
0.650	2.111	2.812	2.703	2.689	2.651
0.700	1.917	2.534	2.496	2.505	2.475
0.750	1.781	2.367	2.348	2.379	2.336
0.800	1.633	2.253	2.261	2.304	2.243
0.850	1.544	2.176	2.194	2.230	2.171
0.900	1.478	2.110	2.155	2.146	2.093
0.950	1.528	2.062	2.110	2.047	2.021
1.000	1.521	2.027	2.064	1.976	1.962

(Coefficients $\times 10^3$)

TABLE 29: Model 6b Residuary Resistance ($C_T - C_{F_{ITTC}}$)

Fn	Monohull C_R	S/L = 0.2 C_R	S/L = 0.3 C_R	S/L = 0.4 C_R	S/L = 0.5 C_R
0.200	1.755	2.864	2.297	2.933	2.353
0.250	2.136	3.217	3.235	3.203	2.335
0.300	2.255	3.769	3.162	3.251	2.833
0.350	2.150	3.667	3.299	3.502	3.158
0.400	2.639	4.007	3.721	3.913	3.479
0.450	2.696	4.534	4.092	3.950	3.570
0.500	2.510	4.379	3.771	3.592	3.393
0.550	2.338	3.734	3.202	3.196	3.085
0.600	2.084	3.144	2.762	2.866	2.662
0.650	1.900	2.738	2.507	2.635	2.565
0.700	1.747	2.477	2.355	2.468	2.378
0.750	1.656	2.311	2.249	2.339	2.268
0.800	1.575	2.184	2.158	2.241	2.214
0.850	1.527	2.093	2.068	2.172	2.112
0.900	1.523	2.052	2.056	2.129	2.064
0.950	1.482	2.020	2.046	2.089	2.048
1.000	1.426	2.001	2.001	2.063	2.036

(Coefficients $\times 10^3$)

TABLE 30: Model 6c Residuary Resistance ($C_T - C_{F_{ITTC}}$)

Fn	Monohull C_R	S/L = 0.2 C_R	S/L = 0.3 C_R	S/L = 0.4 C_R	S/L = 0.5 C_R
0.200	1.882	2.979	1.909	2.608	2.515
0.250	2.395	3.169	3.328	3.056	2.911
0.300	2.581	3.539	3.401	3.252	3.191
0.350	2.666	3.531	3.309	3.385	3.366
0.400	2.785	3.684	3.774	3.813	3.629
0.450	2.816	4.229	3.932	3.813	3.676
0.500	2.626	4.154	3.719	3.527	3.446
0.550	2.394	3.573	3.256	3.187	3.145
0.600	2.177	3.080	2.855	2.866	2.851
0.650	2.006	2.809	2.595	2.609	2.608
0.700	1.866	2.504	2.437	2.432	2.487
0.750	1.754	2.305	2.331	2.345	2.358
0.800	1.682	2.165	2.199	2.232	2.297
0.850	1.633	2.138	2.167	2.210	2.249
0.900	1.568	2.108	2.120	2.174	2.227
0.950	1.628	2.078	2.121	2.149	2.227
1.000	1.672	2.067	2.134	2.157	2.193

(Coefficients $\times 10^3$)